Stratosphere Troposphere Interactions Associated with the Dynamical Processes in the Atmosphere

Thesis submitted to the

Cochin University of Science and Technology

in partial fulfilment of the requirement for the Degree of

DOCTOR OF PHILOSOPHY

in

ATMOSPHERIC SCIENCE

By

V. SATHIYAMOORTHY

Department of Atmospheric Sciences
Cochin University of Science and Technology
Lake Side Campus, Cochin 682 016

July 2001

CERTIFICATE

This is to certify that the thesis entitled ***Stratosphere Troposphere Interactions associated with the Dynamical Processes in the Atmosphere*** *is a bonafide record of research work done by* ***Mr. V. Sathiyamoorthy*** *in the Department of Atmospheric Sciences, Cochin University of Science and Technology. He carried out the study reported in this thesis, independently under my supervision. I also certify that the subject matter of the thesis has not formed the basis for the award of any Degree or Diploma of any University or Institution.*

Certified that ***Mr. V. Sathiyamoorthy*** *has passed the Ph.D qualifying examination conducted by the Cochin University of Science and Technology in September 1999.*

Cochin 16
July 02, 2001

(K. MOHANKUMAR)
Supervising Teacher

Dr.K.Mohan Kumar, Ph.D.
Professor & Head
Department of Atmospheric Sciences
Cochin University of Science & Technology
Cochin-682 016, India

Preface

The lowest two layers of the atmosphere namely the stratosphere and the troposphere have entirely distinct structure, composition, dynamics, etc. Atmospheric trace constituents like ozone, CFCs, Methane, etc have their source regions in one of these regions and sinks in the other. The transport and mixing of mass and chemical species between stratosphere and troposphere, also known as stratosphere-troposphere exchanges, affect climate in numerous ways; eg. the impact of aircraft emissions on the ozone layer, the vertical structure of greenhouse gas distributions in the upper troposphere/lower stratosphere and midlatitude ozone depletion.

The aim of the present study is to understand the biennial scale stratosphere-troposphere interactions over India, and synoptic to interannual timescale meridional stratosphere-troposphere exchanges caused by upper tropospheric/lower stratospheric longwaves using NCEP/NCAR reanalysis data and satellite measured total ozone data.

The doctoral thesis consists of 7 chapters. In chapter 1, elaborate introduction on the dynamical processes in the lower and middle atmosphere is given. In addition, role of ozone as the tracer of atmospheric motion in upper troposphere/lower stratosphere, its production, destruction, transportation mechanisms are presented. Based on published works in various scientific journals, books and reports a review on the literature is given chapter-2. Details regarding the data, their accuracy, limitations, etc are described in chapter-3.

Nature of the biennial scale stratosphere-troposphere interactions over Thumba, a near-equatorial station is studied using radiosonde measured temperature and wind data and is presented in chapter-4. Tropospheric temperature over this station shows a significant biennial variability. Marked differences in amplitude and phase of QBO and TBO are noticed between the decades 1971-81 and 1982-92. The decadal change in phase coherence between TBO and QBO in temperature suggests that they are different phenomena. The strong relation existing between the phase of TBO and Indian summer monsoon activity suggest that the observed biennial variability in the tropospheric temperature over Thumba, may be due to the monsoon-ocean-atmosphere interactions taking place over Indian Ocean in biennial timescale.

In chapter-5, the interannual timescale stratosphere-troposphere ozone exchanges caused by the newly documented Asia Pacific Wave (APW) is presented in detail. This wave is present between 70 hPa and 500 hPa levels in May and the following summer and autumn seasons and couples the stratosphere and troposphere directly. This wave shows a phase shift of 20° longitudes between extreme Indian summer monsoon rainfall years. The large amplitude portion of this wave is situated in the tropopause break region and found to exchange ozone-rich extratropical lower stratospheric air and ozone-poor tropical upper tropospheric air. The ozone exchanges caused by APW is illustrated using the gridded global TOMS total ozone data.

Chapter-6 deals with synoptic scale stratosphere-troposphere ozone exchanges caused by upper troposphereic/lower stratospheric longwaves in winter and summer seasons. The winter time Upper Tropospheric Troughs

(UTT) and the ridges following and preceding it occasionally penetrate deep into South Asia and generates synoptic scale total ozone anomalies (TOA) as mentioned above. Values of positive and negative TOA reached upto 25-30% during this condition over Asia. In summer season, Upper Tropospheric Blocking High and Trough (UTBHT) situation develops over Asia during break periods in Indian summer monsoon. This situation persists for a few days to a few weeks and generates negative and positive TOA over Asia. The negative TOA reached even 50% less than the long-term mean in some areas over Asia and generated a sort of *ozone mini-hole* like situation.

The summary and conclusions of the research work carried out in the thesis is presented in the last chapter, chapter-7. References are listed at the end of the thesis in alphabetical order.

CONTENTS

Chapter –1

Introduction

1.1 Relevance of the study

Although stratosphere and troposphere have distinctive dynamical, physical and chemical characteristics and separated by the tropopause barrier, they interact dynamically, chemically and radiatively. For instance, anthropogenic species transported from the troposphere into the stratosphere initiate much of the chemistry responsible for stratospheric ozone depletion. Conversely, transport of stratospheric trace chemicals into troposphere constitute the main removal mechanism for many stratospheric species, including those involved in ozone depletion, but also represents a significant input of ozone and other reactive species into troposphere chemical system (Holton et al., 1995).

Both observational and numerical studies have presented strong evidences that the variations in the stratosphere are coupled to those in the troposphere and *vice-versa* in the contexts of mid-winter stratospheric warmings in Polar regions, Quasi-Biennial Oscillations (QBO) in zonal wind and the Arctic Oscillation (AO). Planetary scale wave activity in the troposphere is believed to be the cause for the biennial timescale wind reversal in the equatorial lower stratosphere and mid-winter stratospheric warmings. Several statistical works revealed the presence of close relationship between the phase of QBO and the frequency of cyclone incidences, extreme Indian summer monsoon activity, etc. Exchanges of ozone between the troposphere and stratosphere must be understood because of the central role it plays in several important environmental problems such as: controlling the amounts of biologically damaging ultraviolet radiation that reaches the earth's surface, its impact on air quality

as an oxidizing pollutant that is harmful to biosphere, and as a greenhouse gas that contributes to the earth's radiative balance.

These results indicate that the troposphere and the stratosphere should be considered as a dynamically, chemically and radiatively coupled system. However, fundamental nature of the exchange processes that take place in the stratosphere-troposphere coupled system has not fully been understood. Proper understanding of the stratosphere and troposphere interactions such as the dynamical transport and mixing of trace chemical species, biennial scale interactions, etc are important for global change prediction studies.

1.2 Justification of the study

Several statistical works showed significant correlation between the phase of QBO and Indian summer monsoon activity. Indian summer monsoon rainfall shows dominant biennial variability. Yasunari (1989) showed the existence of vertical phase coherence between the biennial oscillations in the stratosphere and the troposphere over Singapore and few other equatorial Pacific stations. So it is interesting to know, whether such a phase coherence exist between QBO and the biennial variability in the troposphere over India. High-resolution (vertical) radiosonde measurements over Thumba, Trivandrum made during January 1970 to December 1992 provided an opportunity to study the presence of such vertical phase coherence over Indian region.

Lower stratosphere is rich in ozone and the troposphere is poor. Stratosphere-troposphere exchange generates wide range of spatial and

temporal total ozone variability over a region due to the presence of sharp gradient in ozone abundance between stratosphere and troposphere. Planetary scale stationary waves in the upper troposphere/lower stratosphere generates global scale total ozone anomalies on intraseasonal, interannual and decadal timescales by stratosphere-troposphere exchange processes. Total ozone over a region undergoes substantial short-term fluctuations associated with synoptic weather systems. Both horizontal and vertical ozone exchanges between the stratosphere and the troposphere are attributed to these fluctuations.

All these random variations in total ozone associated with stratosphere – troposphere exchanges have to be considered properly for the realistic estimation of long-term trend in total ozone over a region.

Good quality total ozone measurement available from Total Ozone Mapping Spectrometer (TOMS) instruments on various satellites provide an opportunity to study these wide range of total ozone fluctuations associated with stratosphere-troposphere exchanges in great detail. Total ozone anomalies generated by the recently documented Asia Pacific Wave (APW) and synoptic scale long waves have been studied in detail employing the most recent available release (version-7) of the total ozone data measured by Nimbus-7 satellite. This version utilized a re-calibration of the raw data, notably improving the quality of data retrieved for low solar zenith angles over earlier versions.

1.3 General circulation of the lower and middle atmosphere

The availability of large number of good quality data sets from *in situ* and remote sensing measurements since the International Geophysical Year (IGY) provide a clear picture about the general circulation of the middle atmosphere. Two of the most basic general circulation parameters are temperature and zonal wind. These two parameters are in approximate thermal wind balance in lower and middle atmosphere.

Fig. 1.1 and fig. 1.2 show the latitude-height plot of the zonal mean temperature and zonal mean zonal wind for solstice condition from surface to 100 km altitude (adopted from Andrews et al., 1987). Typical features seen in these figures are as follows. In the lower atmosphere, tropical tropopause is the coldest region. Stratopause over summer pole is warmer than winter pole. In the upper mesosphere, temperature increases from the summer pole to winter pole. The overall wind distribution is in thermal wind balance. Troposphere is characterized by westerly jet streams in both the hemispheres at about 30° latitude. The winter hemispheric westerly jet is stronger than summer hemispheric one. The middle atmosphere is characterized by easterlies in summer hemisphere and westerlies in winter hemisphere; both with core situated around 60 km altitude over 30° latitude. The westerly jet is stronger than the easterly jet. The middle atmospheric circulation undergoes a strong annual cycle in which the zonal winds in each hemisphere change from westerly to easterly between summer and winter. The interannual variability of the middle atmosphere is large in winter because of the occurrence of sudden stratospheric warmings during which the stratospheric winds reverse temporarily affecting the circulation

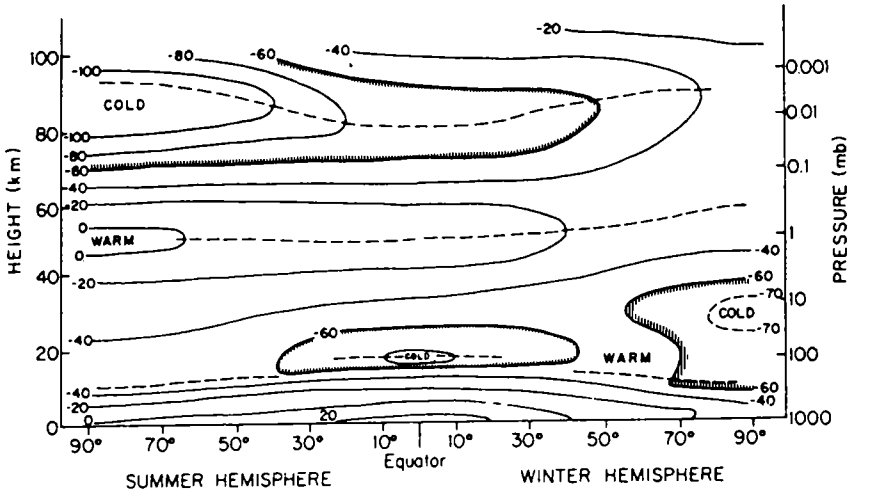

Fig. 1.1 Schematic latitude-height section of zonal mean temperature (° C) for solstice conditions. Dashed lines indicate tropopause, stratopause, and mesopause levels. (Andrews et al, 1987).

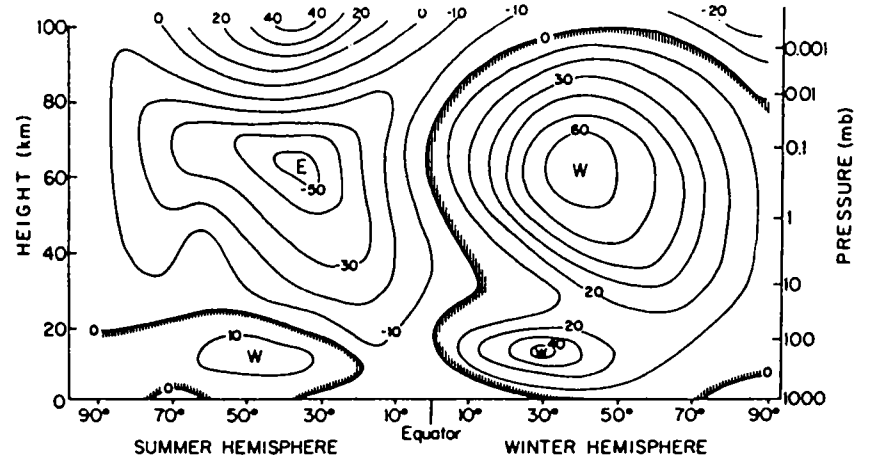

Fig. 1.2 Schematic latitude-height section of zonal mean zonal wind (ms^{-1}) for solstice conditions; W and E designate centers of westerly and easterly winds, respectively. (Andrews et al, 1987).

for several weeks. Circulation of the equatorial stratosphere is dominated by quasi-biennial time scale wind reversal.

1.4 Quasi-biennial oscillation

The QBO in the equatorial lower stratosphere was discovered independently by Reed et al., (1961) and Veryard and Ebdon (1961). It is a quasi periodic, downward propagating oscillation between easterly and westerly zonal wind regimes in the tropical stratosphere. In fig. 1.3, time-height section of monthly mean zonal wind components at Canton Island (January 1953 – August 1967), Gan/ Maledive Islands (September 1967 – December 1975), and Singapore (January 1976 – December 2000) is presented. This oscillation extends from tropopause to 35 km altitude (100 hPa to 10 hPa), but significant QBO signals have been detected at altitudes as high as 50 km (Angell and Korshover, 1970). The amplitude and period of this oscillation are highly variable, with average amplitude greater than 20 ms^{-1} and period about 28 months. The average descend rate of the phase is ~1km/month.

The equatorial zonal wind QBO is believed to be a result of momentum transfer by vertically propagating tropical waves forced in the troposphere, primarily Kelvin and Rossby gravity waves (Lindzen and Holton, 1968, Holton and Lindzen, 1972).

1.5 Sudden stratospheric warming

During some midwinter seasons, the zonal mean configuration of temperature and zonal wind is disrupted dramatically in the polar

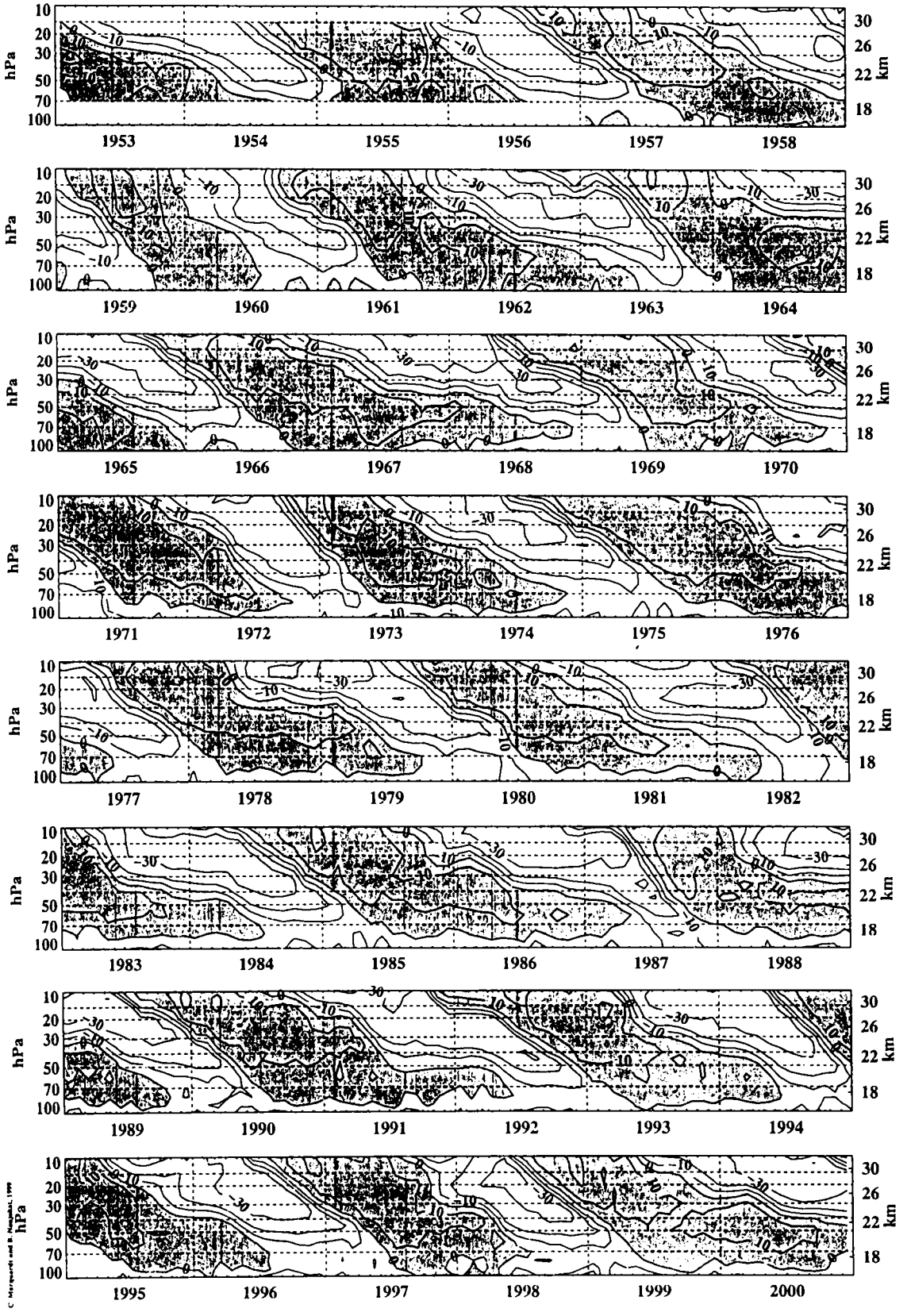

Fig. 1.3 Time-height section of monthly mean zonal wind components (m/s) at Canton Island (January 1953-August 1967), Gan/Maledive Islands (September 1967 - December 1975), and Singapore (January 1976 - December 2000); westerlies are shaded (update from Naujokat, J. Atmos. Sci., 43,1873-1877, 1986).

stratosphere. This sudden increase in polar stratospheric temperature, which persists for a few weeks, is referred to as Sudden Stratospheric Warming (SSW). These events have been classified in to major and minor warming.

During major SSW, the North Pole warms dramatically with reversal of meridional temperature gradient and breakdown of polar vortex occurs. The polar vortex is replaced by a high over this region. The westerlies in the Arctic at 10 hPa are replaced by easterlies so that the center of the vortex moves south of 60°-65° N during the breakdown of polar vortex. The vortex is either displaced entirely or split into two. This type of warming has not been observed in the Antarctic.

Minor warmings can indeed be intense and sometimes also reverse the temperature gradient, but they do not result in a reversal of the circulation at the 10 hPa level. They are found in the Antarctic as well as Arctic regions.

1.6 Static stability of the stratospheric air

The stratospheric temperature increases with height. As the air parcel displaced above becomes cooler than the surrounding, convection rarely occurs in the stratosphere. Potential temperature (θ) is a measure of static stability of the atmosphere.

$$\theta = T\,(P/P_s)^K$$

Where T is the Temperature

P_s is 1000 hPa

$K = R/C_p$

It is the temperature an air parcel would have if compressed adiabatically from its existing pressure level to 1000 hPa level. If the potential temperature increases with height, the air is said to be stably stratified. If it decreases with height, the air is said to be unstable. In stratosphere, the potential temperature increases with height (fig. 1.4). At altitudes around 20 km, the potential temperature is about 500 K or 227° C. As the potential temperature becomes very high at the higher levels in the stratosphere, it is extremely difficult for air parcels in that level to move up or down. The air will tend to remain in an isentropic surface (equal potential temperature surfaces) for several days. Potential temperature is widely used as vertical co-ordinate in stratospheric studies. The most obvious reason to use this co-ordinate system is that the vertical velocity $D\theta/Dt$, equals to the diabatic heating Q. Thus, when $Q = 0$ (adiabatic flow), vertical velocity vanishes and no motion can take place across isentropic surfaces.

1.7 Tracers and their transport in middle atmosphere

Any quantity that labels fluid parcels in the atmosphere is called tracer. Tracers may be chemical or dynamical, conservative or non-conservative, passive or active. Chemical tracers are the minor atmospheric constituents like ozone, methane, etc that have significant spatial variability. The most well known atmospheric dynamical tracer is the potential temperature (θ), which is conserved during adiabatic parcel movements. Somewhat, less familiar dynamical tracer is Ertel's potential vorticity 'P', defined by

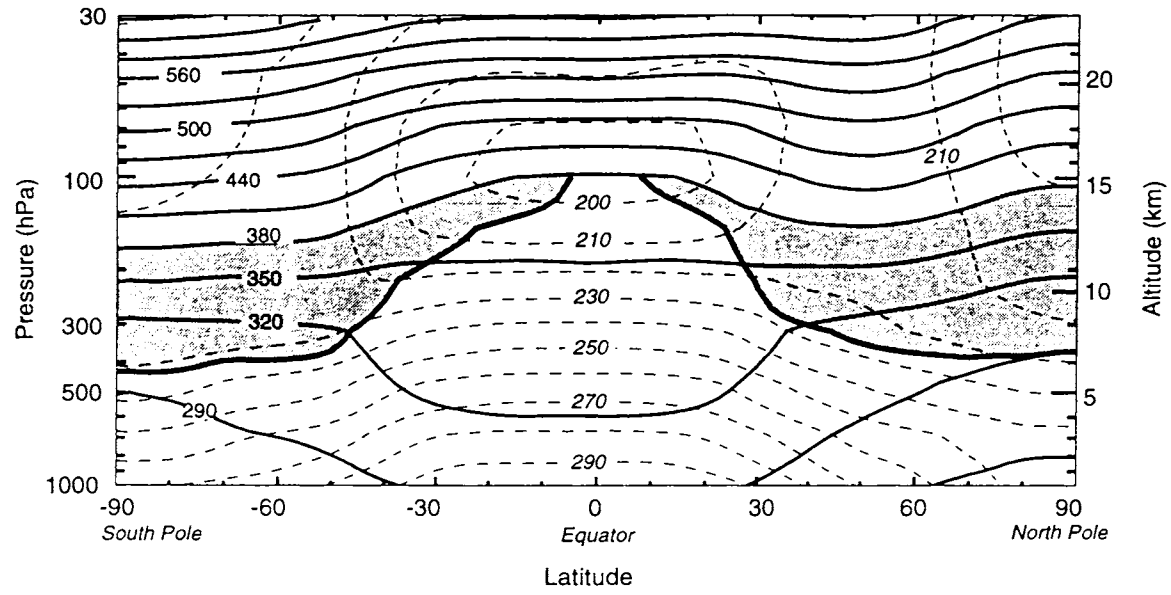

Fig. 1.4 Latitude-altitude cross section for January 1993 showing longitudinally averaged potential temperature (solid contours) and temperature (dashed contours). The heavy solid contour (cut off at the 380-K isentrope) denotes the 2-PVU potential vorticity contour, which approximates the tropopause outside tropics. Shaded areas denote the "lowermost stratosphere", whose isentropic surfaces span the tropopause. (Holton et al, 1995).

$$P = \rho^{-1} (\omega + 2\Omega). \nabla\theta$$

Where ρ is atmospheric density

ω is $\nabla \times U$ (Relative vorticity)

Ω is Earth's rotation vector

Potential vorticity is conserved for adiabatic frictionless flow. In the case of conserved tracers, the amount remains constant in time following each air parcel. The tracers, whose rate of change following the motion are very small for the time scales of interest are referred as long lived tracers. The dynamical, thermodynamical or chemical properties of the dynamically active tracers influence the flow fields that transport them. The dynamically passive tracers do not have such effect.

1.8 Stratosphere – troposphere exchange

The transport and mixing of stratospheric and tropospheric airmasses, chemical species is called as stratosphere – troposphere exchanges (STE). For STE studies dynamics of stratosphere and troposphere are distinguished separately. Main reason for this is that the timescales of vertical transport within the troposphere is very much short compared to the stratosphere. STE can take place in two ways. Meridional exchange takes place along quasi-isentropic surfaces between tropical troposphere and extratropical lowermost stratosphere and vertical cross-isentropic transport between troposphere and stratosphere. These two exchange processes are dealt separately in STE studies because of the different dynamics involved in them.

Some of the processes that cause STE listed by Andrews et al., (1987) are:

a) *the large-scale mean diabatic circulation (Brewer-Dobson cell),*

b) *transverse secondary circulations associated with subtropical and polar jet streams,*

c) *cumulonimbus cloud penetrating into the stratosphere,*

d) *tropopause folds involving baroclinic wave activity,*

e) *radiative cooling in the vicinity of high level cirrus anvil clouds, etc.*

1.9 Dynamical aspects of stratosphere – troposphere exchanges

Holton et al., (1995) summarized the dynamical processes responsible for the transport across the tropopause (fig. 1.5). They emphasized that it is useful to distinguish between transport across and along isentropic surfaces. At middle latitudes where the climatological mean tropopause intersects the isentropes, irreversible exchange of air and chemical constituents can occur in the form of adiabatic eddy motion (heavily shaded region). In this region mesoscale phenomena like tropopause folds and cut-off lows dominate the transport across the tropopause. The global scale diabatic circulations, which account for the largest part of the transport across the isentropic surfaces is illustrated by broad arrows. The light shaded region denotes waves induced forcing responsible for the poleward and downward transport of tropical stratospheric air into the extratropical troposphere.

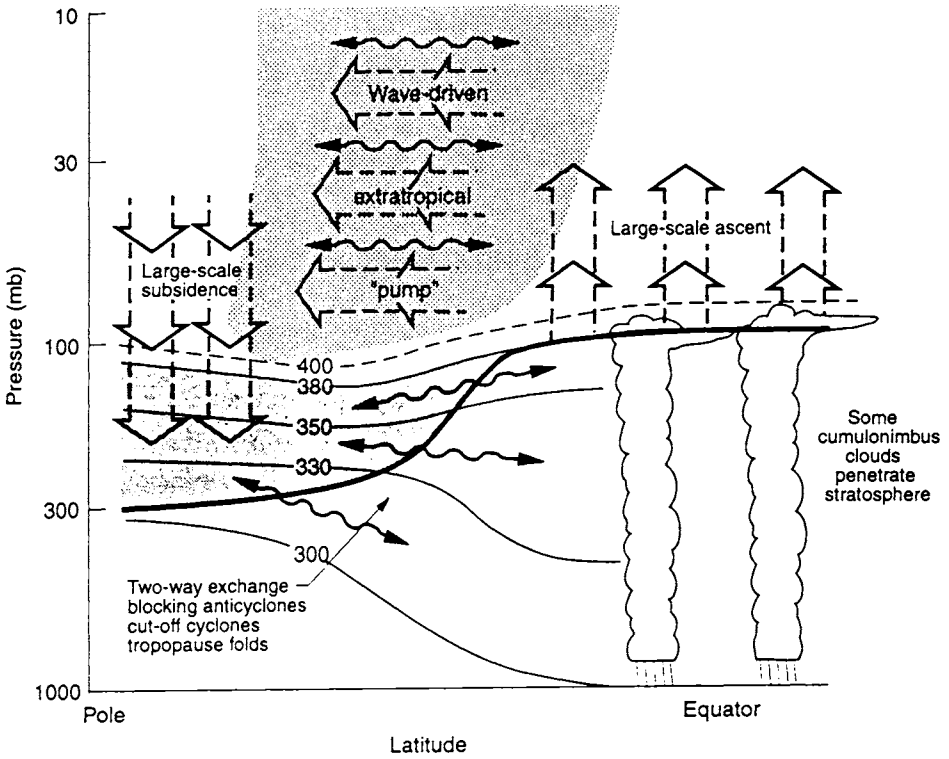

Fig. 1.5 Dynamical aspects of stratosphere-troposphere exchange. The tropopause is shown by the thick line. Thin lines are isentropic surfaces labeled in Kelvins. The heavily shaded region is the lowermost stratosphere, where isentropic surfaces span the tropopause and isentropic exchange by tropopause folding occurs. The region above the 380-K surface is the overworld, in which isentropes lie entirely in the stratosphere. Light shading in the overworld denotes wave-induced forcing. The wavy double-headed arrows denote meridional as well as their midlatitude counterparts including folds. The broad arrows show transport by the global-scale circulation, which is driven by the extratropical pump. The global-scale circulation is the primary contribution to exchange across isentropic surfaces that are entirely in the overworld. (After Holton et al, 1995).

According to them, the generation of large scale and small-scale waves mainly in the troposphere, followed by their propagation into the stratosphere and mesosphere and their dissipation produces a predominantly and persistently westward wave induced zonal force. In the extratropics, which are strongly influenced by the earth's rotation, such a persistent westward force tend to come into balance with the Coriolis force associated with a mean poleward mass flux, which is referred to as midlatitude pumping action (waves induced forcing).

1.10 International activities about stratospheric processes and their role in climate

Stratospheric processes play a significant role in the earth's climate. The absorption of solar radiation in the stratosphere by ozone modulates the solar forcing of climate. The concentrations of some atmospheric gases, principally ozone, carbon dioxide and water vapour, determine significant radiative forcing terms, and there is two-way interaction between stratospheric and tropospheric dynamics.

Recognising the importance of these processes for the climate system, the World Climate Programme (WCRP) set up, in 1992, a research project to study Stratospheric Processes and their Role in Climate (SPARC). SPARC has taken initiatives on the following themes:

1. *Detection of stratospheric trends (temperature, ozone, water vapour), which indicate climate change or could affect climate,*

2. *Understanding stratospheric processes (Chemistry and microphysics of stratosphere, gravity wave processes, QBO and its possible role in coupling the stratosphere and troposphere, etc), and*

3. *Modelling stratospheric processes and trends and their effects on climate.*

An assessment of temperature trends conducted for SPARC has confirmed that a cooling of the stratosphere is taking place. SPARC has also initiated work to assess the current ability to simulate the climatology and variability of the circulation of the middle atmosphere using those general circulation models, which include the middle atmosphere. Work is being undertaken jointly with the International Ozone Commission (IOC) and Global Atmospheric Watch (GAW) to assess the consistency of different ozone measurements and to improve the understanding of trends in the vertical distribution of ozone. SPARC is strongly co-ordinating with other international research programmes and activities like Global Climate Observing System (GCOS), The WMO Global Atmosphere Watch (GAW), The IGBP International Global Atmospheric Chemistry Project (IGAC), International Ozone Commission (IOC), etc in several climate change related issues.

1.11 Ozone measurement from space

Since 1960's, several methods of remote measurements of ozone from space were devised and tested. The most promising techniques for stratospheric sounding seem to be the back scatter UV system for ozone profile and total ozone monitoring and the limb infrared emission system

for investigations requiring good vertical resolution of ozone profile and complementary information on air temperature and trace constituents. A number of satellite systems are currently measuring total atmospheric ozone and its vertical distribution throughout the atmosphere. Some are capable of providing full daily coverage over the sunlit part of the Earth and have the benefit of providing their information in near-real-time. The Total Ozone Mapping Spectrometer (TOMS) onboard Nimbus-7 satellite provided daily global coverage of the earth's total ozone by measuring the backscattered earth radiance in the six 1 nm bands listed below.

TOMS wavelengths (nm): 379.95, 359.88, 339.66, 331.06, 317.35 and 312.34.

Total ozone amount is determined using *pair determination method*, in which radiances at two wavelengths, one sensitive to atmospheric ozone and the other not is used to measure atmospheric total ozone. Detailed radiative transfer calculations are used to determine the backscattered radiance as a function of total ozone. TOMS instruments are also available onboard Meteor-3 and Earth Probe satellites. The Meteor-3-TOMS was operational only for a few years, from 22 August 1991 to 24 November 1994. The Earth Probe TOMS is operational since 25 July 1996 and it gives good quality ozone data continuously until now.

1.12 Vertical distribution of ozone

Mid-latitude standard ozone concentration profile adopted from (Andrews et al., 1987) is presented in fig. 1.6. Major part of the atmospheric ozone is contained in the lower stratosphere with maximum ozone concentration at about 22 km. Ozonopause is the height where the vertical

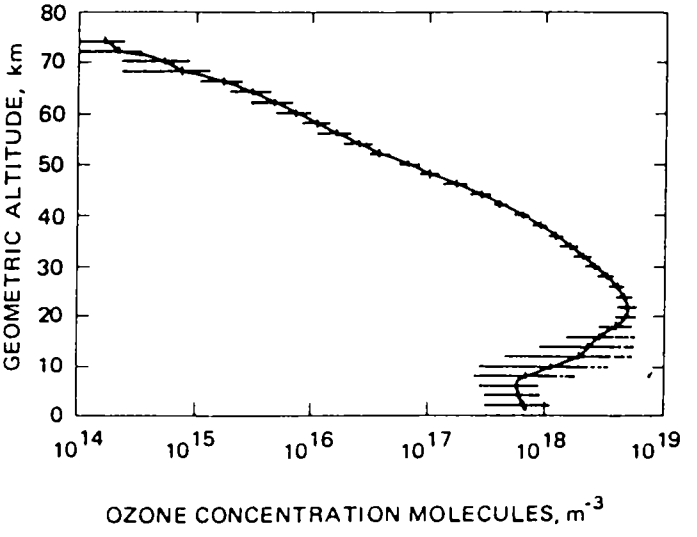

Fig. 1.6 Midlatitude standard ozone concentration profile (molecules m^{-3}). Horizontal bars show the standard deviation about the mean for observed profiles. (Andrews et al, 1987).

ozone gradient goes up from a tropospheric value, less than 5 ppbv km^{-1} to a stratospheric value of about 50 ppbv km^{-1}. Ozonesonde measurements report the atmospheric abundance of ozone in partial pressure.

1.13 Geographical distribution of total ozone

Bowman and Krueger (1985) presented four year averaged total ozone map based on total ozone measurements from TOMS onboard Nimbus-7 satellite. It is presented in fig. 1.7. Total ozone is minimum over equator and maximum near the poles. The isolines of total ozone are fairly parallel to the latitude circles in the mid-latitudes. The regions of maximum total ozone occur in the regions of stationary planetary wave troughs in the upper troposphere.

In fig. 1.8, the time-latitude plot of total ozone adopted from Bowman and Krueger (1985) based on TOMS measurements is presented. This clearly shows the presence of annual cycle in total ozone. In both the hemispheres, the total ozone maximum occurs during the spring season. Area of maximum total ozone occurs at 90° N latitude in Northern Hemisphere and at 60° S in Southern Hemisphere.

1.14 Photochemical lifetime of ozone

Photochemical lifetime of atmospheric ozone is relatively small between 25-80 km altitudes. So photochemical processes mainly control the ozone concentration in this region and the dynamics has little role to play on it. Below 25 km, where major portion of the atmospheric ozone resides, the photochemical lifetime is large and the ozone concentration is mainly

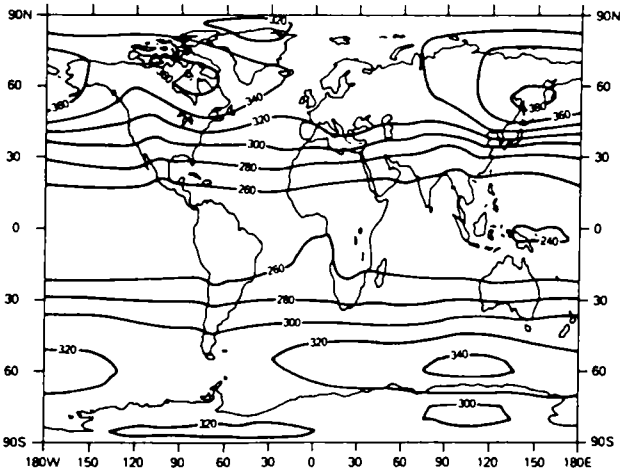

Fig. 1.7 Global distribution of total ozone (Dobson units) based on 4-years of observation with the TOMS instrument on the Nimbus-7 satellite. (After Bowman and Krueger, 1985)

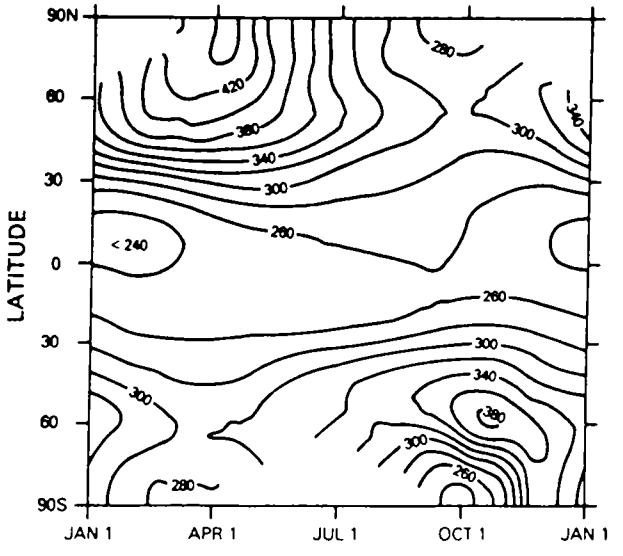

Fig. 1.8 Time-latitude section showing the seasonal variation of total ozone (Dobson units) based on TOMS data. (After Bowman and Krueger, 1985).

controlled by dynamical processes of the atmosphere. Fig. 1.9 taken from Subbaraya and Lal (1999) shows the relative importance of photochemical and transport processes in ozone distribution.

1.15 Meteorology and ozone variability

Satellite measured total ozone distribution reveal the presence of complex and highly dynamical variabilities, with fluctuations as large as 30-60% in Northern Hemisphere. As mentioned above, at 10-20 km altitude the photochemical lifetime of ozone is less compared to the timescales of advection. The time scale of radiative transfer is relatively long of the order of weeks (Kiehl and Solomon, 1986) so that the parcel is adiabatic and move along isentropic surfaces.

So the deflections of the quasi-horizontal surfaces of equal potential temperature mark the vertical motion of individual bodies of air (Salby and Callaghan, 1993). Because of adiabatic nature, the parcel conserves potential vorticity.

$$Q = (\zeta + f) / (dp/d\theta)$$

where ζ is the relative vorticity.

Total ozone variability occurs mainly by one among the few ways mentioned below.

a) *By meridional transport of ozone from the region of photochemical production to the polar region by direct diabatic 'Brewer – Dobson circulation'.*

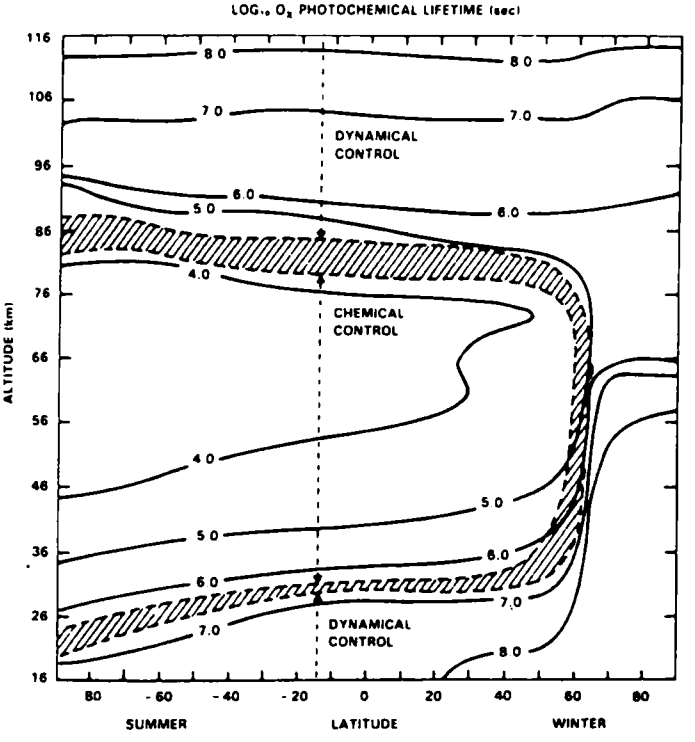

Fig. 1.9 Relative importance of photochemical and transport processes in ozone distribution. (Subbaraya and Lal, 1999).

b) *By horizontal displacement of airmass from one region with particular ozone mixing ratio* $\mu_{o3} = n_{o3} / n_{air}$ *to another region with different ozone mixing ratio and inturn increase or decrease the columnar ozone content over the region (Here* n_{o3} *is ozone number density and* n_{air} *is number density of air).*

c) *By displacement of concentrated total ozone layer downward (upward) in some region, ozone rich air will undergo compression (expansion) which increases (decreases) the ozone number density and hence the column abundance in that region.*

In fig. 1.10 (adopted from Salby and Collaghan, 1993) schematically explains the relation between the disturbances around the tropopause region and total ozone variability. The ozone number density n_{o3} (stippled) increases sharply above the tropopause, the mean position of which is indicated by a solid dashed curve, and then decreases due to exponentially following air density. Disturbances to the circulation deflect the tropopause and neighbouring isentropic surfaces (solid). Upper tropospheric troughs bend the tropopause downward and increase the depth of the stratosphere. Ozone rich airmass descend downward along these deflected isentropic surfaces experience compression. The increased stratospheric column and compression increases the n_{o3} and alters total ozone. Reverse happens over the upper tropospheric ridges.

1.16 Catalytic ozone destruction

Recent findings from ground based and satellite based measurements shows that the stratospheric ozone is decreasing over Antarctic and Arctic

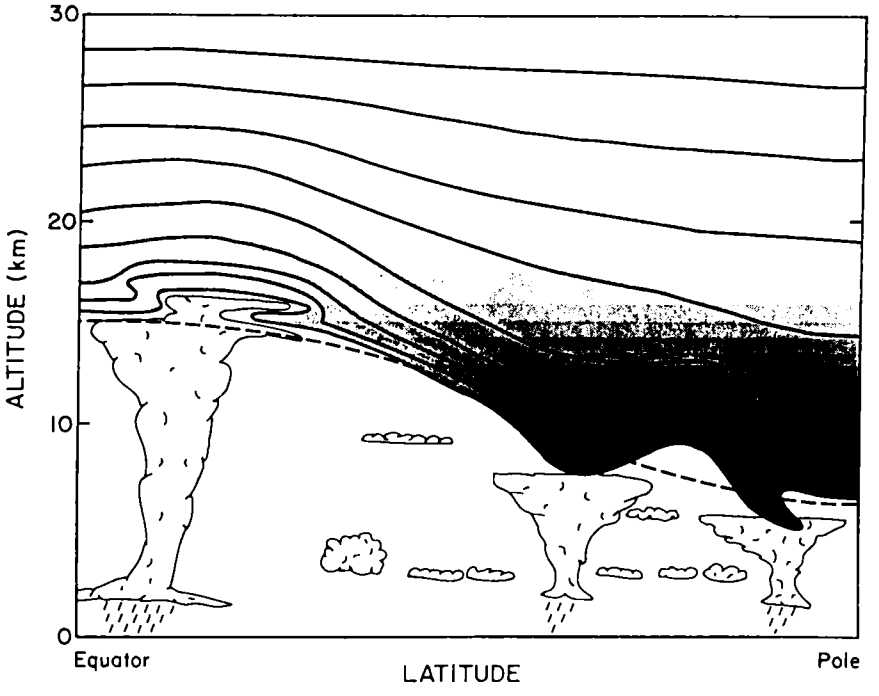

Fig. 1.10 Schematic cross section of the troposphere and lower stratosphere. The ozone number density n_{o3} (stipled) increases sharply above the tropopause, the mean position of which is indicated by a solid dashed curve, and then decreases due to exponentially falling air density. Disturbances to the circulation deflect the tropopause and neighbouring isentropic surfaces (solid). Ozone-rich air descending along those surfaces experiences compression, which increases n_{o3} and alters the column abundance. (After Salby and Callaghan, 1993)

regions; the decrease is very high ranging upto 60% and 20% respectively. Stratospheric ozone is destroyed catalytically by the chlorine compounds derived from CFCs and Nitrogen Oxides as predicted by Crutzen, Rowland and Molina. NO_x is released from the emission from supersonic aircraft and chlorine compounds from CFCs. The catalytic reaction in simplified form is presented below.

Catalytic cycle with NO_2

$$NO + O_3 \rightarrow NO_2 + O_2$$
$$O_3 + h\gamma \rightarrow O_2 + O$$
$$NO_2 + O \rightarrow NO + O_2$$

$$2O_3 \rightarrow 3O_2 \quad \textit{(Destruction)}$$

Catalytic cycle with Cl

$$Cl + O_3 \rightarrow ClO + O_2$$
$$O_3 + h\gamma \rightarrow O_2 + O$$
$$ClO + O \rightarrow Cl + O_2$$

$$2O_3 \rightarrow 3O_2 \quad \textit{(Destruction)}$$

1.17 Depletion of ozone in the polar region

Around 15-20 km in the polar region, the ozone destruction occurs due to heterogeneous chemical reaction that occur in the presence of Polar Stratospheric Clouds (PSC). Three different types of PSCs have now been identified: sulphated, nitrated or aqueous, which form at temperatures varying between 188 K and 195 K (Chanin, 2001). A band of strong winds

called polar vortex, circulating the pole near the polar night terminator plays a crucial role in sustaining the depletion of ozone. The cholorine and bromine activated in the heterogeneous chemical reactions leads to rapid ozone loss when sunlight enters polar region during spring of each year. Due to this process, upto 60% of the columnar ozone is depleted over some parts of Antarctic during austral spring. This phenomenon is known as the *Antarctic Ozone Hole*. About 20-25% of the columnar ozone is depleted over some parts of the Arctic region during Northern Hemispheric spring.

1.18 Consequences of stratospheric ozone depletion

Detailed studies regarding the consequences of stratospheric ozone depletion for climate and society can be found in WMO (1998) and Van der Leun et al., (1995). The most obvious consequence of stratospheric ozone depletion is the increase in UV radiation reaching the ground. This is shown in fig. 1.11, where clear-sky measurements performed at six different stations demonstrate that ozone decreases lead to increased UV-B radiation (for ~10% decrease in ozone, ~20% increase in ground level UV-B) at surface.

Ozone plays a crucial role in the heat balance of the atmosphere. By absorbing UV radiation, the ozone heats the stratosphere. On the other hand, by absorbing terrestrial radiation from earth it traps heat in the troposphere. Deviations in ozone concentration affect the heat budget of the atmosphere over a region.

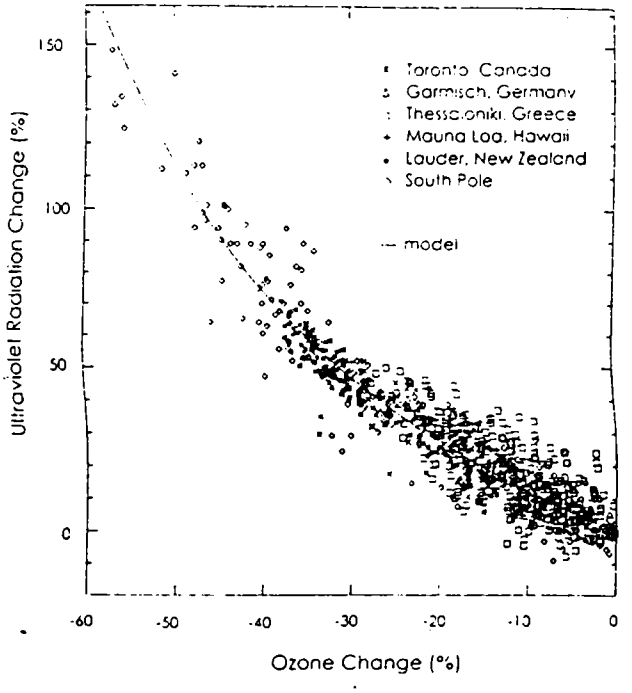

Fig. 1.11 Change (%) in Erythemal UV radiation due to change (%) in ozone.(After WMO, 1998)

1.19 Recovery of ozone layer?

In 1987, the recognition of the potential for chlorine and bromine to destroy stratospheric ozone led to the Montreal Protocol on substances that deplete the ozone layer. Decision was made to limit and then stop the production of CFCs. As a result, the net tropospheric concentration of chlorine and bromine containing compounds started to decrease in 1995 (WMO, 1998). Because of the 3-6 years mixing time required to mix the tropospheric substance to stratosphere, the stratospheric abundance of chlorine started reaching constant level and is expected to decline thereafter.

Chapter –2

Literature Review

2.1 Tropospheric biennial oscillation /Quasi -biennial oscillation

A dominant natural oscillation present in the equatorial lower stratosphere is the QBO in zonal wind. The driving force for the QBO is the vertical transfer of momentum from the troposphere to stratosphere by Kelvin and Rossby-Gravity waves. This oscillation is considered as the instability of the mean zonal flow resulting from equatorial wave-mean flow interaction (Holton and Lindzen, 1972; Plumb and Mc Ewan, 1978). One of the challenging problems is the vertical coupling of the QBO in the middle atmosphere and its influence on the tropospheric weather systems etc. Recently Baldwin et al., (2001) reviewed all aspects of QBO including its possible association with tropospheric weather systems. SPARC has taken initiatives to study the QBO and its possible role in coupling stratosphere and troposphere.

Holton and Tan (1980, 1982) showed that the equatorial QBO is found to influence the high latitude stratospheric circulation features like the amplitude of planetary waves, strength of polar jet stream/polar vortex during winter. They found that the polar night jet is stronger (weaker) than normal during the westerly (easterly) phase of the QBO at 50 hPa. It appears that this relationship is influenced by the 11 year solar cycle also (Labitzke and Van Loon, 1988). Baldwin (2000) reported that the phase and strength of the AO or annular mode especially in the stratosphere, are influenced by QBO. The AO tends to be in its negative phase (weak polar vortex) when the QBO is easterly. He suggested that the high latitude stratosphere – troposphere coupling through AO appears to communicate some effect from the QBO to the earth's surface. Gong et al., (2001) found a significant out-of-phase relationship between the AO and East-Asian winter monsoon. Their study revealed that the AO influences the East Asian

winter monsoon through the impact on the Siberian high. Above the lower stratosphere, QBO is found to influence the descending westerly phase of the semi-annual oscillation in the stratopause region (Dunkerton and Delisi, 1997). The QBO tend to affect the vertically propagating waves and causes a strong QBO while these waves reach the mesopause region.

Mukherjee et al., (1985), Bhalme et al., (1987), Mohanakumar (1996) showed evidences for a link between the Indian monsoon activity and the stratospheric wind. A dominant QBO spectral peak in Indian summer monsoon rainfall and the number of monsoon depressions was also reported (Bhalme and Jadhav, 1984). According to Bhalme et al., (1987), the Indian monsoon rainfall tending to be less (more) than normal during easterly (westerly) phase of the QBO at 10 hPa. He also pointed that large-scale floods never occurred during easterly phase and drought almost never during westerly phase. Gray (1984) identified an association between QBO phase and seasonal incidence of Atlantic tropical cyclones. It is unclear how the Indian monsoon activity or Atlantic cyclone incidence have been affected by the phase of the QBO at 10 hPa or 50 hPa (which propagates downward at a speed of 1km/month) just few months prior to their occurrence.

All these relationships are suggestive and based on statistical relationships. Gray (1992) hypothesized a mechanism where by the QBO of zonal winds alters the distribution of intense deep convective activity throughout the tropical west Pacific. He suggested that in conjunction with the annual cycle and the build up of heat in the Pacific warm pool, the QBO linked variations of deep convection cause variations in the central Pacific trade winds and Walker circulation while in turn govern the occurrence of

ENSO events in the tropical Pacific. Recently, the possibility of a QBO driven monsoon variability was investigated in a number of general circulation model experiments by Giorgetta et al., (1999). These experiments showed that the boreal summer monsoon is significantly influenced by the QBO. They also showed that the QBO influence the austral summer monsoon but the precipitation does not change significantly. QBO seemed to modulate dynamical quantities like temperature, wind, potential vorticity (Baldwin and Dunkerton, 1998; Randell et al., 1997), ozone (Bowman, 1989, Tung and Yang, 1994), and aerosol (Hitchman et al., 1994). QBO influences the properties of the ionosphere also (Chen, 1992).

Several studies have suggested the presence of QBO like biennial oscillation in tropical atmosphere (Angell and Korshover, 1974, 1975; Ebdon, 1975; Terray, 1995; Trenberth, 1975, etc). TBO is seen in the rainfall over India (Mooley and Parthasarathy, 1984), and Indonesia (Yasunari and Suppiah, 1988). It is seen in the sea level pressure, sea surface temperature and air temperature in the Indian Ocean region (Terray, 1995). It is also an important component of the El Nino and Southern Oscillation Phenomena (Rasmusson et al., 1990; Roplewski, et al., 1992) and is an integral part of the Asia-Pacific climate. TBO has irregular periodicities ranging from 2 to 3 years. Compared to the stratospheric QBO, it is irregular in period and longitude.

The cause for the TBO is not clearly known. Several theories and hypotheses have been proposed for the cause, development, evolution, southward movement of active convection zone from Indian region to Australia and its interactions with atmosphere – ocean – monsoon systems

and extratropics. Nicholls (1978) postulated that the seasonally varying interaction between the SST in the west equatorial Pacific – maritime continent, and zonal winds in the overlying atmosphere is the cause for TBO. Meehl (1994, 1997) hypothesized that the TBO is due to the coupled ocean- land interactions in the Indian monsoon, Indian Ocean, west and east Pacific regions. The key role played by the land-atmosphere interaction and tropical-midlatitude interactions are also emphasized in his hypothesis. This hypothesis could explain the southward propagation of the TBO signal from Indian summer monsoon region to Australian region well. Tomita and Yasunari (1996) suggested that the northeast winter monsoon plays an important role in the TBO of the ENSO-monsoon system. According to his hypothesis, the SST anomaly in the South China Sea and the winter monsoon maintain the TBO through the tropical-extratropical interactions. A different concept was proposed by Goswami (1995), which attributes to the TBO as a result of pure internal dynamics (boundary conditions such as SST etc do not have any role in its generation). According to his hypothesis the TBO is arising as a result of the modulation of energetic intraseasonal oscillation by annual cycle. Recently Chang and Li (2000) proposed a theory for TBO, which explains most of the features of the TBO reasonably well. They integrated the ideas of air-sea interaction regulated by annual mean state (Nicholls, 1978, Clarke et al., 1998), those involved in ENSO processes and empherical findings derived from observations or models and developed the theory.

In a rather different explanation, TBO is considered as the result of forcing from the QBO in the lower stratosphere through an unknown stratosphere – troposphere interaction (Khandekar, 1996, 1998). Using zonal wind data form Singapore, Korur and Ponape, Yasunari (1989)

suggested that there exists a coherent phase structure between the lower stratospheric zonal wind QBO and biennial scale zonal wind anomalies in the lower and upper troposphere. He showed that the QBO in the lower stratosphere is also coupled with that in the SST anomalies in the equatorial Pacific. He postulated that the stronger than normal convection over Asian monsoon region through the tropical Pacific from northern summer to winter is related to the downward phase shift of QBO in the lower stratosphere in the same seasons, possibly *via* the stronger than normal Kelvin wave energy.

2.2 Total ozone variability

Ever since the pioneering work of Dobson et al., (1929), the variability of column total ozone levels and its association with meteorological processes such as cut-off cyclones (Wirth, 1995), tropopause folds (Baray et al., 2000), tropical cyclones (Baray et al., 1999; Rodgers et al., 1990; Stout and Rodgers, 1992), equatorial deep convective systems (Suhre et al., 1997), QBO (Bowman, 1989; Tung and Yang, 1994 a; 1994 b; Hamilton, 1995; Holton, 1989; Hollandsworth et al., 1995, Ziemke and Stanford, 1994), western disturbances (Mani et al., 1973), Kelvin waves (Ziemke and Stanford, 1994), Rossby-gravity waves (Stanford and Ziemke, 1993), upper and lower stratospheric planetary waves (Wirth, 1993; Hood and Zaff, 1995; Garcia and Hartmann, 1980; Fusco and Salby, 1999), etc has been a subject of fascinating study.

Wirth (1995) presented a mechanistic axisymmetric Eliassen balanced vortex model for the investigation of the role of diabatic heating in the dynamic evolution of a cut-off cyclone and the related stratosphere –

troposphere exchange. Stout and Rodgers (1992) and Rodgers et al., (1990) showed that the upper tropospheric processes that affect the intensity and motion of tropical cyclone also affect the distribution of ozone in a vertical column. They also pointed that the total ozone distribution is not related to the size of the tropical cyclone but the tropical cyclone's intensity. Baray et al., (1999) analysed a case study of spectacular stratosphere – troposphere exchange directly linked to the strong tropical cyclone *Marlene*, which occurred near Mauritius and Reunion Island on April 1995. With this observation they suggested that the mesoscale tropospheric ozone contaminations, which affect the entire tropical free troposphere, could be due to convective effects.

Data from 'Measurement of Ozone by Airbus In-Service Aircraft' (MOZAIC) project revealed the presence of large ozone peaks (100 to 500 ppbv) associated with tropospheric water vapour mixing ratios (0.4 to 0.6 g kg^{-1}) in the troposphere of the equatorial Atlantic Ocean. These airmasses, rich in ozone and humidity, have been associated with the stratosphere to troposphere quasi-isentropic transport by tropical convection (Suhre et al., 1997).

A number of authors have reported the observational evidence for QBO in total ozone in the tropics and extratropics (Angell and Korshover, 1973; Hamilton, 1989). It is clear from these and other studies that atleast in the tropics the ozone QBO is associated with the well-known QBO in temperature and zonal wind. With a simple one-dimensional model, Holton (1989) showed that horizontal advection by the mean Hadley circulation can account for much of the observed meridional asymmetry of the QBO in total ozone. Bowman (1989) used the nine years of total ozone

measurements from TOMS on Nimbus-7 to study the global structure of QBO in total ozone. He found that the interannual variability of total ozone near the equator (10° N to 10° S) is dominated by the QBO. The equatorial ozone anomalies are independent of season and are well correlated ($r > 0.8$) with the equatorial zonal wind. Tung and Yang (1994 a; 1994 b) clarified the observed picture of how the tropical and extratropical manifestations of the ozone QBO are related. In particular, they found that at very low latitudes the interannual ozone variations very closely follow the variations in the prevailing zonal wind, while poleward of ~10° latitude the ozone anomalies seem to depend on the interaction of the dynamical QBO and the annual cycle. They also explained the presence of two prominent peaks in ozone anomaly spectrum in the extratropics; one (near 30 months) corresponding to the dynamical QBO and one (near 20 months) at the expected beat frequencies between the QBO and annual cycle.

Ziemke and Stanford (1994) investigated the Kelvin wave features in total column ozone using version-6 data from TOMS onboard Nimbus-7. Their results showed eastward propagating zonal waves 1-2 with period ~5-15 days, amplitude ~3-5 DU (1-2% of the time mean), and latitudinal symmetry typical of Kelvin waves. Their analyses and model study suggested that the primary source of the perturbations is slow Kelvin waves in the lower to middle stratosphere. In a study with the same data, Stanford and Ziemke (1993) observed Rossby-gravity waves in total ozone. The observed features are episodic, have zonal wavelengths of ~ 6000 km to 10000 km and oscillate with periods of 5-10 days. The modes exhibit westward phase propagation and eastward group velocity.

With a three-dimensional chemical transport model Hadjinicolaou et al., (1997) showed that the interannual variability in midlatitude ozone can be explained only by meteorological variability in the stratosphere. Their model calculated lowest ozone values during 1993 without the representation of Mt. Pinatubo eruption in the model.

Trend in column ozone between 70° S - 70° N from November 1978 to May 1990 were studied by Niu et al., (1992). They found that trend in the TOMS data are highly seasonal and dependent on location. Near the equator, the estimated monthly trends are not significantly different from zero. In high latitudes, most of the estimated monthly trends are negative. Logan (1994) analysed the vertical distribution of trend since about 1970 and discussed the quality of ozonesonde data and inconsistencies among data records. Stratospheric ozone decreases were found from about 24 km to near the tropopause. Tropospheric ozone showed a mixed trend over different parts of the world with variations with time too. Hood and Zaff (1995) attributed longitude dependence of the total ozone trend in January to the decadal changes in the amplitudes and phases of stationary planetary waves. Steinbrecht et al., (2001) reported that linear regression accounting for the QBO, the 11-year solar cycle, stratospheric volcanic aerosol loading and a long-term trend, accounts for 53% of the interannual ozone variance observed in February at Hohenpeissenberg (48° N, 11° E). When tropospheric circulation patterns are added to the regression, they could get a substantially large fraction (81%) of the observed total ozone variance.

Hood and McCormack (1997) investigated the influence of interannual differences in lower stratospheric dynamics on total ozone trends. Chakrabarty et al., (1998) examined the total ozone trends over

Indian subcontinent using Dobson spectrometer data. They computed trend for six Dobson spectrometer stations and compared with TOMS total ozone data. An increasing trend of this species over the years has been noted at all places except at Varanasi. This increase was attributed, partly to the trend of ozone in the troposphere.

Trends in the vertical distribution of ozone are assessed under SPARC project (SPARC, 1998). Recently Staehelin et al., (2001) presented an extensive review of ozone trends. Solomon (1999) reviewed all aspects of Polar ozone depletion processes in a very detailed way. A number of key problems in atmospheric chemistry are shaped by the strength and character of the various mechanisms acting to move and mix air in the upper troposphere also. Mahlman (1997) examined the transport process from a mechanistic perspective, with primary emphasis on the tropopause and middle-troposphere regions in the extratropics.

Chapter –3

Data and Methodology

3.1. General

Monthly mean radiosonde data over Thumba, Trivandrum, daily and monthly reanalysis data sets from National Centers for Environmental Prediction / National Center for Atmospheric Research (NCEP/NCAR), total ozone measured by TOMS instrument onboard Nimbus-7, Indian summer monsoon rainfall data (Parthasarathy et al., 1994), details of break periods in Indian summer monsoon activity from De et al., (1998) are mainly used in the thesis.

3.2 High-resolution radiosonde data over Thumba, Trivandrum

An Indian radiosonde system working on 1680 MHZ, measuring temperature and wind more or less regularly on weekly basis at Thumba is used in this work. An erstwhile USSR made radiosonde system working on 1780 MHZ is also employed. The course of hydrogen filled balloon release with radiosonde system and corner reflector is tracked by radar and telemetry system and the meteorological parameters, azimuth, elevation and range at 1 minute interval are recorded at the ground.

The accuracy of the wind measurement is 1 ms^{-1} and probable mean square error of temperature is less than 0.4° C, from 40° C to -90° C. The monthly values in the altitude range 0-30 km for a period of 23 years, extending from January 1970 to December 1992, constituted the basis data for this work. The numbers of observations above 30 km being less, data above 30 km were not used for the analysis. The weekly values of wind and temperature

were averaged over a period of each month to obtain the monthly mean values at every 1 km altitude intervals.

3.3 NCEP/NCAR reanalysis data

In chapters 5 and 6, 40-year (1957-96) global NCEP/NCAR reanalysis data set is used to study the circulation of the atmosphere. Reanalysis contrast the 'traditional' data sets in two fundamental ways: (1) an atmospheric general circulation model (AGCM) is an integral component of the analysis system and (2) a wide range of observations are used. Thus, reanalysis not only provides potentially very useful dynamical quantities that cannot be determined by subjective analysis, but may be more accurate than such traditional analyses, particularly in data sparse regions. However, the differences in the AGCMs and the analysis methods will lead to differences in reanalysis. Several inter comparison studies have been made to understand the magnitude and nature of this uncertainty in NCEP/NCAR reanalysis.

The NCEP assimilation system used observations from the COADS surface marine dataset, the rawinsonde network, satellite soundings (the Tiros Operational Vertical Sounder, TOVS data), aircraft data, and satellite (GMS, GOES, and METEOSAT) cloud drift winds. These data were subject to stringent quality control (Kalnay et al., 1996). To interpolate the data into model grid, a spectral statistical interpolation (SSI) was used; this is a three dimensional variational technique. A T62 global spectral model, corresponding to approximate grid point spacing of 208 km was used in NCEP reanalysis. This model used σ-levels as vertical co-ordinate.

The reanalyzed gridded fields have been classified into four classes, depending upon the relative influence of the observational data and the model on the gridded variable (Table 3.1).

Reanalysis outputs are available in 17 standard pressure levels (hPa), 11 isentropic surfaces (K) and 28 sigma levels. The horizontal resolution is 2.5° longitude × 2.5° latitude.

Class	Relative Influence of Observational Data and Model on Reanalysis Variable
A	Strongly influenced by observational data *(most reliable)* *[e.g. upper air temperature and wind]*
B	Model has very strong influence than observational data *[e.g. humidity and surface temperature]*
C	Derived solely from model fields forced by data assimilation to remain close to the atmosphere. *[e.g. clouds, precipitation, and surface fluxes]*
D	Obtained from climatological values and does not depend on model *[e.g. plant resistance, land-sea mask]*

Table 3.1. Classification of NCEP/NCAR reanalyzed fields.

Standard pressure levels (hPa) are 1000, 925, 850, 700, 600, 500, 400, 300, 250, 200, 150, 100, 70, 50, 30, 20, and 10.

Isentropic surfaces (K) are 650, 550, 450, 400, 350, 330, 315, 300, 290, 280 and 270.

Sigma levels are 0.9950, 0.9821, 0.9644, 0.9425, 0.9159, 0.8838, 0.8458, 0.8014, 0.7508, 0.6943, 0.6329, 0.5681, 0.5017, 0.4357, 0.3720, 0.3125, 0.2582, 0.2101, 0.1682, 0.1326, 0.1028, 0.0782, 0.0580, 0.0418, 0.0288, 0.0183, 0.0101, and 0.0027.

NCEP/NCAR reanalysis data have good vertical coverage in the stratosphere also. There are 7 pressure levels and 4 isentropic surfaces present above the tropical tropopause. NCEP/NCAR data set has been validated with observational data sets. In a series of studies (Pawson and Fiorino, 1998a; 1998b; 1999) validated the tropical stratosphere (thermal structure, annual cycle, QBO etc) in NCEP data. They found good agreement between observed values and reanalysis values. At the uppermost level (10 hPa), the reanalysis system found to perform poor due to the proximity of the upper boundary.

3.4 All India summer monsoon rainfall series

Several Indian summer monsoon rainfall series have been prepared with the number of rainguages varying from 300 to 3000 spread all over India for the different lengths of period starting from the year 1841 onwards. But the most systematic rainfall series was prepared by Parthasarathy et al., (1994)

based on fixed network of rainguages. This series is available for the period 1871 to 1993, based on 306 well-distributed rainguage stations over India, one from each of the districts in the plain region (29 subdivisions) of India. The monthly rainfall data at these 306 stations were taken from the records of the India Meteorological Department. Proper weightage for each rainguage station assigning the district area as the weight was given while preparing the rainfall series. The all India summer monsoon rainfall series is presented in fig 3.1.The mean all Indian summer monsoon rainfall (June to September) is 852.4 mm with a standard deviation of 84.69 mm.

3.5 Breaks in Indian summer monsoon activity

Indian summer monsoon activity is characterized by active and break cycles. The India Meteorological Department defines a 'break in the monsoon' as a general cessation of precipitation over most of India with exception of the very south of Peninsular India and the foothills of Himalayas. This rainfall pattern is accompanied by a rise in surface pressure of 2-3 hPa over central India as the monsoon trough moves northward. Enhancements of rainfall and monsoon flow in between the breaks are called as 'active period in the monsoon'. De et al., (1998) identified the break periods during the 30-years (1968-97).

Magana and Webster (1996) argued that the break and active periods in monsoon flow are on a scale much larger than India or even south Asia. They suggested a criterion (see table 3.2) to define active and break periods during

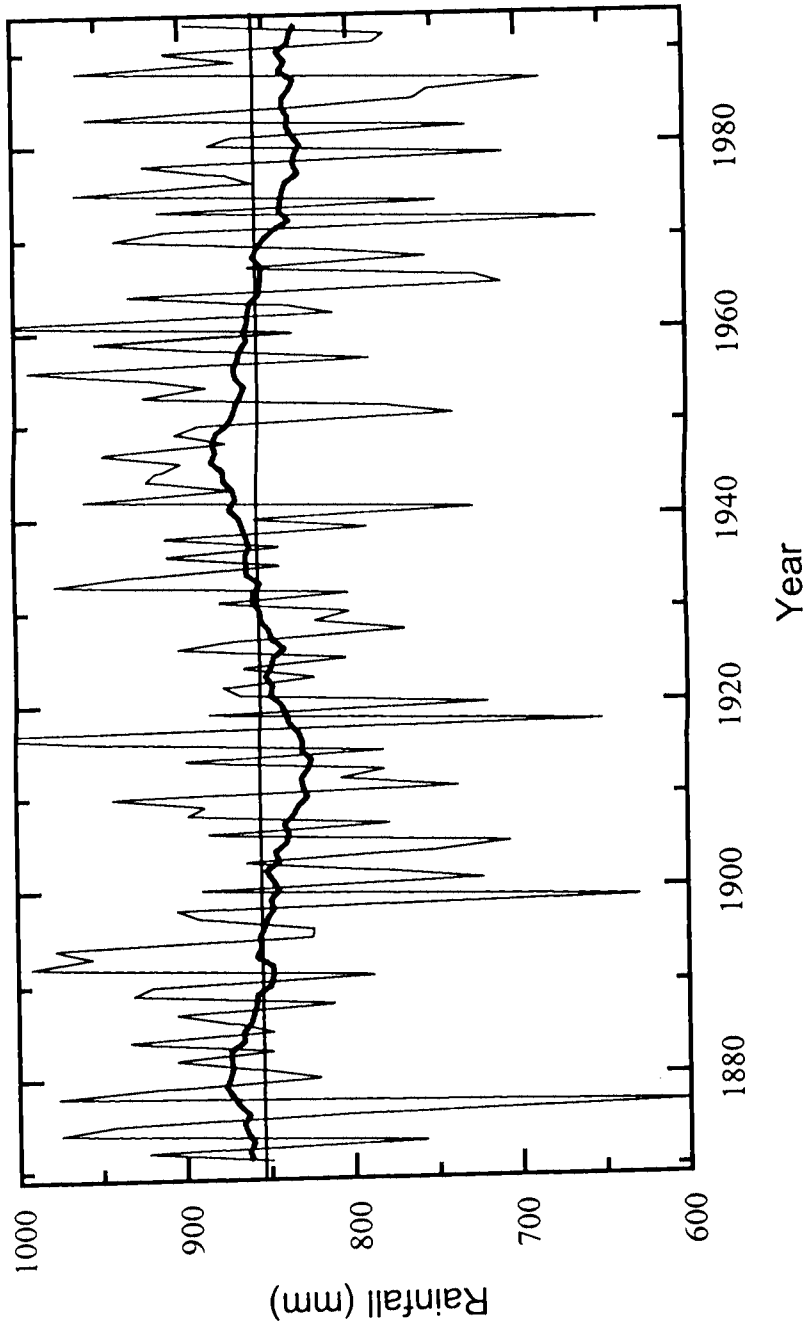

Fig. 3.1 All India summer monsoon rainfall in mm. Thick line is the 31 year adjacent average.(Data from Parthasarathy et al, 1994)

the boreal summer Asian-Australian monsoon and the active/break periods during 1980-93 was tabulated by Webster et al., (1998).

Condition	**Active** (Anomaly)	**Break** (Anomaly)
850 hPa meridional wind at (45° E, 0° N), ms^{-1}	>3	>-3
850 hPa zonal wind at (65°- 95° E, 10°- 20° N), ms^{-1}	>3	>-3
Outgoing longwave radiation at (65°- 95° E, 10°- 20° N), W m^{-2}	<10	>10

Table 3.2 Criteria used to define active and break periods of boreal summer monsoon (After Magana and Webster, 1996)

3.6 Global total ozone data

The TOMS instrument onboard Nimbus-7 provided the global coverage of total ozone on daily basis. The Nimbus 7 spacecraft was in a south-to-north, sun-synchronous polar orbit so that it was always close to local noon/midnight below the spacecraft. Thus, ozone measurements were taken for the entire world every 24 hours. TOMS directly measures the backscattered ultraviolet sunlight from the earth's atmosphere. Total ozone is derived from the differential absorption of scattered sunlight in the ultraviolet region. Ozone is

calculated by taking the ratio of two wavelengths (312 nm and 331 nm, for example), where one wavelength is strongly absorbed by ozone while the other is absorbed only weakly. The instrument has a 50 km square field of view at the sub-satellite point. TOMS collects 35 measurements every 8 seconds as it scans right to left producing approximately 200,000 ozone measurements daily. These individual measurements vary typically between 100 and 650 Dobson Units (DU) and average about 300 DU. This is equivalent to a 3 mm thick layer of pure ozone gas at STP conditions.

Although the total ozone data obtained from TOMS instrument are available from Nimbus-7, Meteor-3 and Earth Probe satellites, the data obtained from TOMS onboard Nimbus-7 are used in this study. This data set is continuous, regular and available for a relatively long period (14.5 years, 31 October 1978 – 6 May 1993).

The TOMS data [version-7] (Mc Peters et al., 1996) are available as (a) gridded daily, (b) gridded monthly average, (c) GIF image, (d) overpass data and (e) zonal means. These data are available in the form of CD-ROMS. Also TOMS data is available in Goddard Space Flight Laboratory's (USA) website *(http://toms.gsfc.nasa.gov)*. TOMS (Nimbus-7) data are available for the period 31 October 1978 – 6 May 1993 (~14.5 years).

(a) Gridded daily

Daily TOMS measurements have been arranged in to 1.25° lon × 1.0° lat grids from 90° S to 90° N and 180° W to 180° E longitude. Thus the

gridded dataset has 180x288 ASCII data arrays. Each total ozone value is in 3-digit integer format. Also local equatorial crossing time is also provided in the data set.

(b) Gridded monthly avergae

The gridded monthly average data also have the same format as gridded daily data. Average over a cell is made only when good quality data was available for the cell at least for 20 days.

(c) GIF image

Each day of data has a corresponding GIF image with 640×480 pixels (full screen in standard VGA) at 256 colours. Images are available in polar (south and north) and Aitoff projections.

(d) Overpass data

Best matching single observation for 371-ground locations worldwide is provided in this data.

(e) Zonal means

Daily and monthly zonal averages in 5° latitude zones are provided in this data.

3.6.1 Comparison of TOMS data with ground-based total ozone measurements

The TOMS version-7 data have been compared with ground based measurements made by a network composed of 30 mid-northern latitude stations with Dobson and Brewer ozone measuring instruments. Only stations had homogeneous data coverage for the entire 14.5 year lifetime of TOMS instrument were included for comparison study. A weekly mean was computed from the daily TOMS-ground differences at each station. These differences from the 30 stations were then averaged to derive a weekly average TOMS-ground difference. In fig. 3.2, the percentage difference between TOMS and ground based ozone measurements as a function of time is presented (from Mc Peters et al., 1996). The difference is smaller than the combined uncertainty of the TOMS and ground based measurements and of the comparison technique, as is the overall trend of 0.2 percent/decade. Thus the two methods of total ozone measurements agree to within the uncertainties.

3.6.2 Problems with the TOMS version-7 data

Volcanic eruptions, solar eclipses, polar stratospheric clouds, high terrain, etc affect the total ozone measured by TOMS instrument. Problems were noticed after the eruptions of El Chichon in April 1982 and Mt. Pinatubo on June 15, 1991. Gaseous SO_2 erupted from these major eruptions absorbed the bands in 290 nm to 320 nm range. Some bands at longer wavelengths coincide with wavelengths used by TOMS to measure total ozone. This produced a false enhancement of total ozone measured by TOMS. This

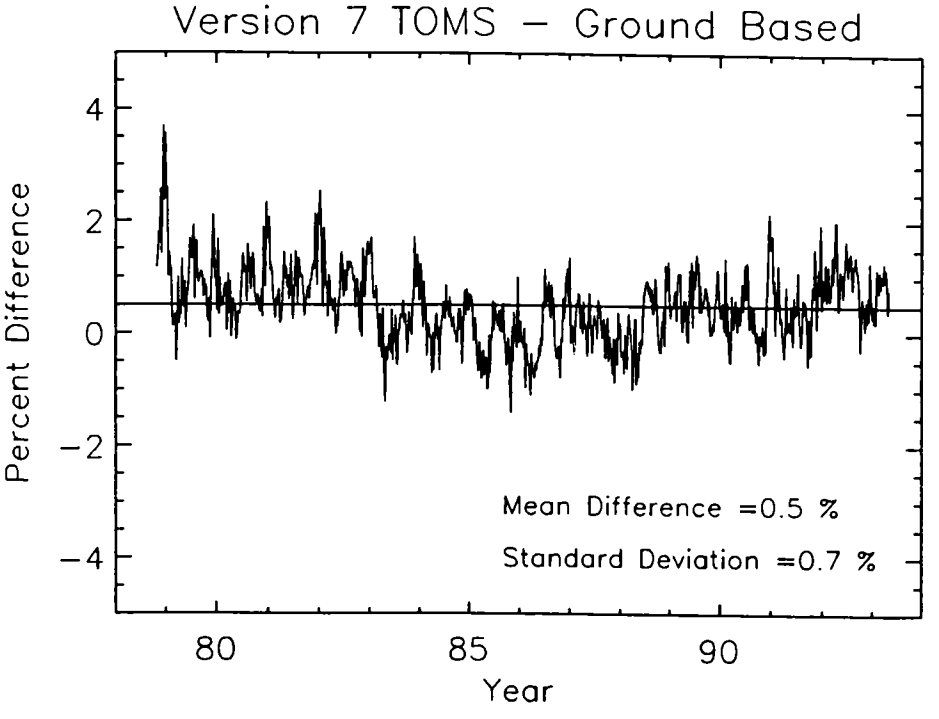

Fig. 3.2 Percentage difference between TOMS and ground ozone. Solid line is linear fit trend. (After McPeters et al, 1996).

problem is short-lived because the SO_2 is converted rapidly to sulfuric acid aerosols. The contaminated data points were marked with a flags for identification.

TOMS measures backscattered sunlight for total ozone estimation. It is not possible to measure ozone when there is no sun. Because of this reason, total ozone data are missing for polar winter season. Another feature observed in TOMS measurements were the low ozone values present over high mountain regions. Because of high terrain, the column of ozone is lower over these regions. This is not an error. TOMS measurements suffered another problem due to the solar eclipses. The decrease in incoming solar radiation leads to a decrease in backscattered radiance. So ozone values were not retrieved for periods of time and ranges of latitude where the radiances are affected by a solar eclipse.

3.7 Wavelet analysis

Wavelet transform is an analysis tool well suited to study multi-scale, non-stationary processes occurring over finite spatial and temporal domain. Since its introduction by Morlet (1983) over a decade ago, this technique has found wide application in diverse fields. The wavelet transforms can be used to analyze time series that contain non-stationary power at many different frequencies. Wavelet analysis gives the localized variations of power within a time scale, by decomposing a time series in time- frequency space and one is able to determine both the dominant modes of variability and how those mode vary in time.

3.7.1 Wavelet transforms

The Wavelet Transform (WT) is a generalized form of Fourier Transform (FT) and a Windowed Fourier Transform (WFT), (Gabor, 1946). The FT uses sine and cosine functions that have infinite span and are globally uniform in time. The FT does not contain any time dependence of the signal and therefore cannot provide any local information regarding the time evolution of its spectral characteristics. In WFT, a time series is examined under a fixed time-frequency window with constant intervals in the time and frequency domains, and hence over-represents high-frequency components and under-represents low-frequency components.

A WT uses generalized local base functions (wavelets) that can be stretched and translated with a flexible resolution in both frequency and time. The flexible windows are adaptive to the entire time-frequency domain, known as the wavelet domain (WD), which narrows while focusing on high-frequency signals and widens while searching the low-frequency background. As a result, high precision in time localization in the high-frequency band can be achieved at the reduced frequency resolution, and vice-versa for low frequency components. A wavelet transform allows the wavelets to be scaled to match most of the high-and low-frequency signals so as to achieve the optimal resolution with the least number of base functions. This Zoom-in property is very unique of the WT that allows the localization of very short-lived, high frequency signals in time, such as abrupt changes, while resolving the low-frequency variability in the time scale or frequency more accurately with relative ease in computation.

Mathematically, a WT decomposes signal s(t) in terms of some elementary functions $\psi_{b,a}(t)$ derived from a Mother Wavelet or analyzing wavelet $\psi(t)$ by dilation and translation:

$$\psi_{b,a}(t) = 1/(a)^{1/2} \quad \psi(t-b/a) \qquad ...(3.1)$$

where b denotes the position (translation) and a(>0) the scale (dilation) of the wavelet, $\psi_{b,a}(t)$ are called daughter wavelets or simply wavelets. An energy normalization factor $(a)^{-1/2}$ keeps the energy of the daughter wavelets the same as the energy of the mother wavelet.

3.7.2 Graphical representation

The choice of octave which is logarithmic with the base of 2 for the frequency or time scale, as a unit to divide the frequency domain allows us to include a broad range of scales, from very small to very large, in an efficient way in a coordinate system with linear interval in octave while logarithmic in frequency scale. In a continuous WT where more scale decomposition is desired, each octave may be divided further by infinite voices. Thus unlike the FT that maps a 1-D time series to a 1-D spectrum, the WT maps a 1-D time series to a 2-D image that portrays the evolution of scales and frequencies with time.

3.7.3 Wavelet choice

There are many commonly used analyzing wavelets that can be grouped into two main categories; continuous wavelets and orthogonal wavelets (a discrete wavelet transform may not be orthogonal.) One of the most widely wavelets in geophysics is the complex Morlet Wavelet, which consists of a plane wave modified by a Guassian envelope. Another commonly used continuous wavelet is the Mexican Hat, which is the second derivative of the Guassian Function. The simplest orthogonal wavelet is the Harr wavelet, which is based on a Box function. In our analysis we have used the Morlet Wavelet whose function.

Chapter –4

Stratosphere – Troposphere Interactions in Biennial Timescale

4.1 Introduction

Inferences obtained by Yasunari (1989) about the possible link between the QBO in the stratosphere and the biennial oscillation in troposphere (mentioned in Chapter-1) is based on the results obtained from the analysis of zonal wind and SST over a few stations (Singapore and a few stations in equatorial Pacific). It is interesting to know whether this kind of phase coherence is present between TBO and QBO over Indian monsoon region (Indian summer monsoon activity has a strong biennial component). It is interesting to check the vertical phase structure of the biennial oscillations in the troposphere and stratosphere over the near-equatorial Indian station, Thumba (8°23' N, 76°52' E) which has relatively long (22 years) and continuous record of high resolution (vertical) radiosonde measured temperature and wind data. Thumba, which is located in the southern end of the Indian peninsula and far away from Singapore, is under the influence of both southwest and northeast monsoons and tropical lower stratospheric QBO. So it is an ideal place to verify the phase coherence between the biennial oscillations of stratosphere and troposphere.

4.2 Data and methodology

Radiosonde measured monthly mean temperature and zonal wind data at 1 km interval for the altitude range 1-27 km during September 1971 to December 1992 over Thumba (Trivandrum) constitute the basic data for the study in this chapter. Beyond this period, the radiosonde data are not available in this station. Temperature anomalies of each month from the 256 month mean were computed for each level. Data of Indian Summer Monsoon Rainfall (ISMR) has been taken from Parthasarathy et al., (1994).

To analyse the multi-timescale oscillations present in zonal wind and temperature anomaly, Morelet wavelet transform is used. It is an useful tool to analyse the time series that contain non-stationary power at many different frequencies (Daubechies, 1990). Wavelet tranform transforms an one dimensional time series into two dimensional frequency-time domain. So it is possible to know the frequency content of the signal at every time-step. Wavelet transform uses generalized wave functions called wavelets that can be stretched and translated both in time and frequency.

Wavelet decomposes a signal s(t) in terms of some elementary function $\psi_{b,a}$ (t) derived from a analyzing wavelet or mother wavelet ψ(t) (Weng and Lau, 1994). The wavelet transform of a real signal s(t) with respect to the analyzing wavelet ψ(t) may be defined as

$$W(b,a) = (1/\sqrt{a}) \int \psi^{*} (t-b/a)\, s(t)\, dt \qquad \ldots(4.1)$$

ψ^{*} is the complex conjucate of
b is the position (translation)
a(>0) is scale (dilation)

The analyzing wavelet ψ(t) for Morelet wavelet transform is $\psi(t) = e^{ik\psi^{t}}\ e^{-|\,t.t\,|\,/\,2}$, which is a plane wave modulated by a Gaussian. Complex Morelet wavelet transform was applied to zonal wind and temperature at each level. This transform provides information of signal on both amplitude and phase. Length of the data is kept as 256 (2^{8}) in order to avoid edge effects caused by data padding and voices per octave are set as 4. Zero octave was fixed as 8 months. Detailed mathematical treatment of the

the wavelet transform is available elsewhere (Lau and Weng, 1995; Torrence et al., 1998).

4. 3 Results and discussion

In figs. 4.1 and 4.2, the time series' of zonal wind and temperature anomaly at two levels, 11 and 21 km representing middle troposphere and lower stratosphere are presented. The real part of the Morelet wavelet transforms for these zonal wind and temperature anomaly time series' are presented in figs. 4.3 and 4.4 respectively. In these figures, y-axes are frequency given in octave. Here 0, 1, 2, 3 octaves corresponds to the periods of 8, 16, 32, 128 months respectively. In zonal wind, annual mode is the only oscillation in the troposphere and both annual and biennial modes are strong in the lower stratosphere. In temperature anomaly, 11-year solar cycle, biennial, annual and semi annual oscillations are seen in both lower stratosphere and troposphere. This clearly shows the presence of biennial oscillations both in lower stratosphere and troposphere in temperature and only in lower stratosphere in zonal wind.

4.3.1 Constant phase of temperature TBO with height

Wavelet analysis shows prominent TBO with periods ranging from 20-32 months in temperature anomaly at almost all levels of troposphere over Thumba. Time series of real part of the temperature anomaly mean wavelet coefficients corresponding to the biennial mode (20-32 months) for the troposphere and lower stratosphere with 2 km uniform interval is presented in fig. 4.5. This is similar to filtering the biennial mode and removing other modes using standard filtering techniques. The time-height

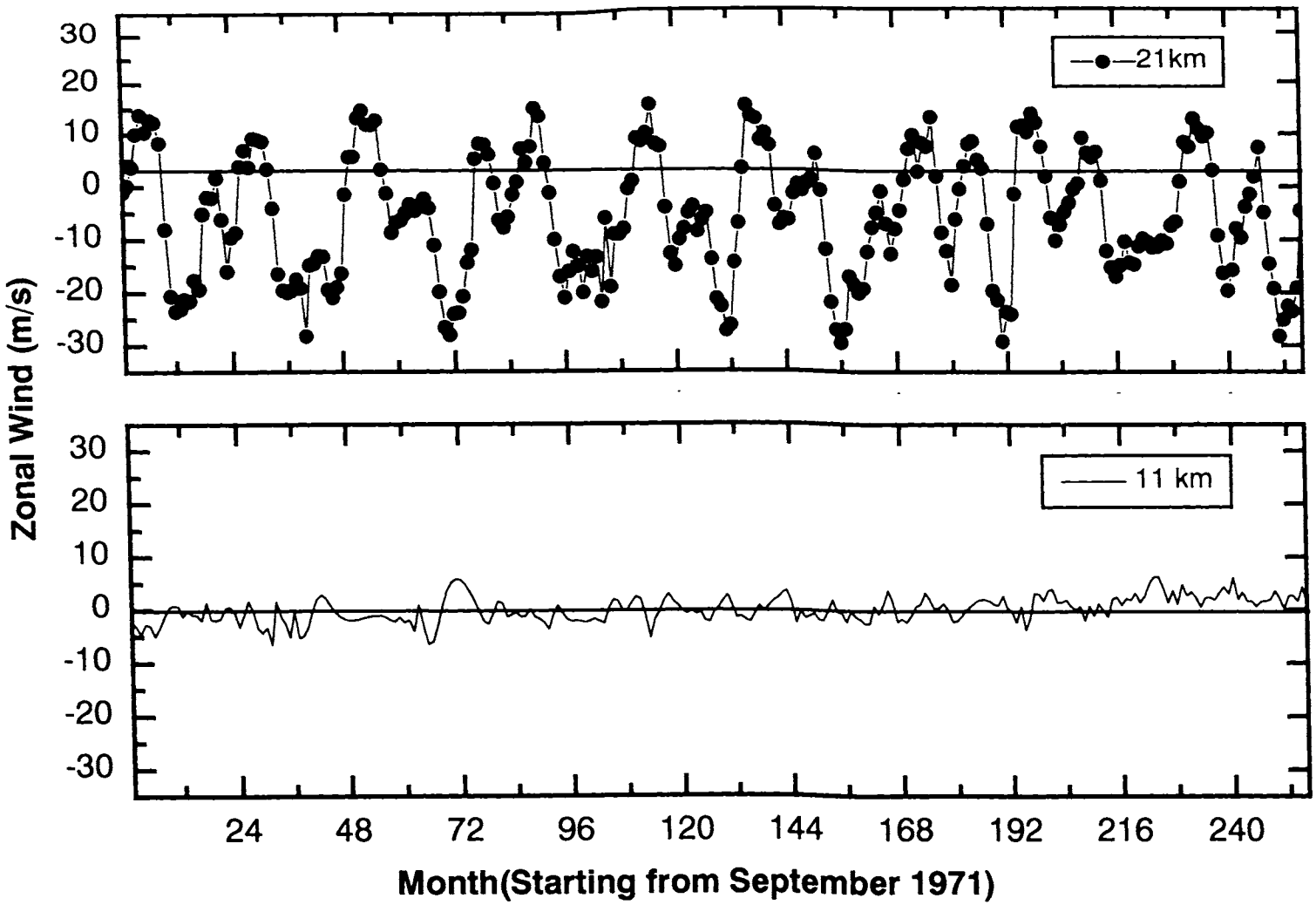

Fig. 4.1 Time series' of zonal wind (ms^{-1}) at 11km and 21 km altitude over Thumba.

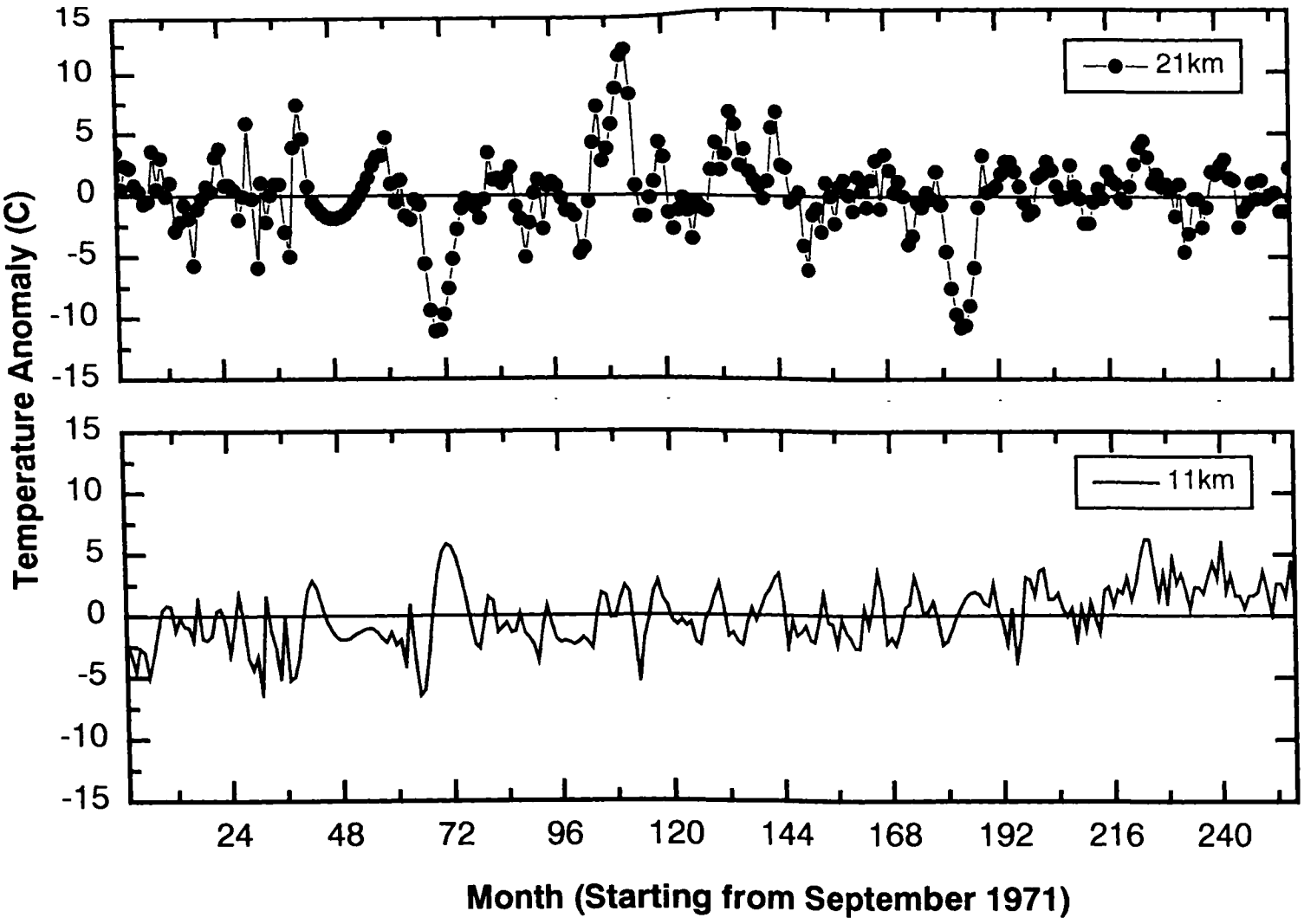

Fig. 4.2 Time series' of temperature (C) at 11km and 21 km altitude over Thumba.

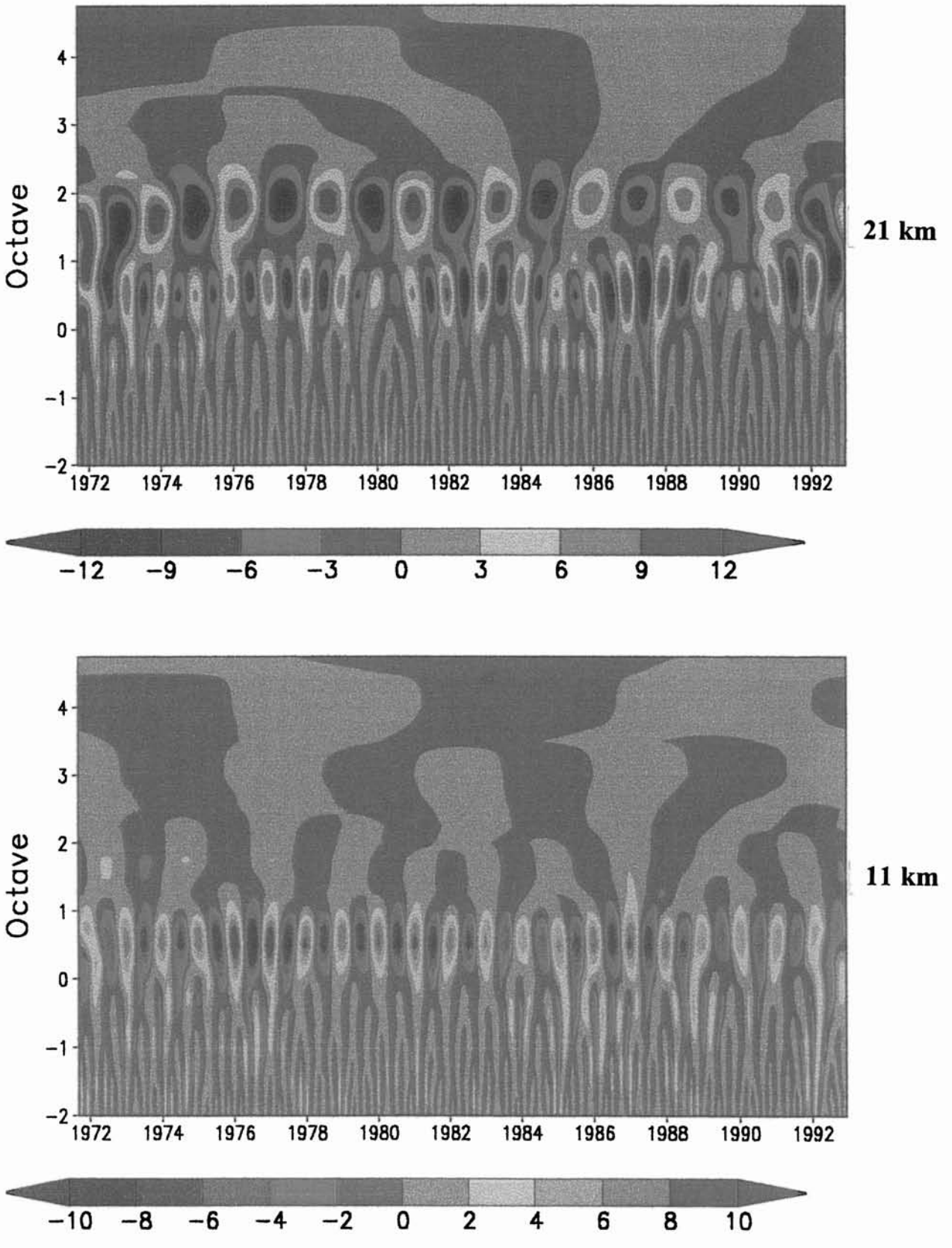

Fig. 4.3 Real part of the Morelet wavelet transform for zonal wind at 11km and 21km over Thumba.

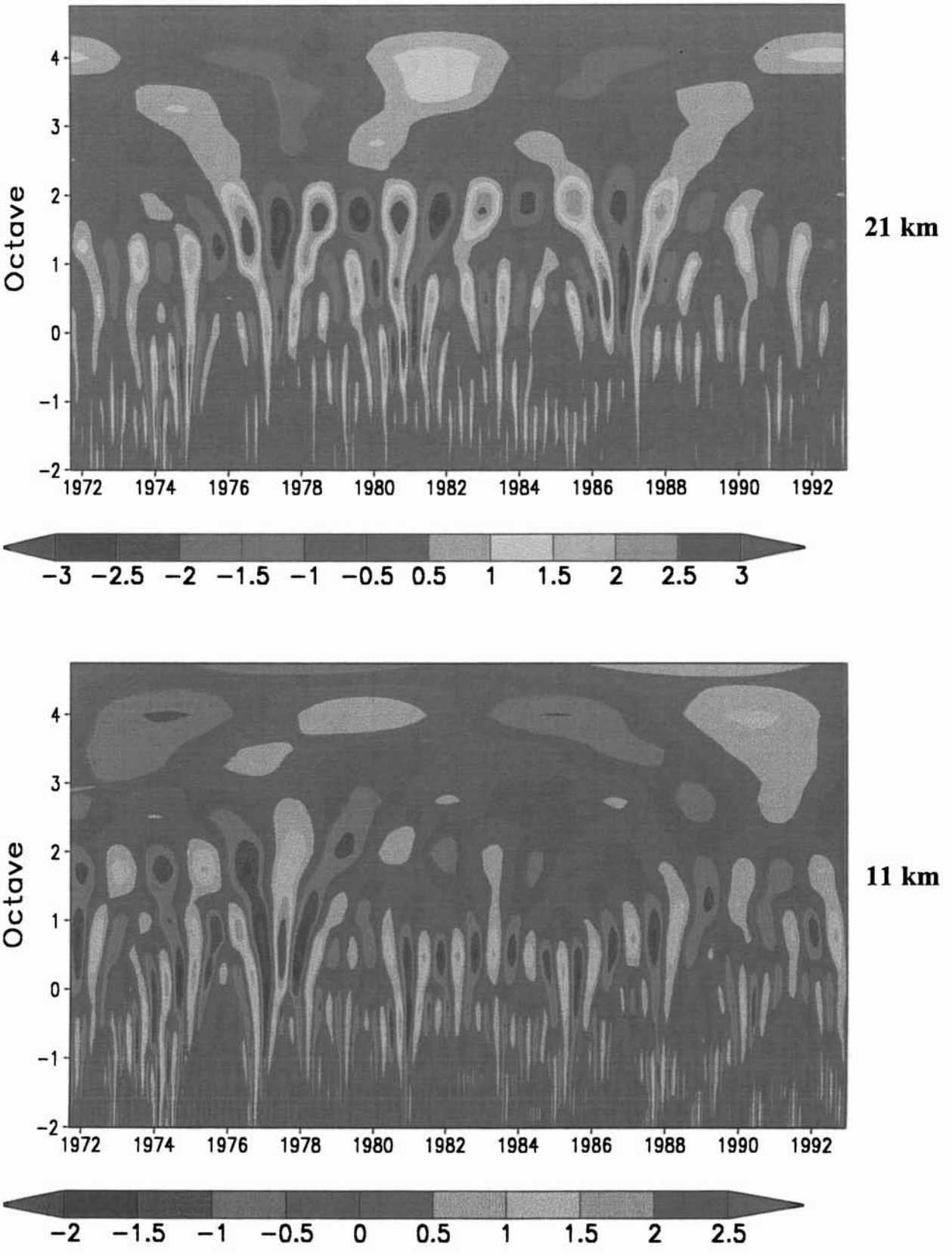

Fig. 4.4 Real part of the Morelet wavelet transform for temperature at 11km and 21km over Thumba.

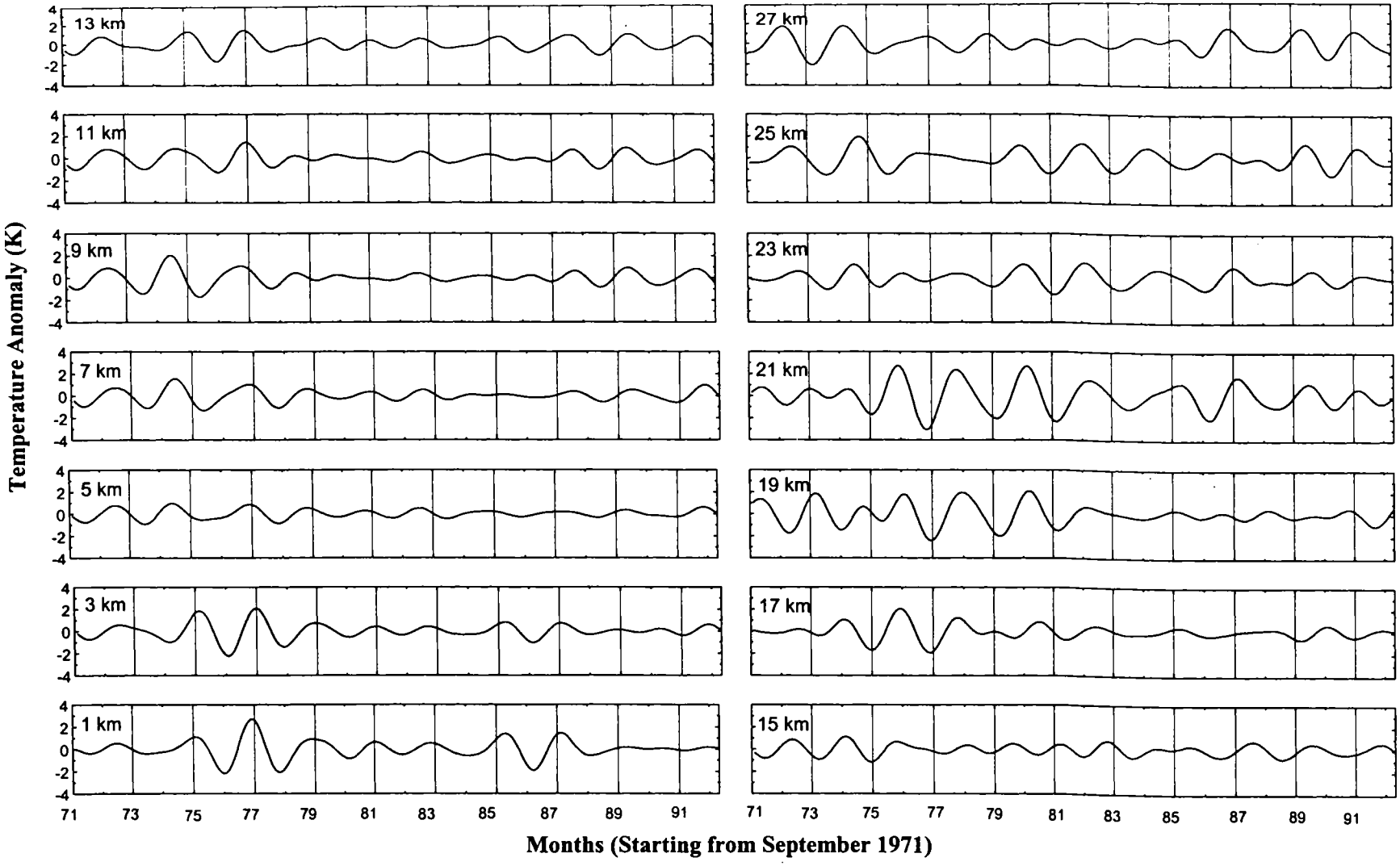

Fig. 4.5 Time series of real part of Morelet wavelet coefficients of temperature anomaly (K) corresponding to biennial mode over Thumba.

plot of the real part of the mean wavelet coefficients of temperature anomaly corresponding to the biennial mode is presented in fig. 4.6. Real part of the wavelet coefficients provides information about both the phase and intensity of a signal at a given time and scale relative to other times and scales (Weng and Lau, 1994). Amplitude of TBO varies with time and height. TBO is found to be strong during 1971-81 in the troposphere, whereas it is relatively weak during 1982-92. It is clear from figs. 4.5 and 4.6 that the phase of TBO in temperature anomaly from surface to tropopause is nearly constant throughout the study period.

4.3.2 Link between QBO and TBO in temperature

Wavelet analysis of temperature anomaly shows QBO in lower stratosphere. Phases of QBO propagate downward with time in the 27-24 km altitudes during 1971-81. Downward phase propagation is disturbed and becomes of constant phase with height at 23-18 km altitudes during the same period. Downward phase propagation of QBO is weak or absent during 1982-92. Phases of QBO and TBO meet at tropopause level or just above 15 km altitude. Where they meet, phases of QBO and TBO are unsynchronized during 1971-81. On the other hand, during 1982-92, phases of QBO and TBO are synchronized there and none of the unusual phenomena of 1971-81 period is manifested.

To get a quantitative idea about the link between QBO and TBO in temperature, the real part of the mean wavelet coefficients of the biennial mode at all levels have been grouped into first (September 1971-December 1981) and second (January 1982-December 1992) decades. Since the QBO signal is prominent at 22 km altitude, QBO at this level is taken as reference

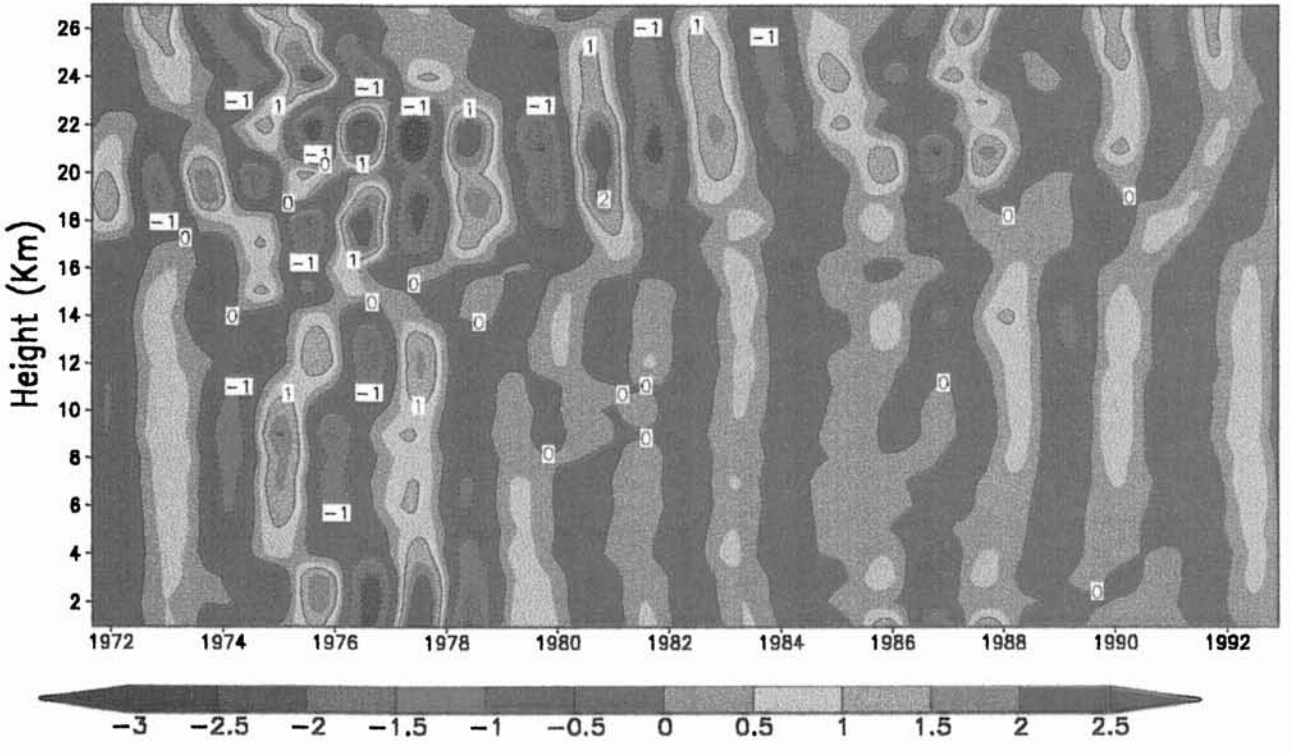

Fig. 4.6 Time-height plot of the wavelet filtered temperature anomaly (K) corresponding to biennial mode. Contour interval is 1K.

QBO and correlation coefficients have been worked out between the real part of the 22 km biennial mode mean wavelet coefficients and those of other levels (1-27 km) for the entire study period and also for the first and second decades separately. The correlation coefficient values are presented in fig. 4.7.

Correlation coefficients of first and second decades show marked differences. In the first decade, correlation coefficient is positive in the 23-15 km levels and negative above 23 km and below 15 km levels. Opposite signs of correlation in 23-15 km and below 15 km levels clearly show that QBO and TBO phases are unsynchronized during the first decade. Opposite signs between 27-24 km and 23-15 km altitudes show the sudden disturbances in the downward propagating phase of QBO at 23-15 km altitudes. In upper and lower troposphere, magnitudes of correlation are high and it is lowest at 9 km. In the second decade, correlation coefficients are positive at all the levels except tropopause. This shows the existence of phase synchronization between TBO and QBO during this period. For the entire period the correlation show a similar pattern as that of the first decade.

4.3.3 QBO/TBO in zonal wind

Wavelet analysis is applied to zonal wind of Thumba for the same 256 month period as that of temperature to study the characteristics of QBO/TBO in it and compare them with those of temperature. In lower stratosphere, clear and regular QBO signal is seen in zonal wind (fig. 4.8). Phase of the zonal wind QBO propagates downward with uniform phase speed of about one km/month without any disturbance at any level. No

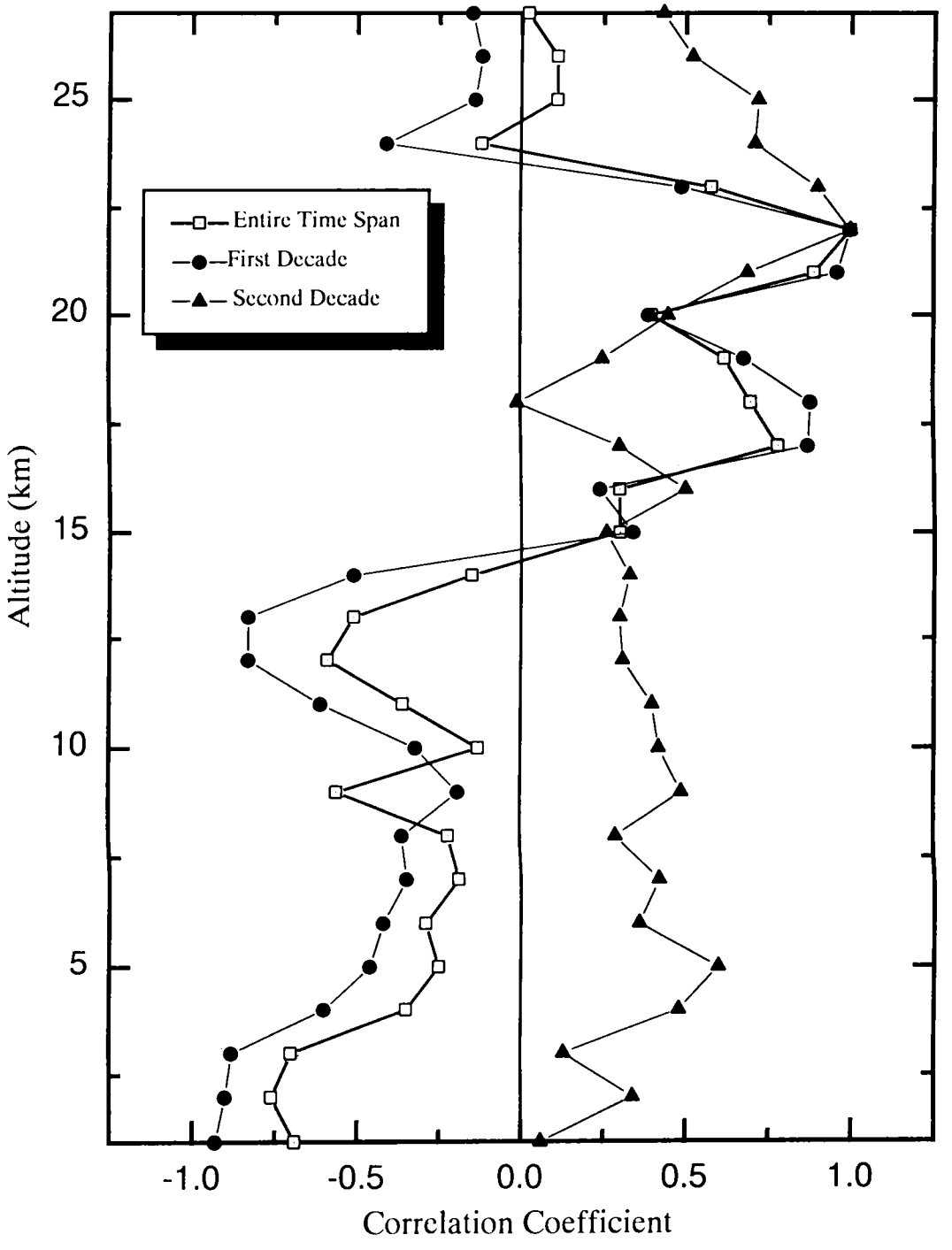

Fig. 4.7 Correlation coefficients between mean real part of the biennial mode wavelet coefficients at 22 km and that of all other levels for the entire period, first and second decades.

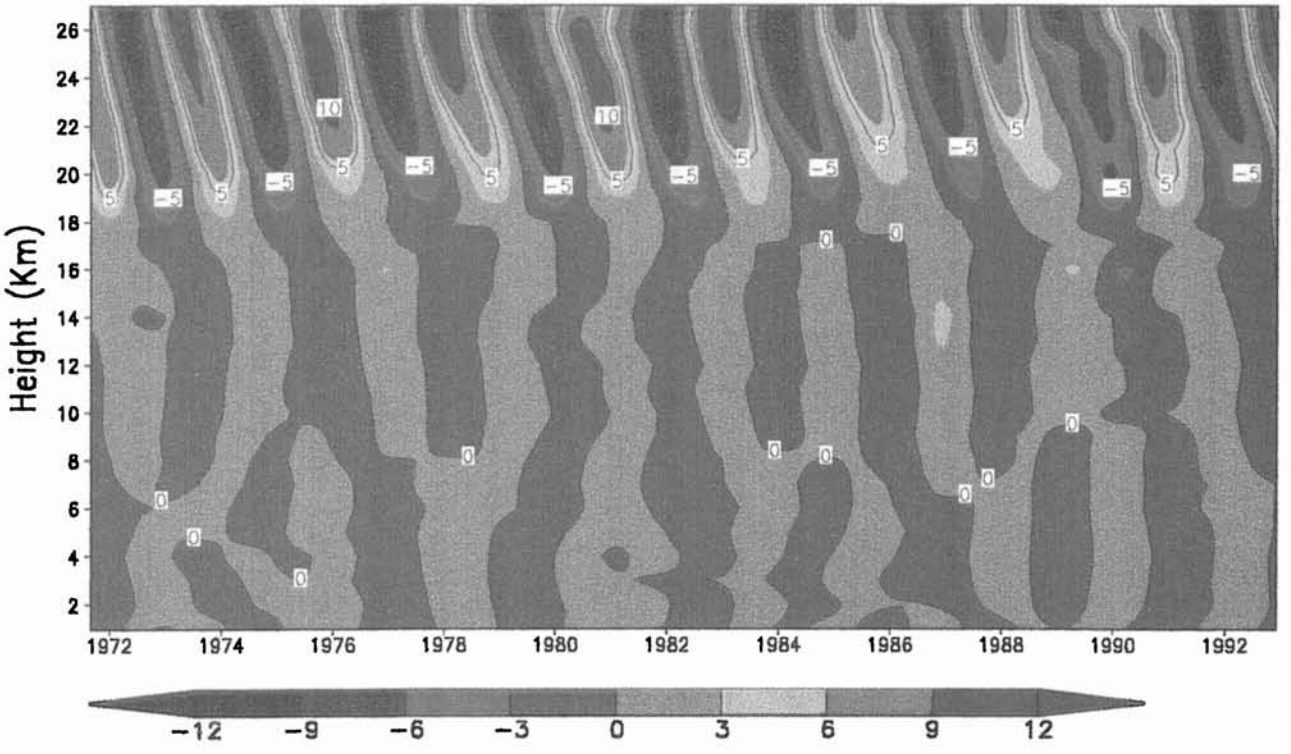

Fig. 4.8 Time-height plot of the wavelet filtered zonal wind speed (ms^{-1}) corresponding to biennial mode. Contour interval is 5 ms^{-1}.

significant variation is noticed in the maximum easterly and westerly amplitudes. Zonal wind QBO does not show marked difference between the two decades unlike in temperature.

Zonal wind hardly shows any TBO signal in the troposphere throughout the study period. As explained by Yasunari (1989), weaker TBO signal over Thumba in zonal wind is due to the location of Thumba near a node or small amplitude area of the wave no 1 or 2 structure of TBO mode around the globe.

4.3.4 Link between monsoon activity and phase of QBO/TBO in temperature and zonal wind

Thumba, located in the southern most part of the Indian peninsula is under strong influence of the Asian summer monsoon circulation. Our analysis shows a significant TBO signal in tropospheric temperature and prominent QBO signal in stratospheric temperature as well as zonal wind over Thumba. Recent studies reveal the existence of biennial time scale variability in Indian summer monsoon activity. According to Meehl (1987, 1997), Indian summer monsoon activity is strongly modulated by biennial time scale variability caused by atmosphere-ocean coupled processes occurring in the Indian and Pacific oceans. Convective activity is strong (weak) over the Indian Ocean area (represented by Thumba data) during strong (weak) Indian monsoons. Kanamitsu and Krishnamurti (1978) pointed out a major shift in the circulation patterns from their normal position over Indian to southeastward during a drought year.

Table 4.1 gives data regarding ISMR for 1972-92. Of these years 1972, 1979, 1982 and 1987 are the weakest monsoons and 1975, 1983 and 1988 are the strongest monsoons of the period.

Year	Indian Summer monsoon Rainfall in mm (June-September)	Percentage departure from long term mean (1871-92)
1972	652.6	-23.44
1973	913.4	7.16
1974	748.1	-12.24
1975	962.9	12.96
1976	856.8	0.52
1977	883.2	3.61
1978	909.3	6.68
1979	707.8	-16.96
1980	882.8	3.57
1981	852.2	-0.02
1982	735.2	-13.75
1983	955.7	12.12
1984	836.7	-1.84
1985	759.8	-10.86
1986	743.0	-12.83
1987	697.3	-18.20
1988	961.5	12.80
1989	866.7	1.68
1990	908.7	6.60
1991	784.6	-7.95
1992	784.9	-7.92

Table 4.1 Indian Summer Monsoon Rainfall 1972-1992 (Parthasarathy et al., 1994)

During the 3 strong Indian monsoons the temperature TBO is in positive phase. Generally stratospheric zonal wind QBO is in westerly phase during strong Indian monsoon and easterly phase during weak Indian monsoons as pointed out by Bhalme et al., (1987). Of the 4 weak Indian summer monsoons except in 1979 TBO is in negative phase. The results suggest that the observed biennial variability in the tropospheric temperature over Thumba, may be due to the monsoon-ocean-atmosphere interactions taking place over Indian ocean region in biennial time scales as suggested by Meehl (1997).

4.4 Conclusion

Phase coherence between TBO and QBO in monthly mean temperature anomaly and zonal wind over Thumba has been analysed. A strong decadal change in phase coherence between 1971-81 and 1982-92 period is observed in temperature anomaly. Change in phase coherence is reflected in the correlation between these oscillations. All these evidences presented in this chapter suggest not an association between TBO and QBO, but rather lack of association between the two phenomena. The decadal change in phase coherence between TBO and QBO in temperature and correlation between these oscillations suggests that they are different phenomena. Two nearly biennial phenomena with slightly different periods are expected to drift in and out of phase on decadal time scales.

The strong relation existing between the phase of TBO and Indian summer monsoon activity suggest that the observed biennial variability in the tropospheric temperature over Thumba, may be due to the monsoon-ocean-atmosphere interactions taking place over Indian ocean in biennial time scales.

Chapter –5

Interannual Timescale Stratosphere – Troposphere Exchange of Ozone by Asia Pacific wave

5.1 Introduction

Ozone is a chemical tracer in the atmosphere. At altitudes 10-20 km, ozone is considered as a passive tracer because the photochemical lifetime of ozone is several weeks, which is long, compared to the time scale of advection [~1day] (Salby and Callaghan, 1993; Brasseur and Solomon, 1984). It is also considered as active tracer because ozone distribution changes the short-wave diabatic heating distribution and hence changes the temperature and wind distribution (Andrews et al., 1987).

Therefore changes of ozone number density and hence of column abundance

$$\Sigma O_3 = \int_o^\infty n_{o3}\, dz \qquad \ldots(5.1)$$

where n_{o3} is ozone number density or total ozone are controlled by the circulation of the 10-20 km region which redistribute O_3 molecules.

Several studies showed the presence of such strong relationship between meteorological circulation and total ozone variations on regional to global scales. (Bowman, 1989, Hadjinicolaou et al., 1997, Salby and Callaghan, 1993 and many others, see chapter 2).

In this chapter, the meridional ozone exchange caused by a newly documented upper tropospheric Rossby wave in May and the following summer and autumn seasons between tropical upper troposphere and extratropical lower stratosphere is studied. Planetary scale Rossby waves are seen in the Northern Hemispheric middle latitude upper troposphere throughout the year. In Northern Hemispheric winter season, when the Sun is in the Southern Hemisphere, these waves are caused by convective heating due to land-sea contrast and by orography. In fig. 5.1, the monthly

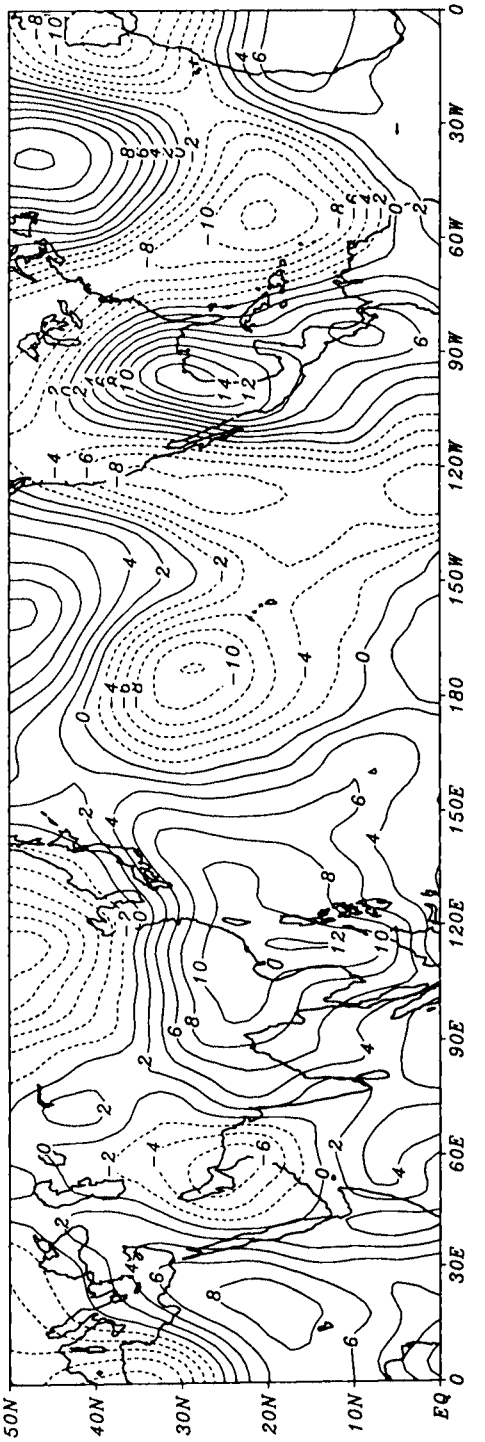

Fig. 5.1 Monthly mean meridional wind (ms^{-1}) at 200 hPa for February 1987.

mean meridional wind at 200 hPa for February 1987 is presented as an example. This clearly shows the presence of such a planetary scale wave with wave number 3 structure in zonal direction.

Localized changes in latent heat release such as those associated with slowly varying sea surface temperatures (SST) are widely believed to affect the circulation in distant places around the globe. Sardeshmukh and Hoskins (1988), using a simple vorticity equation model showed that the upper level divergence associated with the tropical heating can lead to a Rossby wave source in the subtropical westerlies. They also showed that the wave could be relatively insensitive to the longitudinal position of the equatorial divergence (Rossby wave source).

In fig. 5.2, the annual cycle of outgoing longwave radiation (OLR) measured by satellites, reproduced from Webster et al., (1998) is presented. The darkly shaded areas corresponds OLR < 220 wm^{-2}, which is considered to indicate deep convection and heavy rainfall activity (regions of heat source) over the tropics. The hatched area corresponds to the regions of high OLR values or regions of heat sink. In accordance with the apparent migration of the sun to Northern and Southern Hemispheres, the regions of low OLR also migrate. In April, the regions of deep convection are minimal in the globe. Every year the regions of low OLR first enter the Northern Hemisphere in May. According to Sardeshmukh and Hoskins (1988), this heating generates Rossby waves in the midlatitude upper tropospheric westerlies.

Recently Joseph and Srinivasan (1999) (in the following JS) documented the presence of such heat-generated Rossby waves in midlatitude upper tropospheric westerlies. Using NCEP/NCAR reanalysis

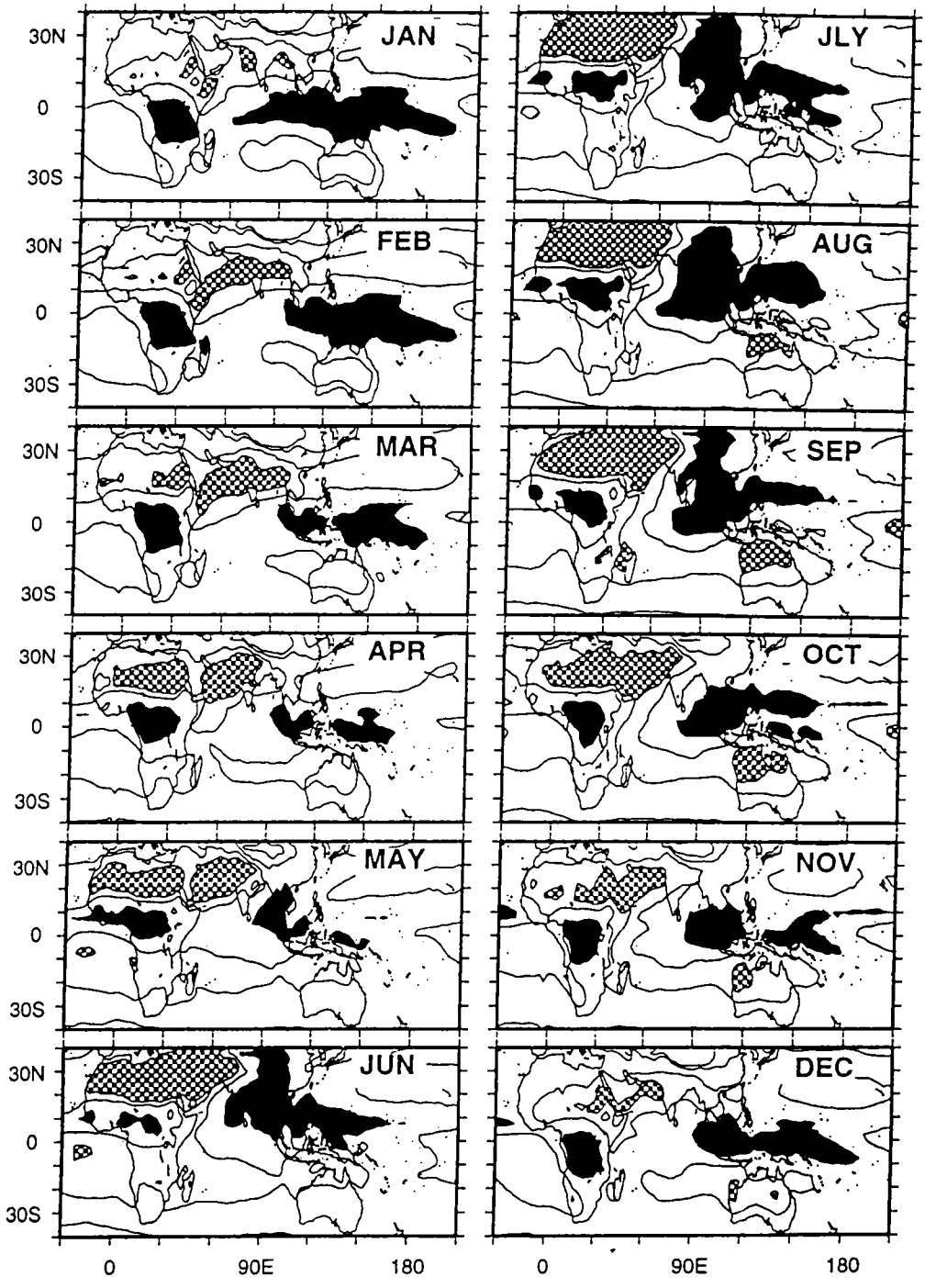

Fig. 5.2 Annual cycle of outgoing longwave radiation (OLR) measured by satellite. Shaded and cross hatched regions indicate OLR < 220 and >300 W m^{-2}, respectively. OLR minima are surrogates for persistent deep convection and latent and radiative heat sources within the troposphere. Regions of maximum OLR, on the other hand, indicate radiative loss to space and hence are heat sinks. (After Webster, 1995)

data (Kalnay et al., 1996) they showed the presence of a large amplitude standing Rossby Wave in the upper tropospheric westerlies during May confined between 10°N and 50° N latitudes. This wave has a wavelength of about 50-60° longitude (zonal wave number 6 or 7) and has a spatial shift of about 20° longitude between deficient and excess Indian Summer Monsoon Rainfall (ISMR) years. According to JS, the spatial shift is due to the shift in the longitudinal position of the convective heat sources associated with the Inter Tropical Convergence Zone. The area occupied by deep convective clouds (highly reflective clouds) in May during weak (DRY) and strong (WET) monsoon years is shown in fig. 5.3. In strong monsoon years, the area occupied by deep convective clouds expands westward, by about 20° longitudes. In the strong monsoon years, the deep convective clouds occur between 70° E and 100° E, where as in weak monsoon years they occur between 90° E and 120° E. The observed sensitivity of the spatial phase of the APW to longitudinal shift of convective heating is contradicting with the model studies of Sardeshmukh and Hoskins (1988).

Due to its geographical location, this stationary Rossby wave was named as Asia Pacific Wave (APW). JS reported that this wave has a large amplitude around 200 hPa, and the amplitude decreases with decreasing height in the troposphere. Although the lower portion of this wave has been studied in detail, the nature above 200 hPa has not been documented. It would be interesting to know whether the APW is seen above 200 hPa in the lower stratosphere, because this region is rich in ozone.

In this chapter the nature of the APW above 200 hPa level is studied. The importance of the location of the APW and possible meridional mass exchange including that of ozone by this wave is highlighted. It is also

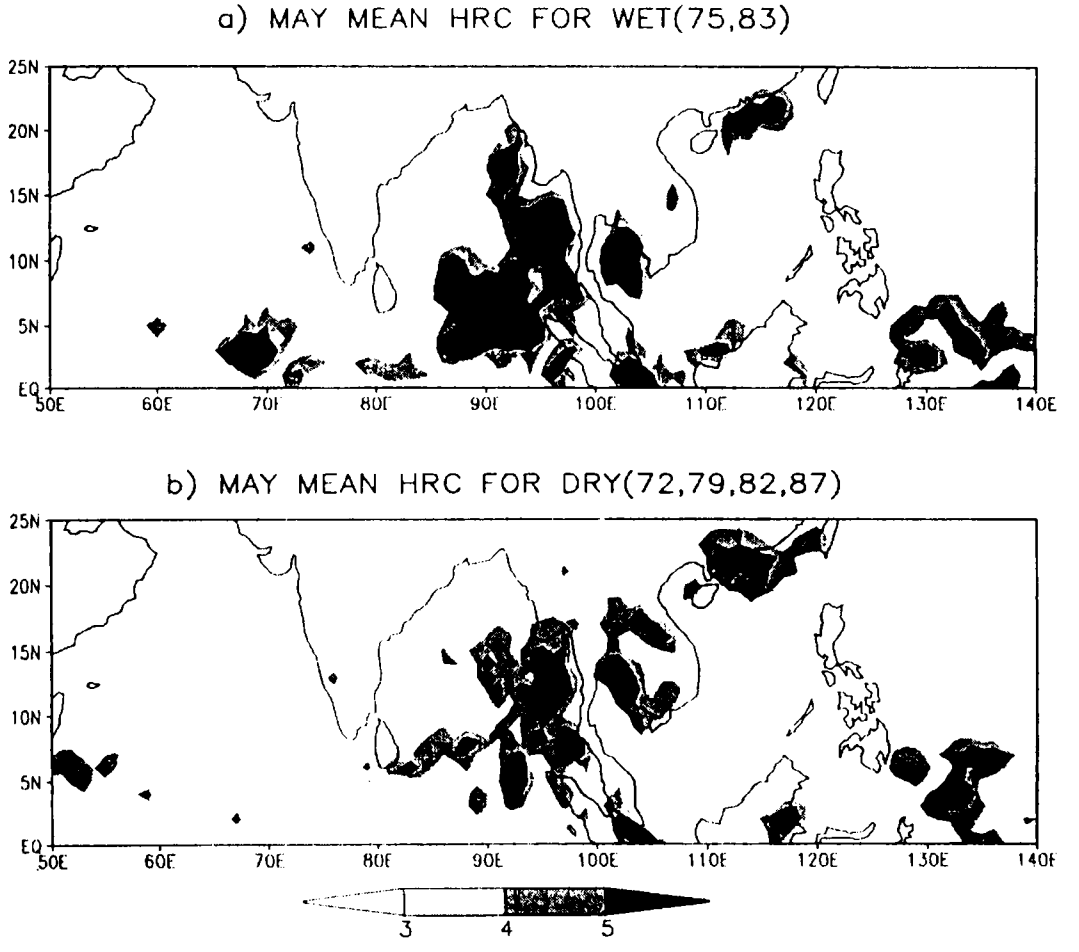

Fig. 5.3(a) May HRC (days per month) wet composite (years 1975 and 1983). (b) May HRC (days per month) dry composite (years 1972, 1979, 1982 and 1987). (After Joseph and Srinivasan, 1999)

shown how the environmental conditions associated with extreme ISMR affect the distribution of total ozone amount over an area in the interannual time scale.

5.2 Data

Monthly mean values of wind (both u and v) at 300, 200, 150, 100, 70, 50, 30, 20 and 10 hPa levels from NCEP/NCAR reanalysis data for the period 1979-1994 were used. Temperature data at all 17 levels have been analysed to understand the tropopause break. Gridded monthly mean total ozone data (version 7) for the period November 1978 to April 1993, measured by the TOMS instrument onboard Nimbus-7 spacecraft was used for the ozone analysis (McPeters et al., 1996). Indian summer monsoon rainfall (ISMR) data were adopted from Parthasarathy et al., (1994). Table 5.1 gives the ISMR for the 1979-93 period. The 3 DRY years are the years of maximum rainfall deficiency while the 3 WET years are the years of maximum rainfall excess. During the period 1979-1993 the years 1979, 1982 and 1987 are DRY monsoon years and 1983, 1988 and 1990 are WET monsoon years. All these years have rainfall excess/deficiency more than one standard deviation from the long period average except 1990 (Table 5.1).

5. 3 The Asia Pacific Wave in the lower stratosphere

In order to study the characteristics of the APW, gridded NCEP/NCAR mean meridional wind data during the month of May were used. Data for the 13 year period 1982-1994 available in the CD-ROM supplied along with Kalnay et al., (1996) for the 9 levels considered (300,

200, 150, 100, 70, 50, 30, 20, 10 hPa) were used to calculate meridional wind anomalies at each grid point for composites of DRY and WET years.

Year	Percentage departure (mm) from 1871 -93 mean
1979	-16.96
1980	3.57
1981	-0.02
1982	-13.73
1983	12.12
1984	-1.84
1985	-10.86
1986	-12.83
1987	-18.20
1988	12.80
1989	1.68
1990	6.61
1991	-7.91
1992	-7.91
1993	2.89

Table 5.1 Indian Summer Monsoon Rainfall (mm)
(Parthasarathy et al., 1994)

In Fig. 5.4 meridional wind anomalies for the composite WET years for 4 levels viz., 300, 200, 100 and 70 hPa and in Fig. 5.5, meridional wind anomalies for the composite DRY ISMR years for 200 hPa level only are presented. A prominent stationary Rossby wave signal is seen in these figures at all levels. It has a wave number 6 or 7 in zonal structure and is confined between 10° N and 50° N latitudes. It is seen from Fig.5.4, that the areas of southerly and northerly meridional wind anomalies of the WET composite above 200 hPa levels match with the same at 200 hPa and below. Thus, the wave seen above 200 hPa level is an integral part of the APW reported by JS for 200 hPa and below. The amplitude of this wave decreases both above and below 200 hPa and the wave is very weak above 70 hPa (figures not shown).

From Fig. 5.4 and the study by JS it is clear that the wave is present between 500 and 70 hPa levels with maximum amplitude around 200 hPa. Above and below 200 hPa its amplitude decreases. Over the Indian region, northerly anomalies are seen during WET years and southerly anomalies during DRY years. It is seen from the 200 hPa WET (Fig. 5.4c) and DRY (Fig. 5.5) composites that the APW shows a phase shift of about 20° longitude between extreme ISMR years as reported by JS. It is clear from this study that the APW affects both the upper troposphere and the lower stratosphere. In other words, APW couples the lower stratosphere and troposphere directly. JS showed that the APW at 200 hPa and below possesses major characteristics of a stationary barotropic Rossby wave, which has no phase shift with height. It is clear from Fig. 5.4 that the wave above the 200 hPa level also does not show any phase shift with height.

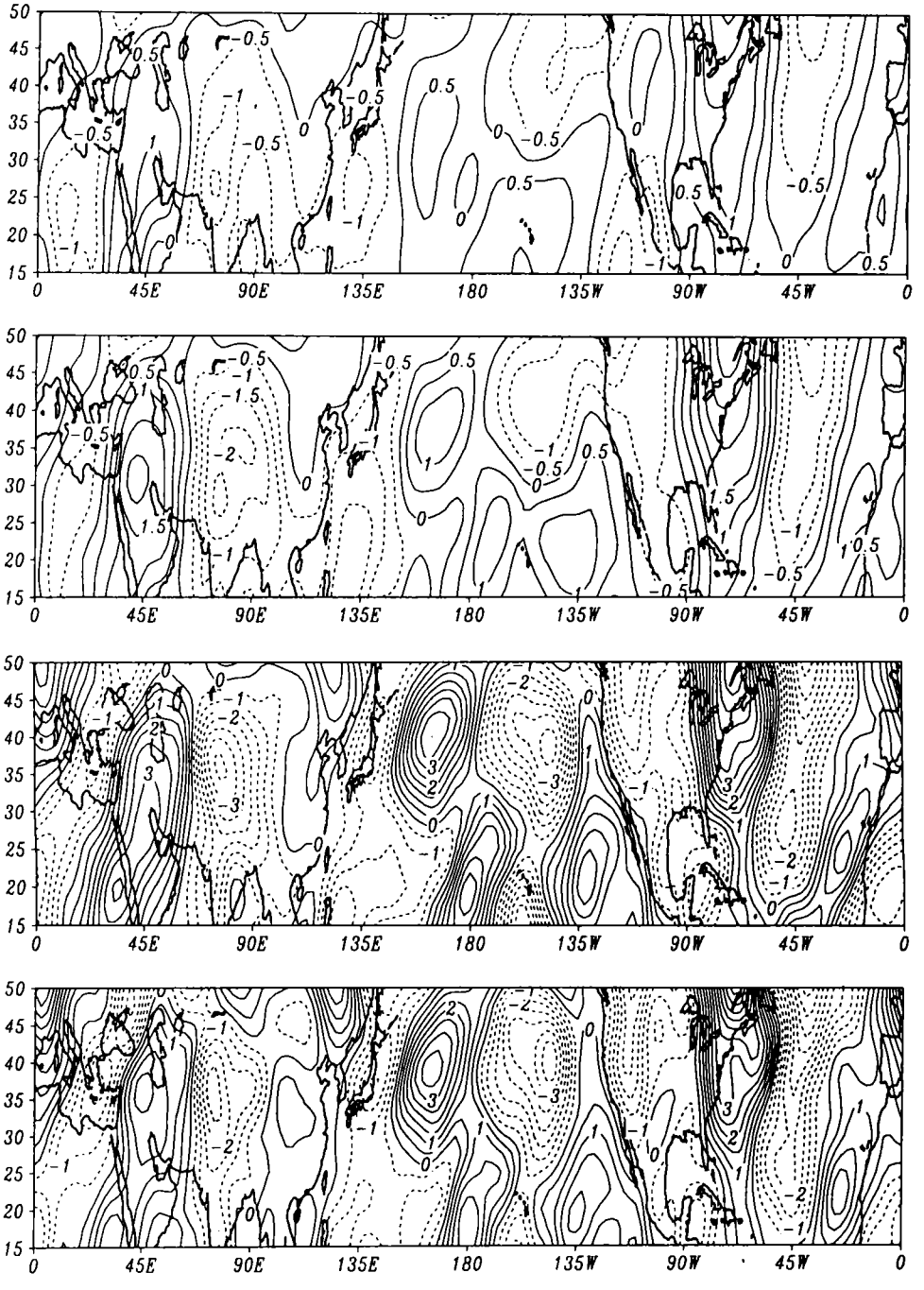

Fig. 5.4 Meridional wind anomalies (ms^{-1}) of a) 70, b) 100, c) 200 and d) 300 hPa levels for WET composite. The contour interval is 0.5 ms^{-1}.

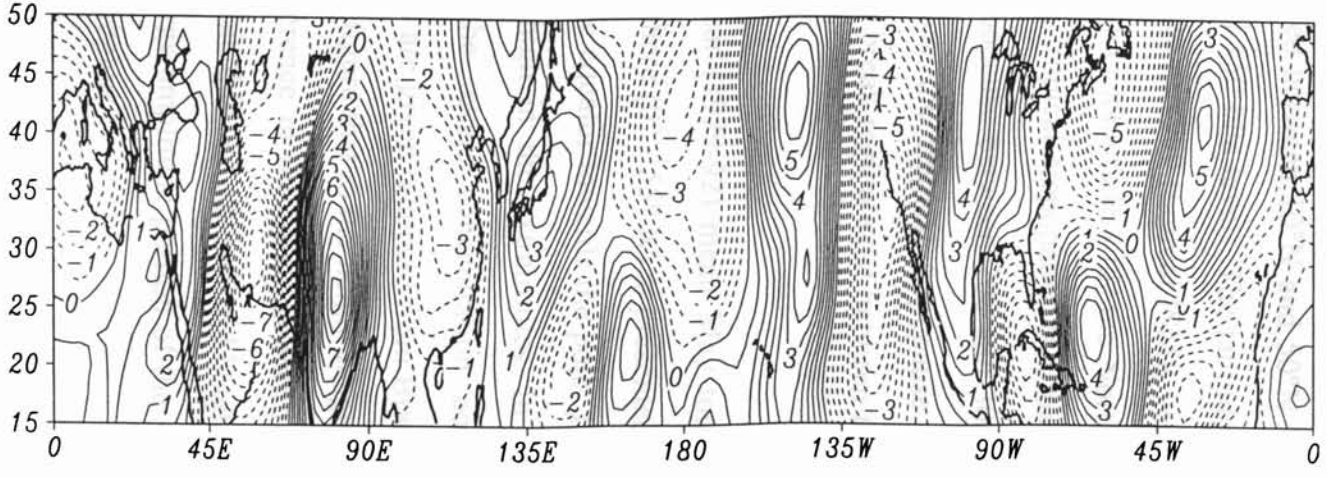

Fig. 5.5 Meridional wind anomalies (ms^{-1}) of 200 hPa for DRY composite. The contour interval is 0.5 ms^{-1}.

5. 4 The Asia Pacific Wave and meridional mass exchange

APW follows the subtropical westerly jet stream over the Asian region and then moves southeastwards to North America. This wave is generally confined between 10°N and 50°N latitudes with large amplitude between 300 and 150 hPa levels. The latitude-height plot of the mean May temperature values of 1989 (normal ISMR year) averaged between 50-100° E longitudes (Indian longitudes) for the Northern Hemisphere is presented in Fig. 5.6. The tropical tropopause is situated around 100 hPa and the extratropical tropopause between 200 and 300 hPa levels. Over 30°N and adjoining latitudes, the tropical tropopause lies above the extratropical tropopause and a break region exist between them, which is the tropopause break.

The 14 year (1979-92) mean May total ozone distribution for the Northern Hemisphere (0° - 55° N) is presented in Fig. 5.7. The total ozone increases from the equator towards the pole. The ozone gradient is weak in the tropics and high in the extratropics. In Fig. 5.8, the mean vertical distribution of the ozone concentration according to observations at different latitudes are given (adopted from Brasseur and Solomon, 1984). It is clear from this figure that in the height range of 8 km to 20 km, there is a considerable difference in the ozone concentrations between 20° and 60° latitudes. It is within this latitude belt and height range the tropopause break is located. The large amplitude portion of the APW train is situated in this tropopause break region.

The maximum amplitude of APW is in the tropopause break. It is suggested that the large amplitude meridional wind anomaly associated with APW is able to transport ozone rich extratropical lower stratospheric

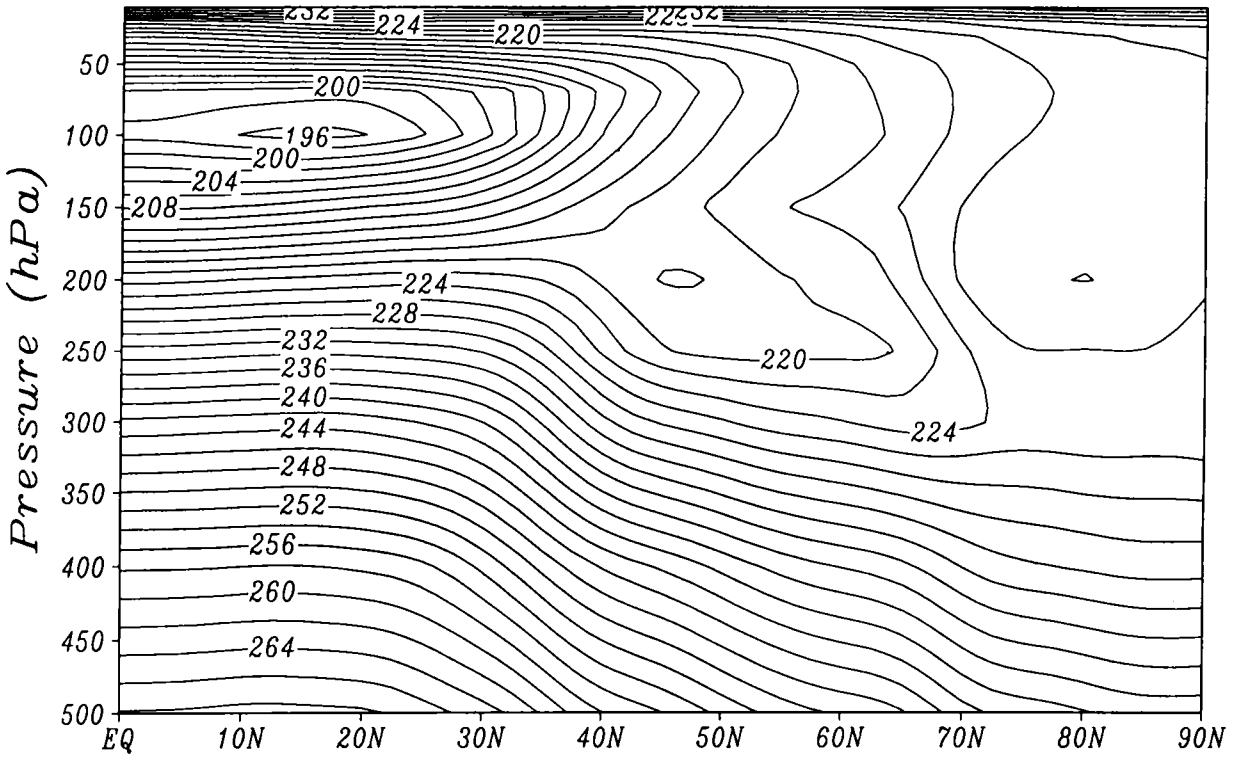

Fig. 5.6 Latitude-height plot of the temperature averaged between 50° and 100° E longitudes for May 1989.

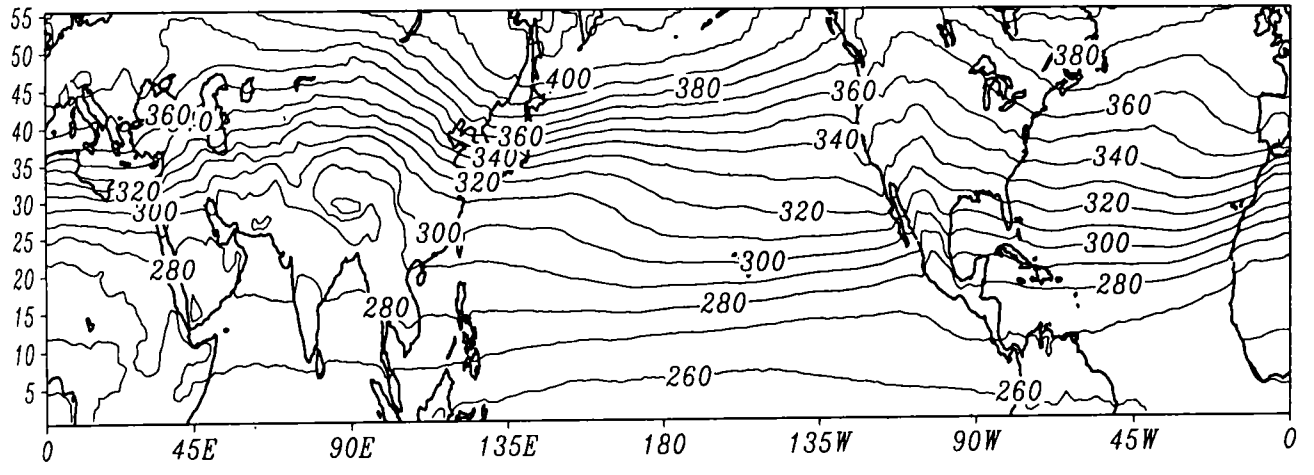

Fig. 5.7 Total Ozone Climatology of May. Contour interval is 10 DU.

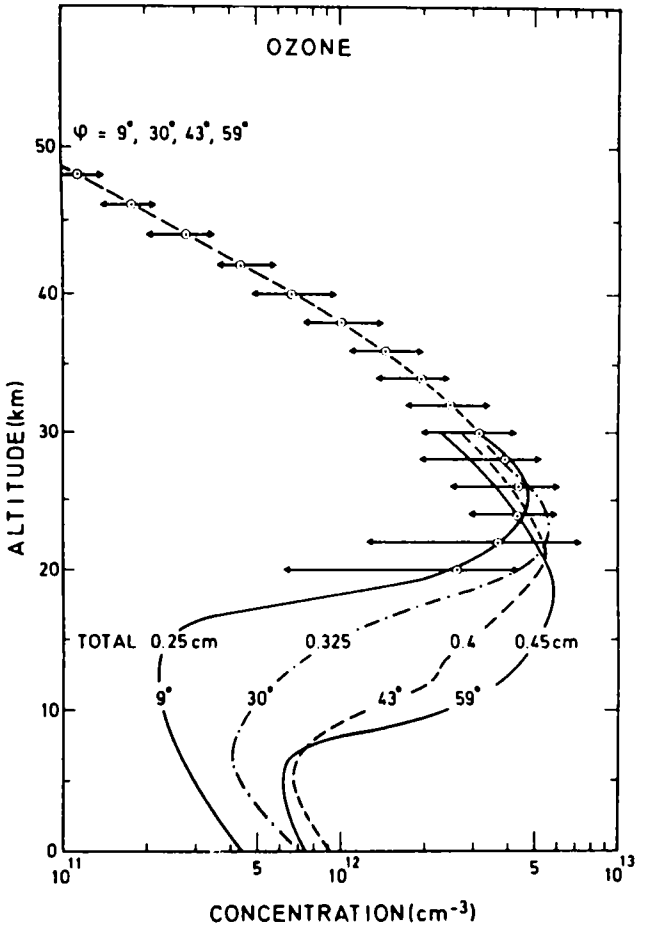

Fig. 5.8 Mean vertical distribution of the ozone concentration according to observations at different latitudes - adopted from Brasseur and Solomon, 1984.

air into tropical upper troposphere and ozone poor upper tropospheric air into the extratropical lower stratosphere effectively through the tropopause break region, which in turn can affect the total ozone distribution.

5. 5 Signature of Asia Pacific Wave in total ozone

In order to check the possible presence of APW induced meridional mass exchange *via* the tropopause break, the total ozone anomaly of May was examined. Ozone is an ideal tracer for this study because relatively long period satellite measured total ozone data are available on global scale. Gridded monthly mean TOMS total ozone data in the latitude range 0.5°N to 50.5°N for the period 1979-92 were available for analysis. Total ozone anomalies from the 14 year climatology were computed for May for each grid point. In Fig. 5.9 total ozone anomalies for the composites of WET and DRY years are presented. Areas of positive and negative total ozone anomalies are seen in the zone between 10°N and 50°N latitudes. It has a wave number 6 or 7 structure in the zonal direction just like APW. Areas of positive (negative) total ozone anomalies correspond to northerly (southerly) meridional wind anomalies of APW. Thus, over north India in May of DRY (WET) years there are negative (positive) anomalies in total ozone as can be seen from Fig. 5.9. In some regions the areas of total ozone anomalies show small eastward shift while compared to the corresponding locations of the meridional wind anomaly. It is interesting to note that the Indian summer monsoon, is associated not only with the spatial phase of the APW but also with the total ozone distribution around the globe in the interannual time scale.

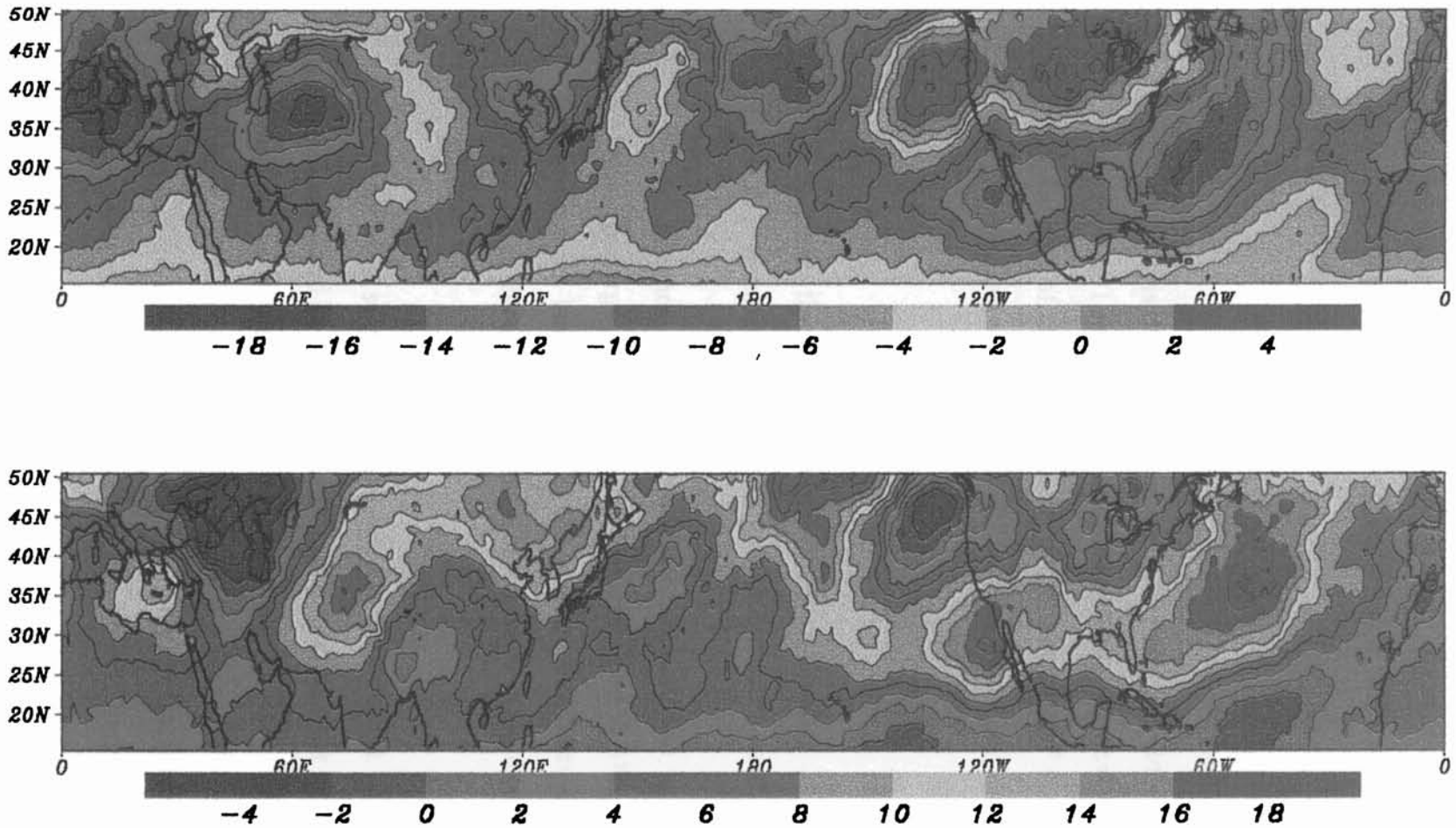

Fig. 5.9 Total ozone anomaly (DU) of May for a) WET and b) DRY composites. (Colour scale is different for each figure)

5. 6 The Asia Pacific Wave during the monsoon season

In a barotropic atmosphere, Rossby wave is an absolute vorticity conserving motion. Zonal phase speed of the Rossby wave relative to mean wind is written as

$$C_x = -u + (\beta/(k^2 + l^2)) \qquad \ldots(5.2)$$

β is df/dy; the variation of Coriolis parameter with latitude.

k, l are zonal and meridional wave numbers respectively

In case of stationary Rossby wave like the APW, $C_x = 0$ and l=0. Thus the zonal wave number of APW can be written as

$$k^2 = \beta / u \qquad \ldots(5.3)$$

It states that the square of the wave number of APW is directly related to β parameter and inversely related to zonal wind speed.

In summer monsoon season, the midlatitude upper tropospheric westerlies undergo some changes when compared to May; (1) they shift to further northern latitudes and (2) the velocity decreases moderately. These changes affect the structure of the Rossby wave in summer season as stated in equation 5.3.

APW is seen in monsoon season also. In Fig. 5.10, the 200 hPa meridional wind anomalies of peak ISMR months (July and August) for the composite WET and DRY years are presented. This figure illustrates the presence of APW in monsoon season too. Since the ITCZ reaches its northernmost position around 30° N in summer monsoon season and the westerly belt also moves northwards, the APW is found further to the north

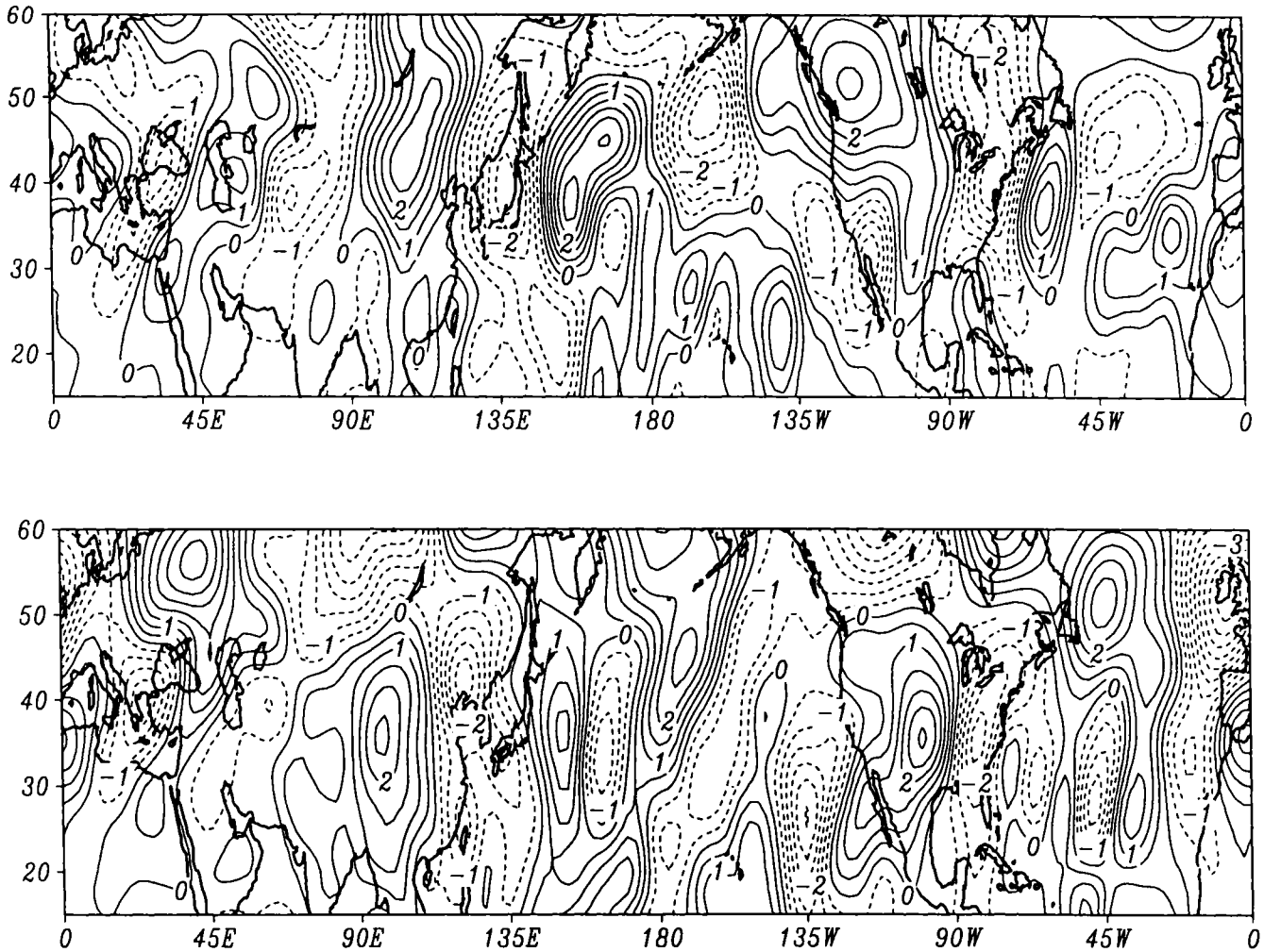

Fig. 5.10 Meridional wind anomalies of peak monsoon months (July and August) (ms^{-1}) of 200 hPa level for a) WET and b) DRY composites. The contour interval is 0.5 ms^{-1}.

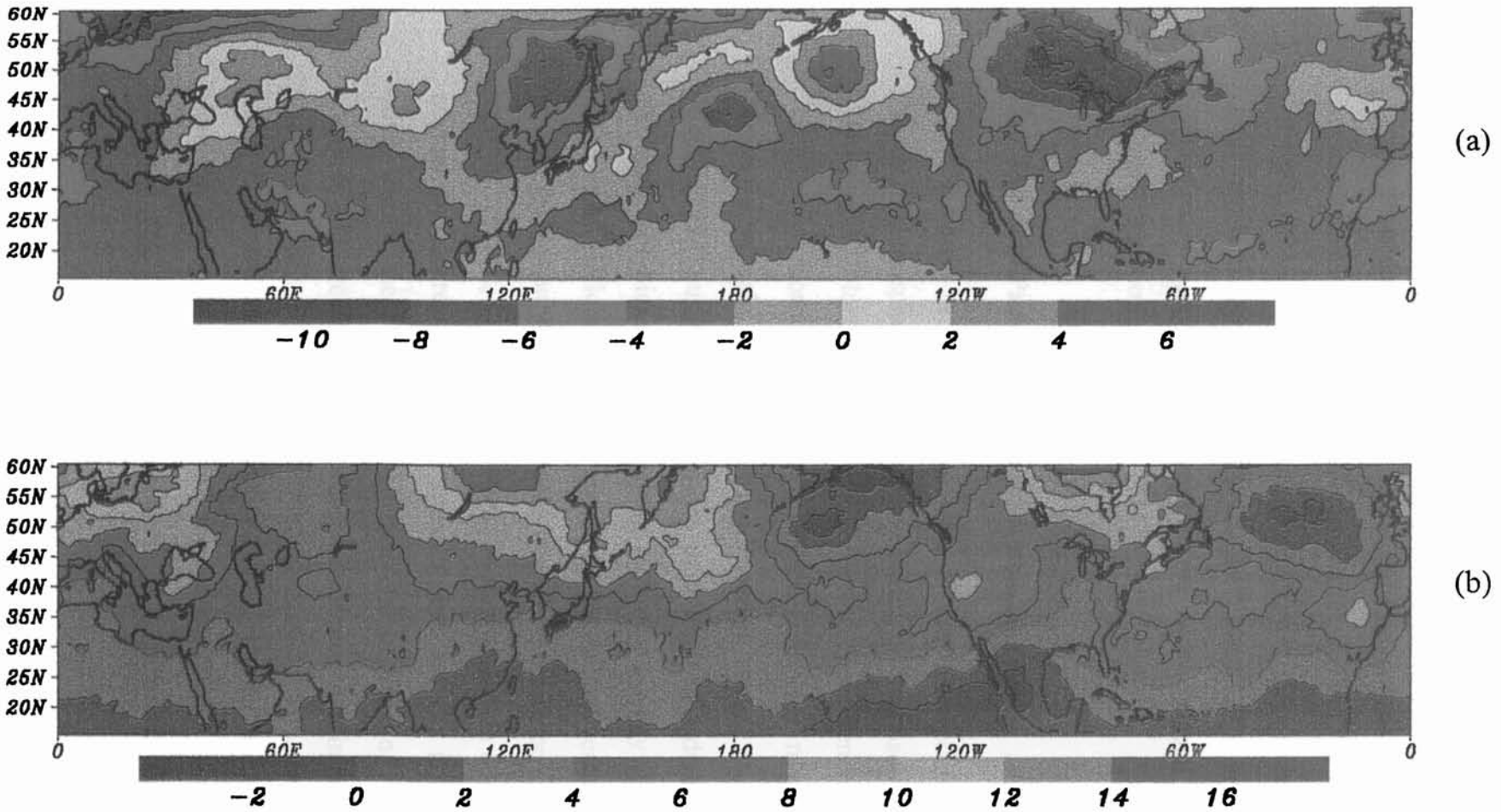

Fig. 5.11 Total ozone anomalies (DU) of peak monsoon months (July and August) for a) WET and b) DRY composites (Colour scale is different for each figure).

during this season than during May. The spatial phase is however the same during May and the following summer monsoon season.

In order to study the APW induced anomalies in total ozone in monsoon season, the total ozone anomalies for WET and DRY composites of peak ISMR months July and August were calculated. In Fig. 5.11 the total ozone anomaly composites for WET and DRY years are presented. This clearly shows the presence of the APW in total ozone during the summer monsoon season also.

5. 7 The Asia Pacific Wave in post-monsoon season

As seen in fig (5.2), the areas of deep convection are seen in the Northern Hemispheric tropical region during post monsoon season (October - November). Normally this tropical heating could generate Rossby waves during post monsoon season also. Indian summer monsoon has strong biennial timescale variability as evidenced in second and fourth chapters. Meehl (1994) suggested that air-sea interaction in Indian Ocean might be the cause for biennial variability in monsoon activity. He suggested that following a deficient summer monsoon the Indian ocean is warmer than normal and favourable for increased winds and monsoon activity in the next year. In contrast, following an excess monsoon, Indian ocean is cooler than normal and decreases the wind and monsoon activity in the next year. In other words, the state of sea surface temperature in the post-monsoon season is an indicator for the performance of monsoon in next year.

Examination of the spatial phase of the APW in May and post-monsoon season in 1982 and 1987 showed the change of phase from DRY condition (eg. southerlies over India and Japanese islands) to WET

condition (northerlies overthese regions) in post-monsoon season. This phase change of APW in post-monsoon season can be used to predict the performance of summer monsoon in the following year well in advance. But this result is based on the analysis of only two sets of dry followed by wet ISMR years, and detailed examination of several such years are needed to get more conclusive result. In fig (5.12) the APW for the months of May 1982 and November 1982 are presented as an example. It is clear that the strong northerly anomalies (phase reversal) appear over India during November 1982 indicating the presence of favourable condition for WET monsoon in the following year. Although the phase reversal is found over India in November 1982 and May 1983, the APW shows slight difference in the overall spatial phase structure due to the change in latitudinal position and velocity of the westerlies and changes in the longitudinal position of heating regions between these months.

In fig (5.13) the total ozone anomalies for the months May 1982 and November 1982 are presented. Clear signatures of APW are reflected in these months. The major feature observed between these figures is the phase reversal in total ozone anomaly throughout the globe between May 1982 and November 1982.

5. 8 Counter-part of Asia Pacific Wave in Southern Hemisphere

At the end of austral spring, the regions of low OLR enter the Southern Hemisphere every year. These heat sources can generate planetary scale waves in the Southern Hemispheric midlatitude upper tropospheric westerlies and in turn affect the total ozone in Southern Hemisphere. The meridional wind anomaly for December 1987 (random choice) at 200 hPa

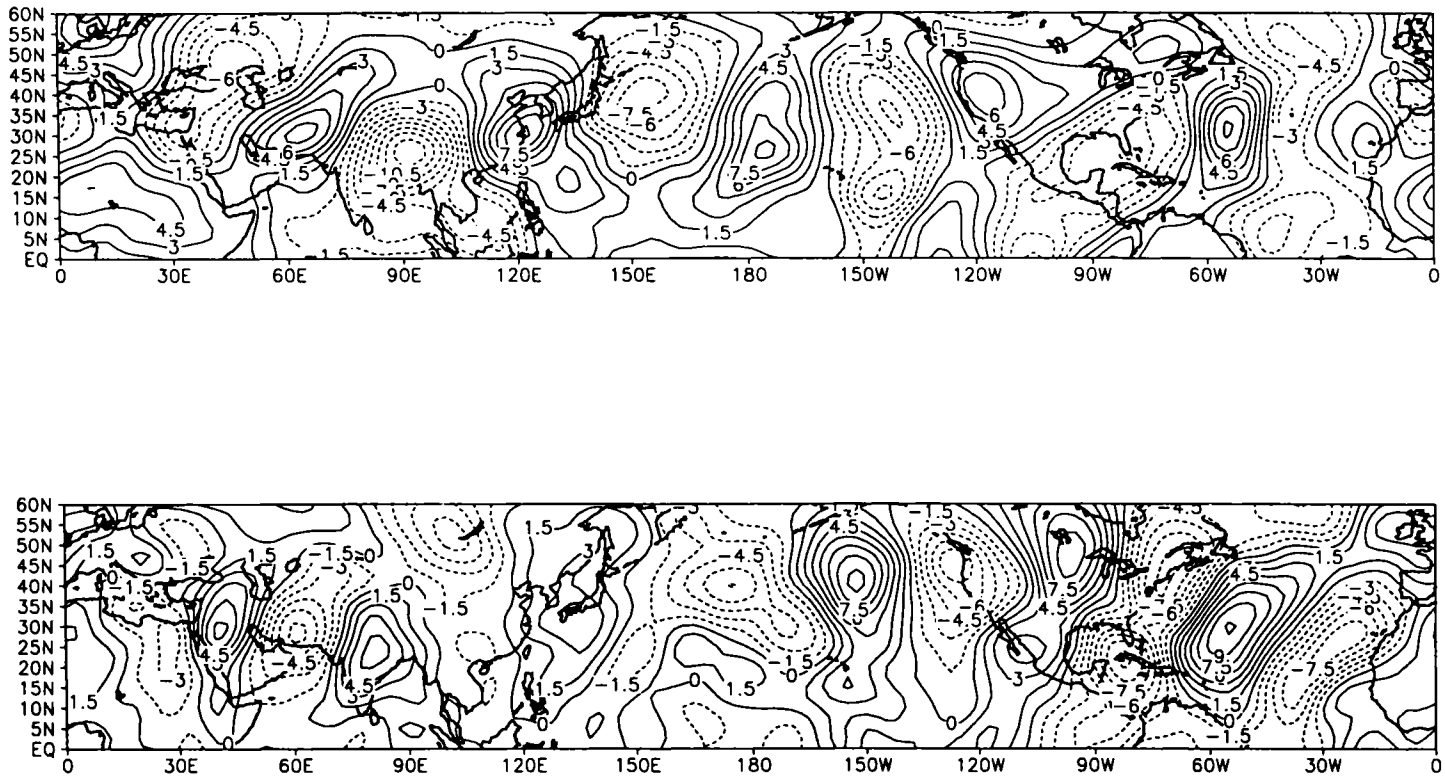

Fig. 5.12 Meridional wind anomalies (ms^{-1}) at 200 hPa for a) November 1982 and b) May 1982.

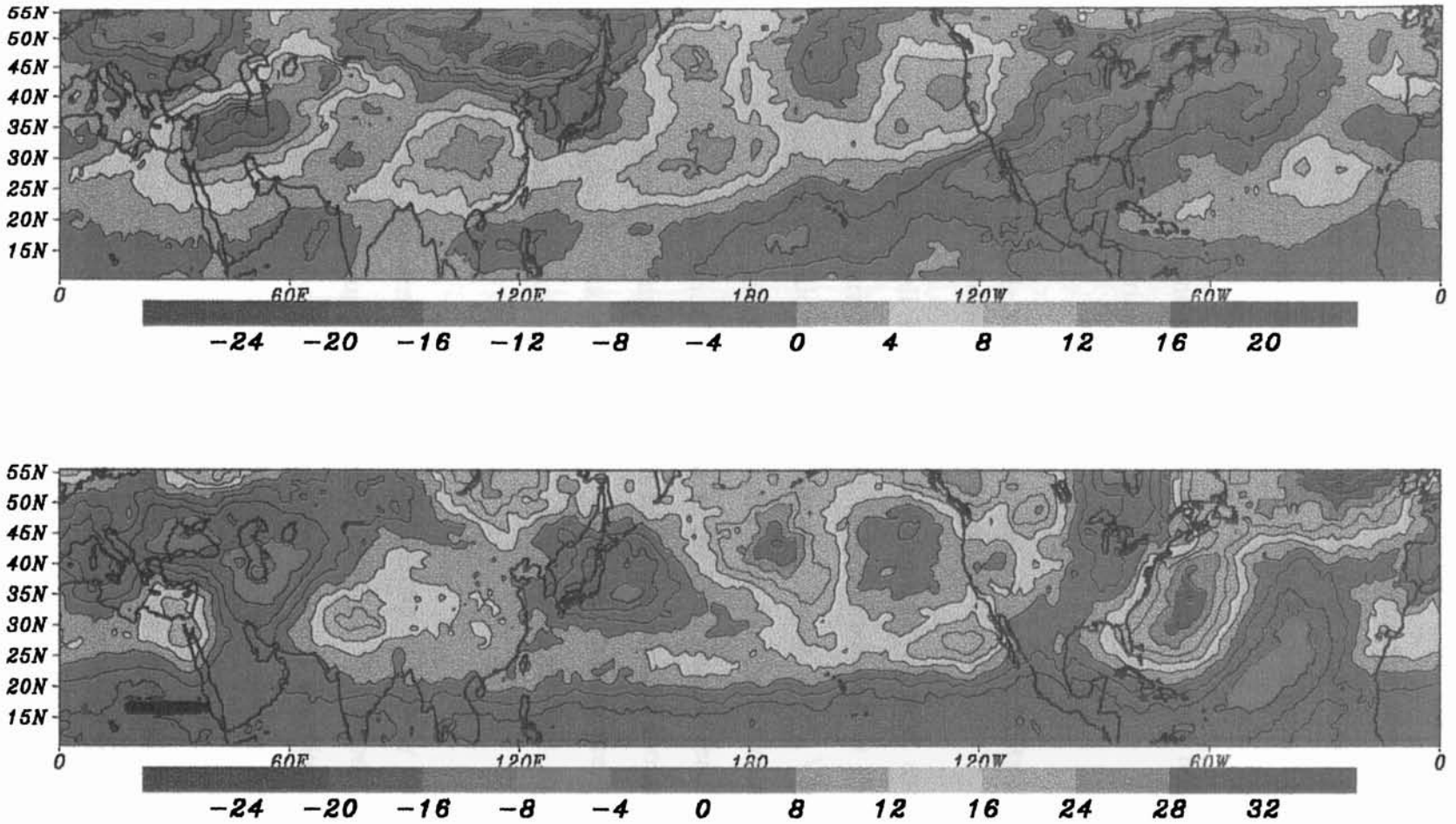

Fig. 5.13 Total ozone anomaly (DU) for a) November 1982 and b) May 1982.

(fig 5.14) shows the presence of such heat-induced waves along the subtropical westerly jet stream. This also exchange tropical upper tropospheric ozone poor airmass and extratropical lower stratospheric ozone rich airmass and generate ozone anomalies (figure not shown). Caution is needed in determining the total ozone anomalies caused by these stationary Rossby wave because the polar vortex breaks down during the austral spring and ozone poor airmass from Antarctic ozone hole strongly mix up with the ozone rich airmass outside the polar vortex.

5. 9 Asia Pacific Wave induced total ozone variability and its possible implication on total ozone trend

It is well known that the decrease of total ozone increases the amounts of harmful ultraviolet (UV-B) radiation at the earth's surface, which is considered a health hazard (Chanin, 2001; Van der Leun et al., 1995; WMO, 1998). Studies have shown that the decrease of total ozone by 10% causes about 20% increase in the UV radiation reaching the surface of the earth. During May and the following summer monsoon months, solar radiation is maximum in the Northern Hemisphere, and the negative anomalies in ozone thus pose health hazards due to increased UV-B radiation there.

Long-term decline of total ozone is largely caused by ozone depletion through anthropogenic chlorine (Solomon, 1999). However, particularly at northern mid-latitudes, the full magnitude of the observed decline, its annual and longitudinal variation, have not been explained well by two-dimensional photochemical models (Jackman, 1996). Recent explanations for such discrepancies range from additional chemistry to purely dynamical changes in transport (Solomon, 1999; Hood et al., 1997).

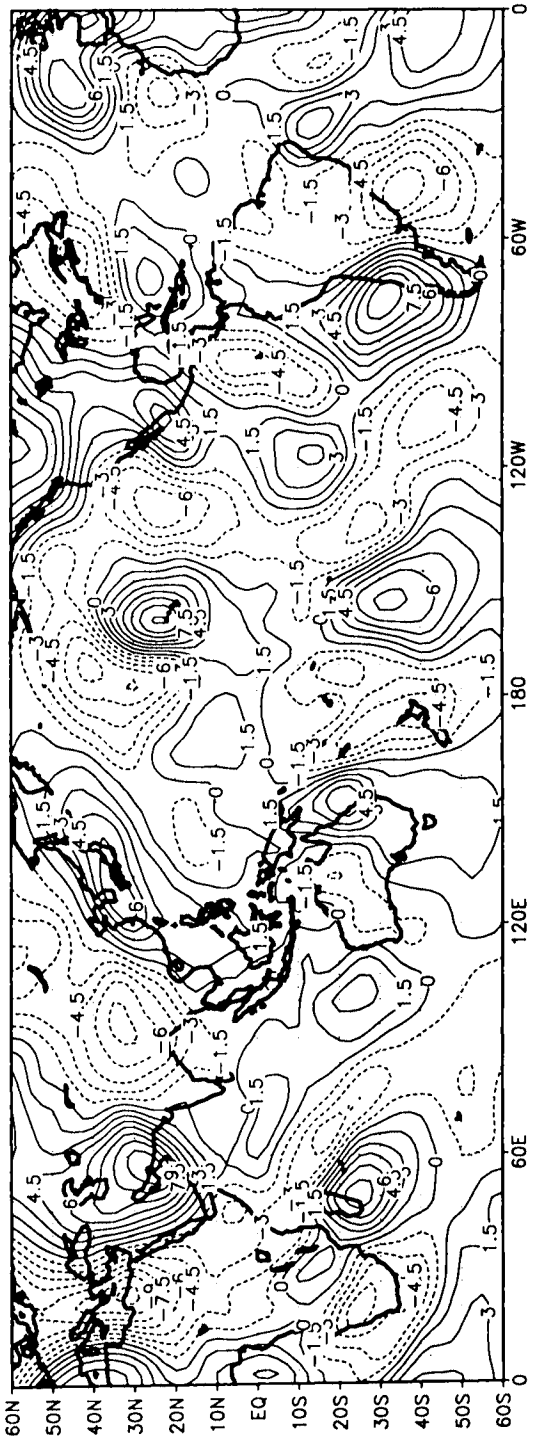

Fig. 5.14 Meridional wind anomalies (ms^{-1}) at 200 hPa for December 1987.

Total ozone measured from TOMS onboard Nimbus-7 revealed a trend in column abundance that maximizes at midlatitudes of the Northern Hemisphere. The zonal mean trend reaches a maximum during February, when it exceeds –6% per decade (Jackman et al., 1996). In contrast the zonal mean trend during September and October is only 2% per decade. Geographical distribution of total ozone trend taken from Niu et al., (1992) is already presented month wise in chapter-1. Hood and Zaff (1995) explained the longitude dependence of middle latitude total ozone trend in January given by Niu et al., (1992) on the basis of decadal changes in the amplitudes and phases of stationary planetary waves. He also showed that owing to horizontal and vertical transport, ozone-mixing ratio maxima tend to occur where geopotential height in the lower stratosphere is a minimum (wave trough), and a temperature maximum occurs where the change in geopotential height with pressure is a maximum.

The so-called random interannual total ozone variability mentioned in the literature may be understood by the total ozone anomalies caused by APW between May and November months. Since the APW in the upper troposphere and associated meridional stratosphere-troposphere exchange is unknown until now, these total ozone variations were described as random variations. These variations are associated, atleast partly with the phase of APW. The magnitude of the total ozone variations associated with APW is between 5-10%.

It has been demonstrated that the phase of APW is strongly related to the performance of Indian summer monsoon activity. Indian summer monsoon activity is characterized by decadal timescale epochs of frequent deficient and frequent excess rainfall years. In fig. 3.1, the all Indian

summer monsoon rainfall series and its 31-year adjacent averaging are presented. This clearly shows the presence of decadal epochs in ISMR. It is also suggested that this decadal timescale ISMR epochs may be reflected in APW and inturn affect the total ozone trend around the globe from May to November. It is to be borne in mind that Hood and Zaff (1995) explained the longitude dependence of middle latitude total ozone trend in January on the basis of decadal changes in the amplitudes and phases of stationary planetary waves. So it is recommended that the interannual and interdecadal variability in APW may have to be considered in the total ozone trend computations in order to get realistic trend estimation.

Chapter –6

Synoptic Scale Stratosphere –Troposphere Exchange of Ozone by Long Waves

6.1 Introduction

Total ozone distribution in the Northern Hemisphere exhibits wide range of temporal and spatial variability. Large-scale ozone anomalies of interannual timescales caused by APW were documented in the previous chapter. It is well known that the total column ozone undergoes substantial short-term fluctuations, which correlate closely to the passage of synoptic weather systems (Dobson et al., 1929). Later Reed (1950) showed that these fluctuations were part of the synoptic scale regions of depleted ozone which were advected under the influence of tropospheric dynamics and exhibited growth and decay on a time scale of a few days. These transient regions of strongly depleted total ozone were referred as *Ozone mini-holes* (Newman, et al., 1988; Mc Kenna et al., 1989). Ozone mini-holes are formed by the horizontal advection of ozone-poor airmass from tropical region to the extratropics and ascent across the tropopause region resulting in divergence of ozone-rich stratospheric air out of the column (James et al., 1997; James et al., 2000). In the region of ozone mini-holes, total ozone amounts may fall by over 100 DU in a couple of days. Petzoldt et al., (1994) and Petzoldt (1999) have shown case studies of exceptionally deep mini-ozone holes that occurred over northern Europe during stratospheric warming. Ozone mini-hole events frequently appear in the Northern Hemispheric mid and high latitudes.

In tropics and mid-latitudes, synoptic scale ozone-rich regions are associated with synoptic scale weather systems. These ozone-rich regions form due to the advection of ozone-rich airmass from higher latitudes to lower latitudes and lowering of tropopause over synoptic scale wave troughs. They also exhibit growth and decay over a few days.

Number of synoptic scale total ozone anomaly events caused by meteorological disturbances is low in the tropics compared to the extratropics. Because of this reason, fewer studies have been made about such ozone variabilites in the tropics especially in Asia. On occasions, remnants of extratropical cyclones and upper tropospheric troughs/ridges, reach tropical Asia (even very close to equator). One such long wave is seen as Upper Tropospheric Trough (UTT) in zonal westerly winds during winter season in tropical Asia and another one as Upper Tropospheric Blocking High and Trough (UTBHT) pattern in summer. Although their circulation characteristics and associated rainfall activity have been studied in detail, relatively less importance has been paid to the total ozone variations associated with them. Since these two waves are present around the tropopause level, they are expected to generate large ozone anomalies by variations of the stratospheric depth also. These waves are also expected to exchange ozone between tropical upper troposphere and extratropical lower stratosphere, *via* tropopause break as noticed by Mani et al., (1973). Aim of the present work is to highlight the total ozone variations caused by these two upper tropospheric long waves over Asia. A few well-developed cases of these two events have been considered randomly for this study. Circulation features of these two types of long waves have been analysed using NCEP/NCAR reanalysis data. Total ozone variations have been studied using satellite measured total ozone data.

6.2. Data

Daily streamline maps of 200 hPa are obtained from NCEP/NCAR reanalysis data for winter (January and February) and summer (July and August) months to identify the presence of UTTs and UTBHTs. Monthly

mean temperature at 17 levels with same horizontal resolution as for wind of 1982-94 period has been taken from NCEP/NCAR reanalysis data to obtain the climatology of the vertical distribution of temperature and the location of tropopause break.

TOMS version-7 (onboard Nimbus-7 satellite) data set has been used to study the variations in total ozone associated with these upper tropospheric long waves over Asia. Details regarding the break periods in Indian Summer Monsoon have been taken from De et al., (1998).

6. 3. The Characteristics of upper tropospheric long waves over Indian subcontinent and associated ozone variations

6. 3. 1 Winter-time westerly Upper Tropospheric Troughs (UTT)

During northern hemispheric winter, upper tropospheric waves of zonal westerly flow in the middle latitudes take more southerly location. On occasions these waves develop into large amplitude north-south oriented troughs that penetrate deep into south Asia. Occasionally some of these troughs extend even upto near equatorial latitudes in winter season. Under the influence of overlying UTTs, lower tropospheric low-pressure systems form, intensify and move eastwards. Indian meteorologists refer to these eastward moving lower tropospheric circulation features as *western disturbances* to differentiate them from the main westward moving tropical disturbances over this region. The western disturbance tracks reach the southern most position in January and February months. Singh (1963), Dutta and Gupta (1967) and Singh (1979) brought out the close relation existing between the UTTs and the formation, intensification and movement

of the lower tropospheric disturbances. Singh (1979) made a detailed case study of vertical structure of a UTT and its interaction with lower troposphere over the Indian region.

Generally the UTTs occur in between 500 hpa and 100 hPa levels and persist for less than a week during winter months over south Asia. UTTs are followed by cold polar jet stream from north. Singh (1979) noticed that the northerly polar jet associated with the UTT becomes more prominent at 200 hPa than the Subtropical Jet stream (STJ) and the later rose to 150 hPa from 200 hPa. He showed that the wind speed in the northerly polar jet is 100 - 165 knots for the December 1974 – January 1975 case. A case study of a UTT is also reported by Joseph (1967).

6. 3. 2 Summer-time Upper Tropospheric Blocking Highs and Trough (UTBTH)

In summer season, the Inter Tropical Convergence Zone moves as far as 30° N in July over south Asia and is accompanied by strong cross equatorial lower tropospheric wind flow from southern hemisphere in the form of Indian summer monsoon. At the same time, the polar front shifts to its northern most position far away from Indian region. India gets about 80% of its annual rainfall during the summer monsoon season (June to September). Indian summer monsoon rainfall (ISMR) activity shows strong intraseasonal variability. Summer monsoon season is characterized by active and break periods. In active period, the whole Indian subcontinent experiences widespread rainfall. During break periods, rainfall activity abruptly weakens over India and dry weather prevails over most parts of India. The low-pressure monsoon trough in the lower troposphere shifts

from its normal position over central India to foothills of Himalayas in the north. Break periods are identified by the weakening of rainfall activity, shift in the position of monsoon trough, departure in the surface pressure, changes in wind direction, and the presence of upper tropospheric trough over India.

It is well known that during break periods (or simply breaks) upper tropospheric westerly troughs in midlatitudes penetrate deep into the south Asian region (Ramaswamy, 1962). Raman et al., (1980) found that the breaks were associated with stagnant upper tropospheric blocking ridge over the east Asia along ~ 100°E, extending from 35°N to 70°N. Raman and Rao (1981) presented a model for the evolution of blocking highs one over East Asia and another over West Asia with a deep wave trough in between during prolonged break monsoon situations.

Details about the breaks in Indian summer monsoon activity has been provided by both De et al., (1998) and Webster et al., (1995). For the present study the break periods listed by De et al., (1998) has been used. They identified 193 break days (33 break spells) during 1968-97 (30 years) period. Breaks appear once or twice in most of the years during summer monsoon season (one in 17 years, 2 in 8 years and zero in 5 years in the above 30 year period). Duration of the break period is highly variable. It varies from few days to a few weeks (20 days in 1979). Once break period comes to an end, widespread rainfall activity gets restored over whole of India again. Breaks that occurred during 1988-97 (ten year) period taken from De et al., (1998) has been presented in Table. 6. 1

Year	No of Breaks	Period	No of Break Days
1988	2	5-8 July, 13-15 August	4, 3
1989	2	10-12 July, 29-31 July	3, 3
1990	2	8-10 July, 27-31 July	3, 5
1991	1	3-9 September	7
1992	-	-	-
1993	1	19-21 July	3
1994	-	-	-
1995	1	12-15 August	4
1996	1	1-5 July	5
1997	-	-	-

Table 6.1 Breaks during 1988-1997 (De et al., 1998)

Daily 200 hPa streamlines obtained from NCEP/NCAR reanalysis wind data have been used to study the circulation characteristics of the UTBTH situation during break periods in ISMR activity. In fig. 6.1, the composite picture of the 200 hPa streamlines corresponding to one of the longest breaks that appeared during 1968-97 period is presented. It started on 17 July 1972 and ended around 3 August 1972 in the middle of the summer monsoon season. This represents the typical upper tropospheric circulation during break monsoon condition with two upper tropospheric ridges, one over East Asia and another over West Asia and a deep trough intruding into south Asia. Detailed examination of the streamline charts corresponding to these break days shows the presence of cut-off low in the trough region on individual days (not seen in composite). The blocking

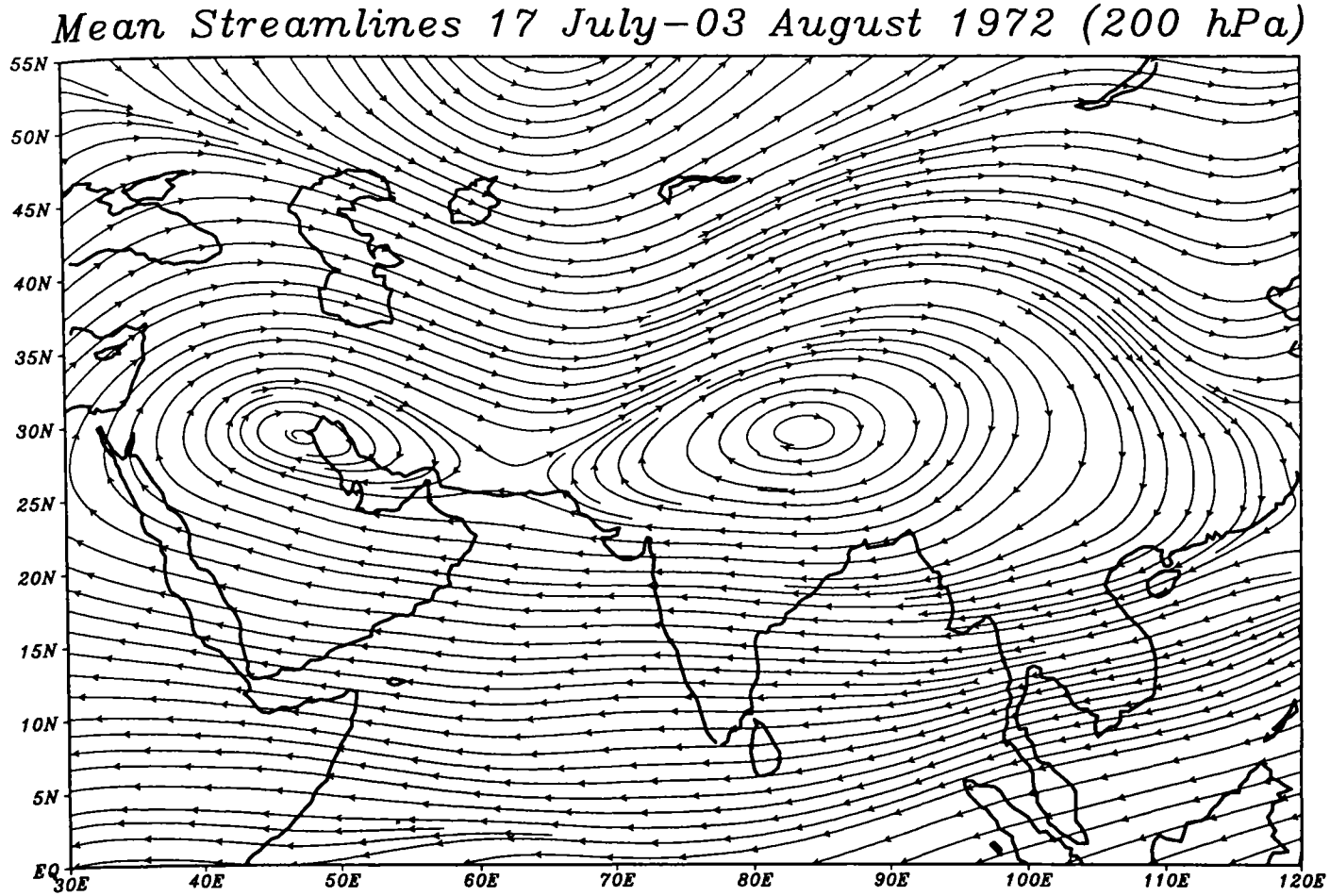

Fig. 6.1 Mean 200 hPa streamlines for the 17 July – 3 August 1972 break period in Indian summer monsoon.

pairs prefer to occur in the same latitude belt and the most favoured latitude for their centers is around 30° N, the east one generally appear over Eastern Tibet and the west one somewhere from Egypt to Iran at 200 hPa. Once the break condition ends and active monsoon condition get established over the Indian region, the Tibetan high shifts westwards. This stationary UTBHT condition persists during break periods in the Indian summer monsoon season over Asia. This wave pattern is similar to the Asia Pacific wave of May reported by Joseph and Srinivasan (1999).

6. 3.3 Upper tropospheric long waves and total ozone variations

In fig. 6.2, the meridional cross-section through India of the 13 year (1982-94) mean temperature averaged over Indian longitudes (50°-100° E) is presented for January-February (winter) and July-August (summer) months. A break is seen between tropical and extratropical tropopauses in these figures. The zone of westerly winds and the break region are at more northern latitudes during the summer season. The 14 year (1979-92) mean January-February and July-August total ozone distribution for the Northern Hemisphere (0°-55°N) are presented in fig. 6.3. The total ozone increases from the equator towards the pole. Gradient of the total ozone is relatively more in the 25°-45° N latitude belt in January-February and 35°-50° N latitudes in July-August. Total ozone variations are negligible in lower latitudes upto 20° N in both the seasons. At about 200 hPa level (~ 12 km altitude) where these two waves are present in large amplitude, steep meridional ozone gradient exist (see fig. 5.8) between tropical upper troposphere and extratropical lower stratosphere and mutual exchange is possible between these two regions due to the presence of tropopause break there. The northwesterly flow to the west of the trough in these two cases is

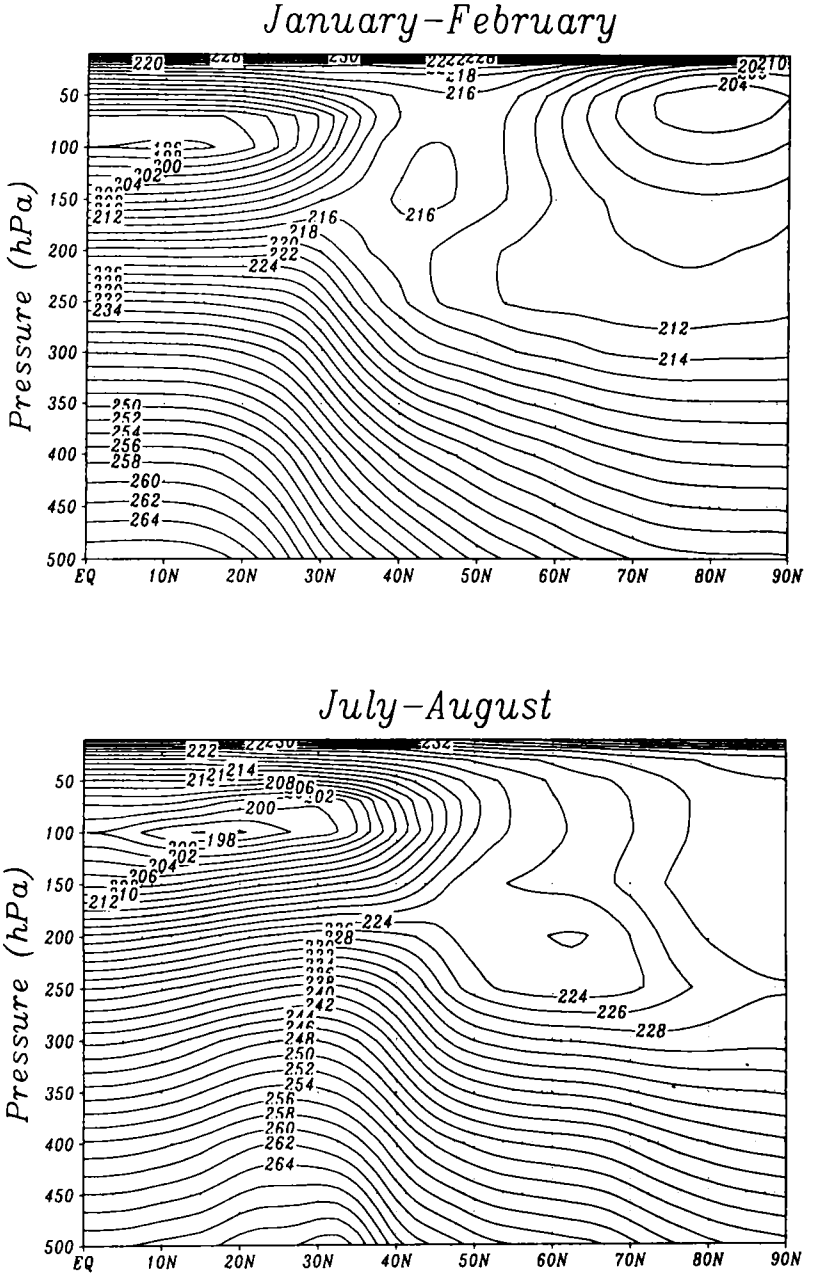

Fig. 6.2. 13 year (1982-94) climatology of the latitude – height distribution of temperature (°K) for January – February (winter) and July – August (summer) months averaged between 50° E and 100° E longitudes. Contour interval is 2°K.

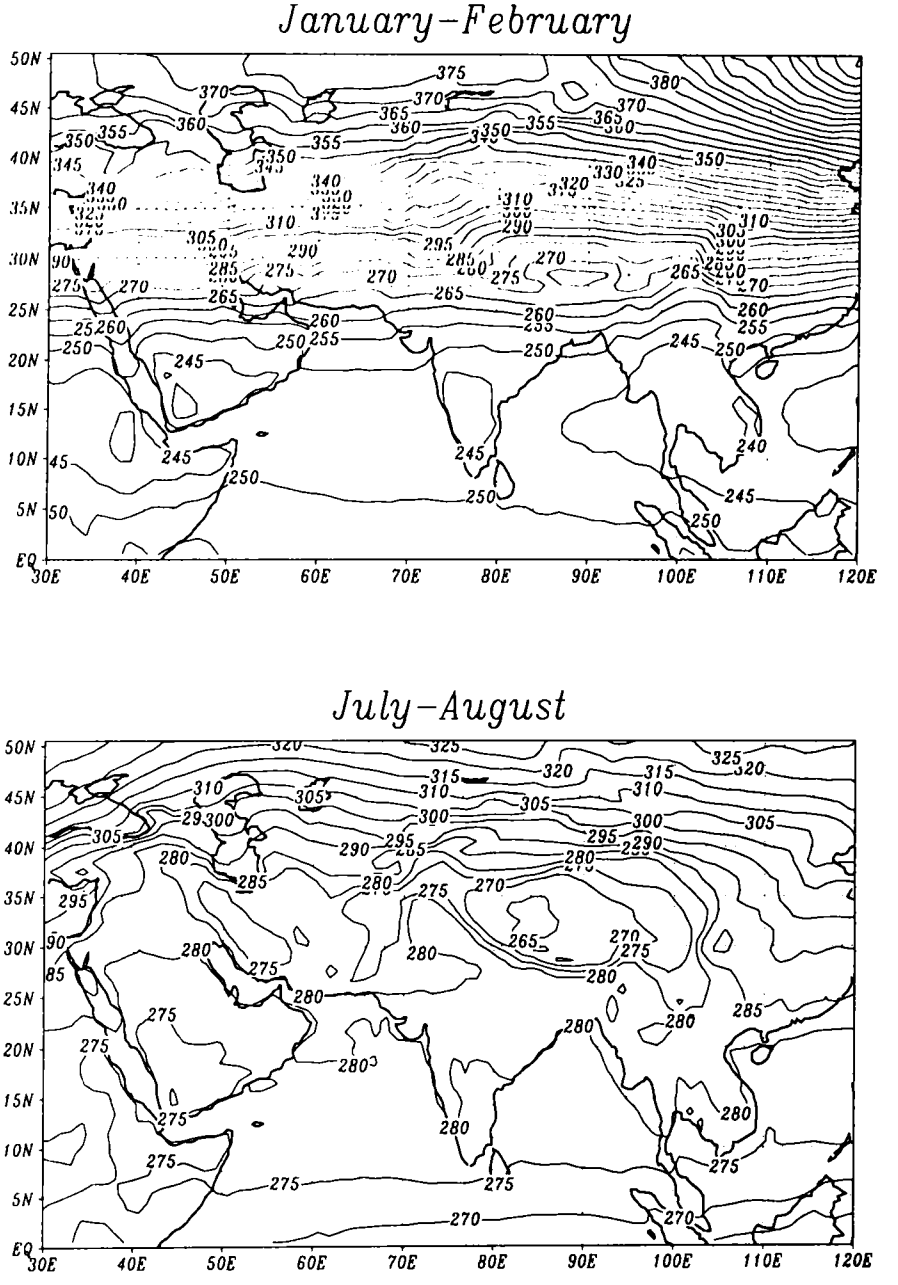

Fig. 6.3 . Climatological (1979-92) distribution of total ozone (Dobson Units) over Asia for January-February (winter) and July-August (summer). Contour intercal is 5 DU.

likely to transport ozone-rich extratropical lower stratospheric airmass into the tropical troposphere over south Asia and increase the total ozone content over this region. In the east of the trough and to the west of the blocking high, the existing southwesterly airflow is expected to transport ozone-poor tropical tropospheric air to the extratropical lower stratosphere.

More importantly a trough in upper troposphere lowers the tropopause, thereby enhancing the stratospheric column and hence the total ozone column. On the other hand, ridge decreases the stratospheric column and hence the total ozone amount. Thus by the transport of ozone rich airmass from higher latitudes and the increase in stratospheric column, total ozone increases over the trough region. Conversely by the transport of ozone poor airmass from low latitudes and the decrease in stratospheric column, total ozone decrease over the ridge region. In the present work, attempt has been made to study the total ozone variations associated with these waves over Asia using satellite measured total ozone.

6. 4. Case studies

6.4.1 Winter season

Case studies of 2 UTTs are presented in this section. The troughs in these cases are at different longitudes, over south Asia and these UTTs moved very slowly eastwards. These typical cases with deep troughs extending across the tropopause region were chosen from the period 1979 to 1992. In general, this large amplitude slow moving waves that penetrate deep into tropical Asia is expected to cause synoptic scale ozone variations for few days like in midlatitudes. But the presence of near uniform total

ozone distribution (also in the upper troposphere, see fig. 6.3) and the increase in the height of the tropopause towards the equator in tropics are expected to make the situation slightly different.

6.4.1.1 January 01-04, 1988 UTT (55° E Longitude)

In the 200 hPa streamline chart, this UTT is seen in the form of a deep cyclonic flow over Caspian sea, Arabian peninsula and Arabian sea on 1 January. The north-south extent of the trough is between 55°N and 5°N latitudes during 1-2 January. The northern portion of the trough moved east and the southern portion remained practically stationary. A well-developed ridge is seen east of the trough at 90°E at this level. The trough weakened after 4 January.

In fig. 6.4, the 200 hPa streamlines at 1200 UTC, geopotential height of 200 hPa at 1200 UTC and Total Ozone Anomaly (TOA) for 3 January 1988 are presented. Anomalies are the deviations from January and February climatological total ozone values. The TOA plot shows the signatures of changes in circulation and tropopause height associated with the upper tropospheric trough/ridge. An area of positive TOA is seen over Saudi Arabia, Iraq and Iran regions. The southward extent of this anomalous region is seen upto 20° N latitude. Maximum TOA over this region is 60 DU, which is about 25% more than the January – February climatological mean over this region. The magnitude of total ozone variability in this case is comparable with those of extratropical ones. Though the cyclonic trough is seen southwards upto 5° N, positive TOA pattern is limited north of 20° N latitude and no signatures of ozone variation is seen beyond this latitude. The uniform ozone distribution

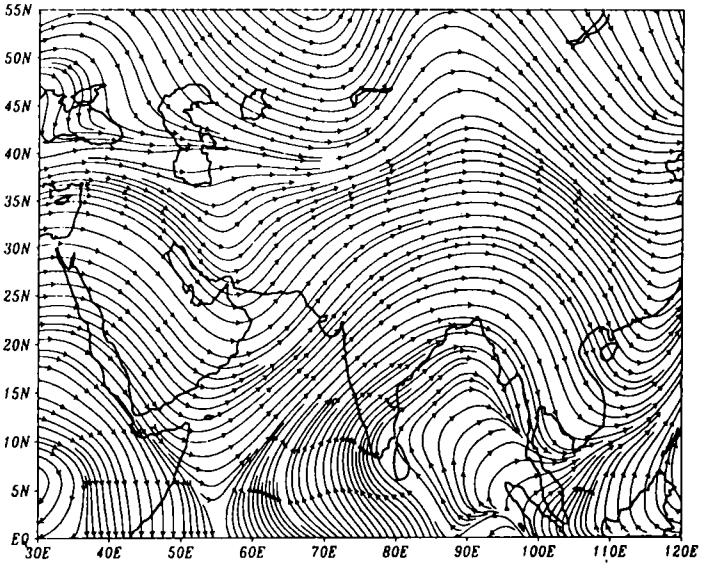

(a)

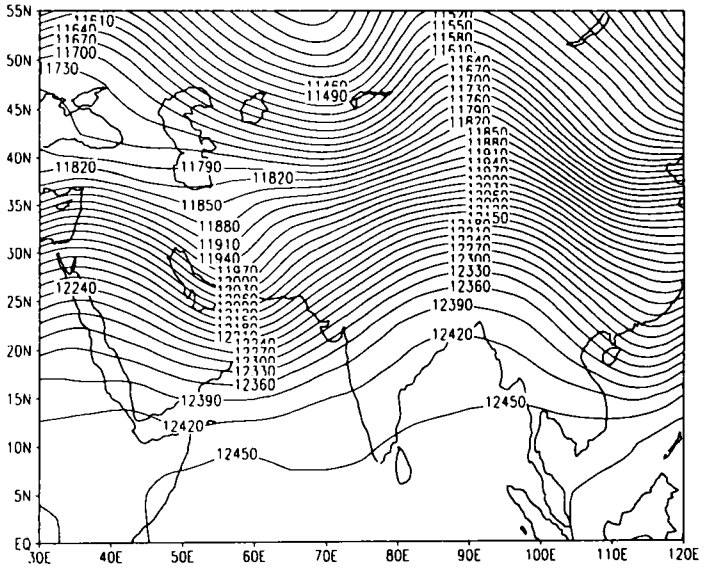

(b)

Fig. 6.4 a) 200 hPa streamlines at 1200 UTC for 3 January 1988 b) Geopotential height (gpm) of 200 hPa at 1200 UTC for 3 January 1988 (Contour interval is 30 gpm) and c) Total ozone anomaly from January-February climatology (Contour interval is 10 DU) in Dobson units for 3 January 1988.

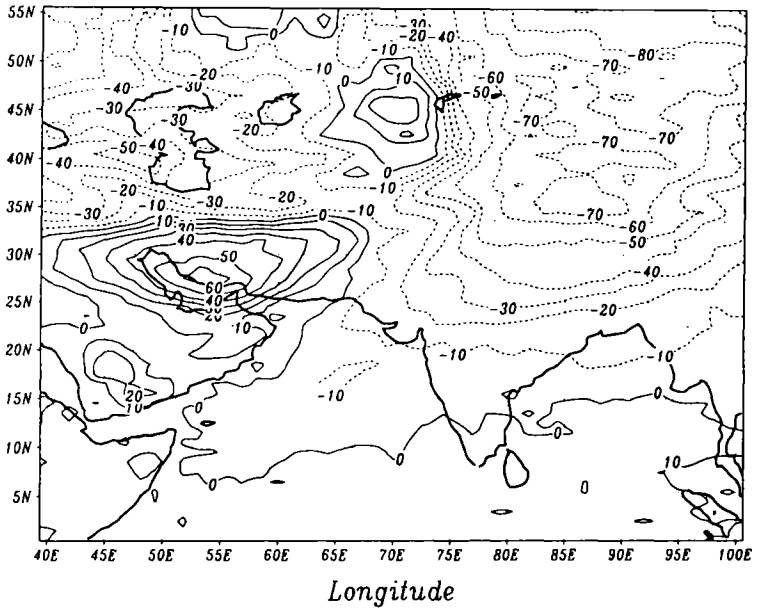

(c)

Fig. 6.4 (Continued)

encountered by the airmass once it reaches 20° N latitude from north and the increase in the tropopause height towards equator may be the cause for the insignificant TOA in the tropical region.

An area of negative TOA is seen east of 85° E longitude and north of 20° N latitude in the region of southwesterly flow west of the ridge and east of the UTT. As suggested earlier, the ozone-poor air transport from tropical upper troposphere to the ozone rich extratropical lower stratosphere and the decrease in stratospheric column may be the cause for this low total ozone over this region. It is seen that both the positive and negative anomalies are elongated in the east-west direction. This may be due to the strong zonal component of the wind that moves the meridionally transported ozone to the east.

6.4.1.2 February 24-28, 1992 UTT (90°E Longitude)

In the 200 hPa streamline chart, trough is seen over India, Bangladesh regions on 24 February, intensified during 25-27 February and weakened afterwards. The trough has shown slow eastward movement and is seen over Indo-China on 28 February. A ridge is seen west of the trough in the same level. In fig. 6.5, 1200 UTC streamline charts at 200 hPa and TOA for 26 February are presented. Area of positive TOA is seen over Bangladesh-Indian region over the trough. The values of the maximum TOA in this case reached as high as 100 DU and the area of positive anomaly is seen upto 15° N latitude. An area of negative TOA with values of 50 DU below the climatological values is seen over a large area in the field of the southeasterly flow west of the ridgeline, which transports ozone-poor air from the tropics.

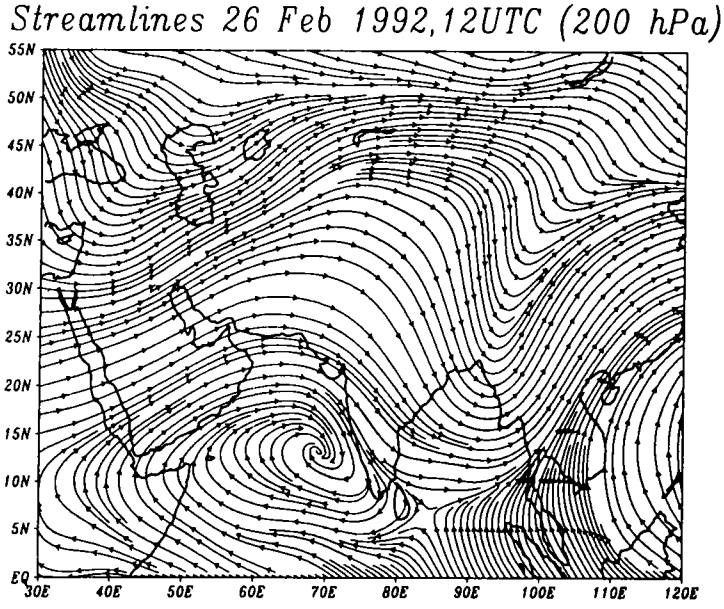

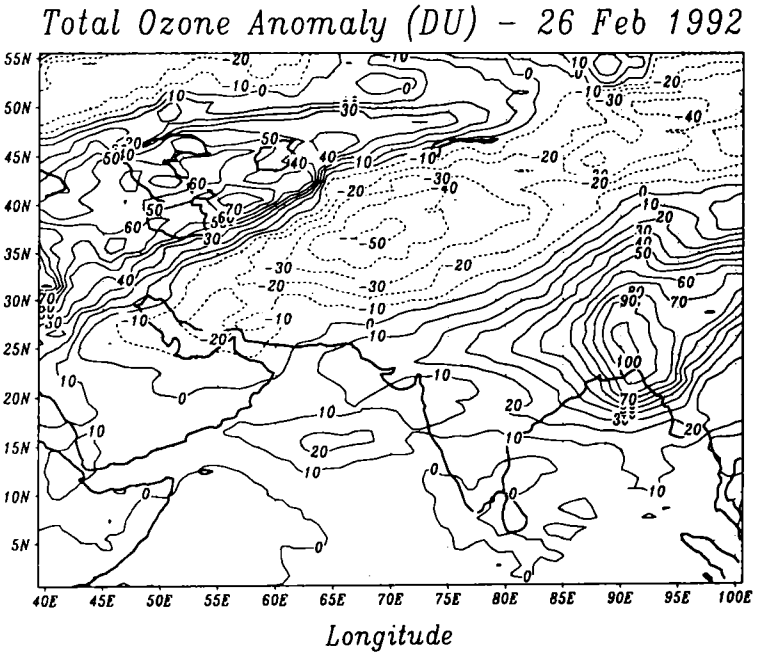

Fig. 6.5 Same as fig. 6.4 (without geopotential height), but for 26 February 1992.

These two cases of UTT show the occurrence of large ozone anomalies in association with the phase of the upper tropospheric waves over tropical Asia.

6.4.2 Summer season

From the 33 break situations listed by De et al., (1998) during 1968-97 period, 2 cases that occurred during the mid-summer monsoon season (July, August) have been selected from the 1979-92 period (TOMS data from Nimbus-7 satellite were available only during this period) to find the ozone variations associated with the UTBTH seen in the upper troposphere during break monsoon period. Daily 200 hPa streamline chart obtained from u, v fields has been analysed to study the circulation features during these two breaks over south Asia. These breaks are characterized by two blocking highs, one over eastern Tibet and another over west Asia accompanied by a trough in between them at 200 hPa level. In these cases, the distance between the blocking highs is relatively small for 1981 case compared to 1987 case. If the blocking highs are relatively much apart, the trough in between them is likely to penetrate deep into tropical latitudes. This is clear from the existence of well-developed trough in between the blocking highs in 1987. On individual days, the trough in this year penetrated deep into the tropical latitudes and a cut-off low formed in the trough region. Generally UTBHT are stationary and we have presented composites for each case.

The mean 200 hPa streamline chart, and composite TOA (deviations from July climatology) for the first break (26 July - 31 July, 1981) are shown in fig. 6.6. The mean 200 hPa streamline chart, mean 200 hPa

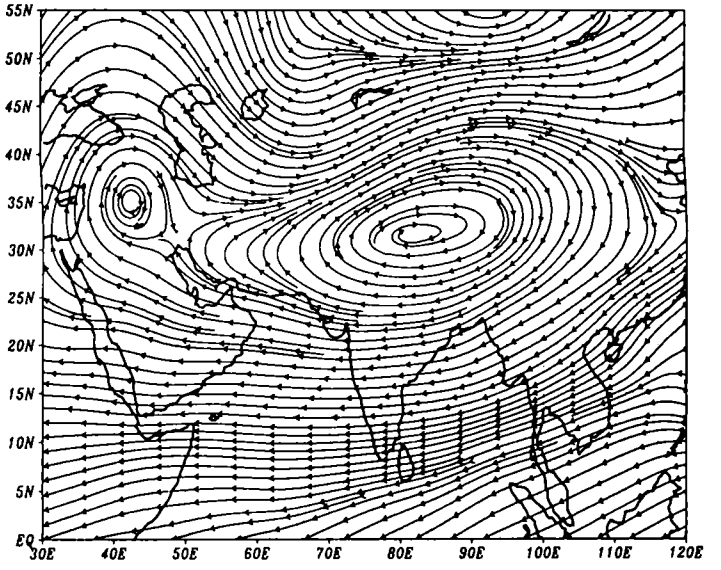

(a)

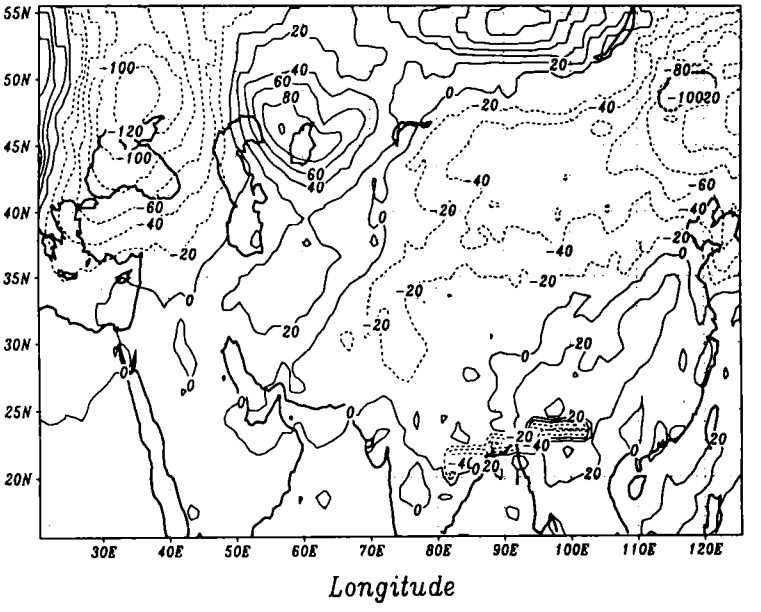

(b)

Fig. 6.6. a) Mean 200 hPa streamlines for the break in Indian summer monsoon during 26-31 July 1981, and b) Mean total ozone anomaly from July climatology for 26 – 29 July 1981 (Contour interval is 20 DU). [Ozone data was missing for some days over Bangladesh, Myanmar regions].

geopotential height for the second break (28 July - 1 August, 1987) and mean total ozone anomaly from July climatology for 28 July - 31 July 1987 are presented in fig. 6.7. To avoid major gaps in the total ozone data, TOA anomaly is computed for the days when adequate data coverage is available. Large amount of ozone variations taking place caused by the wind flow associated with blocking high and trough and variations in stratospheric column is reflected in these plots. Important feature seen in these figures are the large total ozone increase in the trough regions and decrease in ridge regions. The magnitude of ozone variations is comparatively more than the UTT case. Although the 1981 break is seen during 26-31 July period, the TOA composite is computed only for 26-29 July due to the large ozone data gaps present during the remaining two days.

The 1981 ozone anomaly chart shows two areas of pronounced negative TOA associated with the western blocking highs over a region north of Black sea and an area of positive TOA along the trough east of Caspian sea. The maximum value of positive TOA reached as high as 100 DU and negative TOA reached as low as –120 DU, which is about 30% more, and 35% less than the July climatology respectively. The 1987 case also showed large areas of positive and negative TOA. Eastward tilt in the trough from south and its southward extension is reflected well in the positive anomaly pattern. The maximum positive TOA has reached upto 100 DU and negative values upto –80 DU, which is about 35% more, and 25% less than the July climatology. Unlike the UTTs, the UTBHT are stationary in their position. In prolonged break periods, the negative TOA over ridge may increase the ground level UV-B radiation considerably due to the presence of sun near Tropic of cancer.

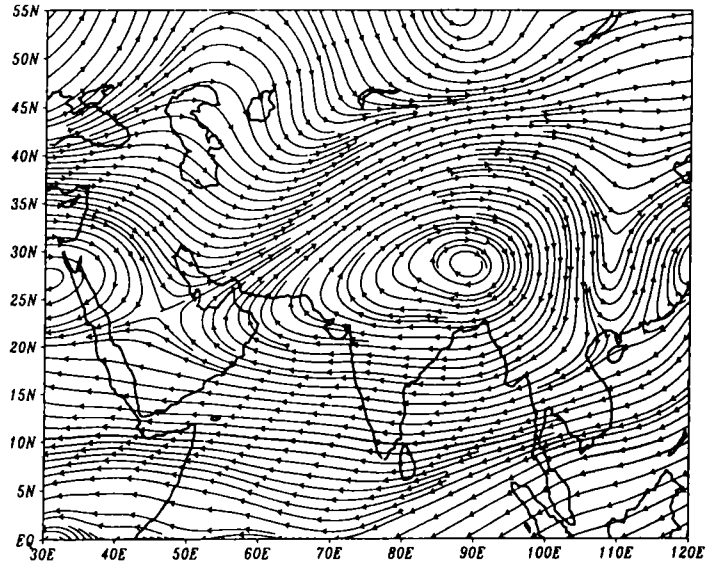

(a)

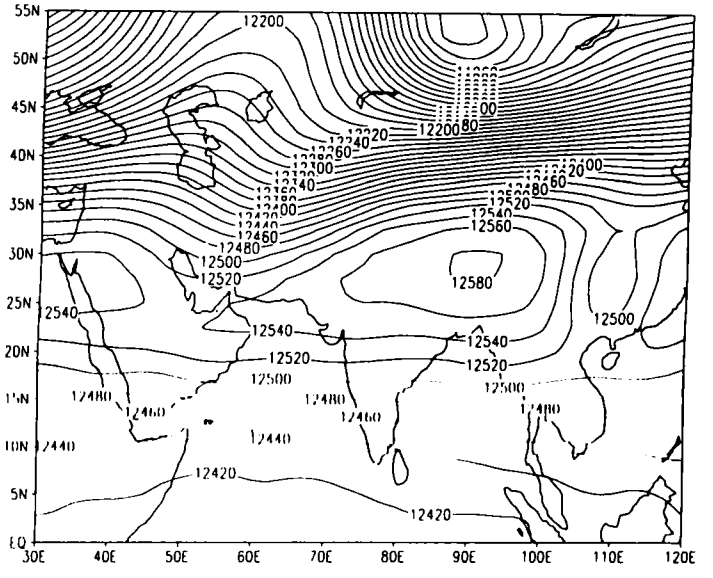

(b)

Fig. 6.7 a)Mean 200 hPa streamlines for the break in Indian summer monsoon during 28 July – 1 August 1987, b) Mean 200 hPa geopotential height (gpm) for 28 July – 1 August (Contour interval 20 gpm) and c) Mean total ozone anomaly from July climatology for 28 – 31 July 1987 (Contour interval is 20 DU). (No data areas are marked by stippling). [Ozone data was missing for some days over Red Sea].

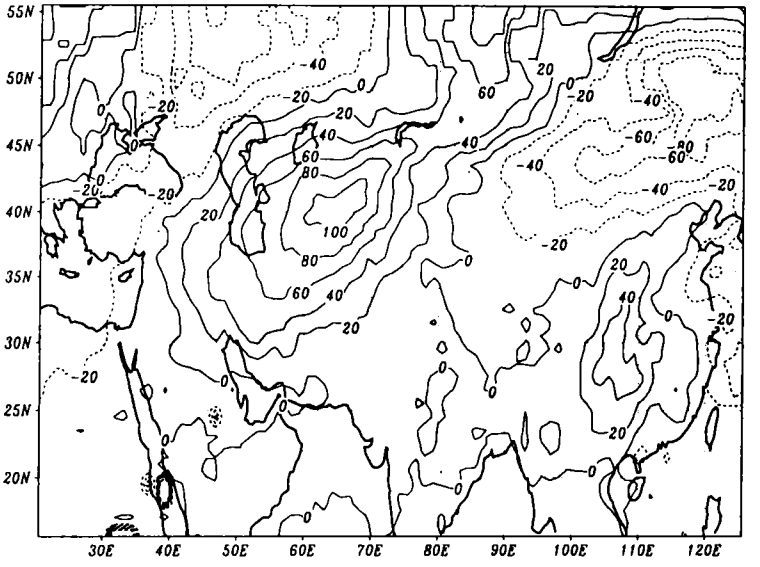

(c)

Fig. 6.7 (Continued)

The UTT moves eastward with time generally with very slow speed. It produces total ozone variations even in the tropical latitudes. The UTBHT is stationary over Asia for several days. The magnitudes of TOA generated by UTBHT are relatively more than that of UTT. The UTBHT produces TOA over latitudes north of India. The intense anomalies associated with UTBHT are possibly because of the stationary nature of UTBHT. The large negative TOA anomalies associated with UTBHT pose severe health threat to the people of central Asia by the presence of overhead Sun in summer and possible increase in surface UVB radiation than that of UTT.

6.5 Summary

Ozone perturbations caused by two upper tropospheric long waves in winter and two upper tropospheric blocking high and trough of summer seasons over south and central Asia were presented. The wintertime UTT and the ridges following and preceding it occasionally penetrate deep into south Asia on synoptic time scales and create positive and negative TOA over these areas. Values of TOA reached upto ± 25-35 % during this condition over south Asia.

In summer season, UTBHT situation develops over south Asia during the break periods in the Indian summer monsoon. This situation persists for a few days to a few weeks and creates negative and positive TOA over south and central Asia. Positive TOA reaches values of the order of 100 DU and negative TOA upto –140 DU depending upon the strengths of the blocking highs and troughs. The negative TOA reached even 50% less than the long-term mean in some areas during these episodes and

created a sort of *mini ozone hole* like situation. Negative total ozone perturbations are likely to increase the amount of harmful UV-B radiation reaching the ground considerably in these situations particularly as UTBHT occur during summer with sun over head which increases the solar UV radiation over these areas for a period of few days to weeks. Increased columnar ozone over the trough decreases the ground level of UV radiation over the trough region.

Chapter –7

Summary and Conclusions

7.1 Summary and conclusions

Some aspects of stratosphere-troposphere interactions like biennial timescale interaction over near equatorial region, the interannual to synoptic timescale stratosphere-troposphere ozone exchanges caused by longwaves are studied using NCEP/NCAR reanalysis data, high-resolution radiosonde data, satellite measured global total ozone data, etc and the results are discussed in this thesis. Major outcomes of the study are presented as follows.

The biennial timescale interactions between lower stratosphere and troposphere over Thumba is analyzed using high-resolution radiosonde data. Signals of oscillation with periods ranging from 20-32 months were found in the tropospheric temperature over this near-equatorial Indian station. The phase of the TBO in temperature did not vary with height from surface to the level of tropopause and was associated with the intensity of the Indian monsoon rainfall. A QBO signal is seen in temperature in the lower stratosphere. Examination of the phase of the biennial mode in temperature in lower stratosphere and troposphere showed decadal change in the phase coherence between 1971-81 and 1982-92 periods. Marked differences in amplitudes of QBO and TBO were also noticed between these dacades. During the first decade the downward propagating phase of QBO was disturbed in the 18-23 km altitude.

These results and the correlations suggested not an association between TBO and QBO, but rather a lack of association between the two phenomena. The results suggest that TBO and QBO are two different phenomena with nearly biennial periodicity. Strong relation exists between TBO in temperature over Thumba and Indian summer monsoon activity.

During strong Indian monsoons the temperature TBO is in positive phase. Of the 4 weak Indian monsoons except in 1979 TBO is in negative phase. The results suggest that the observed biennial variability in the tropospheric temperature over Thumba may be due to the monsoon-ocean-atmosphere interactions taking place over Indian Ocean region in biennial time scales.

Interannual timescale meridional stratosphere-troposphere exchanges caused by the newly documented Asia Pacific Wave (APW) were analyzed using ozone as tracer of atmospheric motion. Analysis of the NCEP/NCAR reanalysis wind data showed the presence of a stationary Rossby wave in the lower stratosphere during May. This wave is seen prominently below 70 hPa level, confined between 10°N and 50°N latitudes and has a zonal wave number of 6 or 7. It is an extension into the stratosphere of the Asia Pacific Wave of the troposphere documented by Joseph and Srinivasan (1999). This wave shows a phase shift of 20° longitudes between deficient and excess ISMR years. This shift is due to the shift in the longitudinal position of the convective heat sources associated with the ITCZ.

Since the APW is present between 70 hPa and 500 hPa levels, it couples the lower stratosphere and troposphere directly. Since the maximum amplitude of the APW is in tropopause break region, the APW is able to transport ozone rich extratropical lower stratospheric air into tropical upper troposphere and ozone poor upper tropospheric air into the extratropical lower stratosphere effectively through the tropopause break region, which in turn can affect the total ozone distribution. Analysis of the global total ozone measurements by the TOMS instrument onboard Nimbus-7 satellite showed the signatures of the APW. Since the phase of APW changes through 20° longitudes between extreme Indian summer

monsoon years, the APW affects the total ozone distribution over large areas of the globe on interannual timescales. Analysis of the NCEP/NCAR data during the summer monsoon season and the following autumn season showed the presence of APW and its signature on global total ozone distribution during these seasons. The amplitude of the total ozone anomalies caused by APW is about 5-10% from climatology. Counter-part of the APW is also seen in Southern Hemisphere. During May and the following summer monsoon months, solar radiation is maximum in the Northern Hemisphere, and the negative anomalies in ozone thus pose health hazards due to increased UV-B radiation.

Synoptic timescale meridional stratosphere-troposphere exchanges caused by subtropical upper tropospheric long waves over Asia were studied using global total ozone measurements from TOMS. One such long wave is seen as Upper Tropospheric Trough (UTT) in zonal westerly winds during winter season in the tropical Asia and another one as Upper Tropospheric Blocking High and Trough (UTBHT) pattern in summer over Asia. The characteristics of these two waves are studied using NCEP/NCAR reanalysis data. These waves occasionally develop large amplitudes when the associated north-south wave troughs span across the break region between the tropical and extra-tropical tropopauses. Exchanges of ozone poor air mass from the tropical upper troposphere to the extratropical lower stratosphere and ozone rich air mass from the extratropical lower stratosphere to the tropical upper troposphere *via* the tropopause break region occurs associated with these large amplitude waves, due to the presence of steep meridional ozone gradients around these levels. Since these waves are present around the tropopause level, these wave troughs and ridges deflect the tropopause. A trough in upper

troposphere lowers the tropopause, thereby enhancing the stratospheric column and hence the total ozone column. On the other hand, ridge decreases the stratospheric column and hence the total ozone column.

Analysis of the global total ozone data from Nimbus-7 TOMS shows the signatures of the total ozone anomalies generated by these waves. Values of TOA from long climatology reached upto ± 25-35 % during the UTT conditions over south Asia. The summer time UTBHT situation persists for a few days to a few weeks and creates negative and positive TOA over Asia. Positive TOA generated by UTBHT reaches values of the order of 100 DU and negative TOA upto –140 DU depending upon the strengths of the blocking highs and troughs. The negative TOA reached even 50% less than the long-term mean in some areas during these episodes and created a sort of *mini ozone hole* like situation. The negative TOA anomalies associated with the UTBHT is expected to increase the amount of ground level UV-B radiation in Asia over large areas in summer season.

7.2 Scope for future studies

The meridional transport of ozone between extratropical lower stratosphere and tropical upper troposphere by APW, UTT and UTBHT can be studied and quantified using the ozonesonde vertical profiles and potential vorticity maps around tropopause levels. Since the global ozonesonde data can be obtained easily from the archives of World Ozone and Ultraviolet Radiation Data Centre, Canada and the potential vorticity data from NCEP/NCAR reanalysis data sets, detailed study about the vertical structure of the meridional transport can be made. Effect of the interannual timescale total ozone anomalies caused by APW on the long-

term trend in total ozone over a region can be estimated for the realistic computation of the trend. This research work can be extended to study the influence of decadal scale epochal nature in Indian summer monsoon activity on the APW generated total ozone anomalies around the globe and the trend estimates in total ozone. Total ozone anomalies generated by the counter-part of the APW in Southern Hemisphere during austral summer can be studied using TOMS data. Based on these observational evidences, modeling studies can be initiated about the stratosphere-troposphere exchange processes for a better understanding on stratosphere-troposphere interactions.

References

Andrews, D.G., et al., 1987: Middle Atmosphere Dynamics, *Academic Press Inc., Orlando.*

Angell, J. K., and J. Korshover, 1964: Quasi biennial oscillations in temperature, total ozone and tropopause height, *J. Atmos. Sci*, ***21***, 479-492.

Angell, J. K., and J. Korshover, 1970: Quasi biennial, annual, and semi annual zonal wind and temperature harmonic amplitudes in the stratosphere and lower mesosphere of the Northern Hemisphere, *J. Geophy. Res.*, ***75***, 543-550.

Angell, J. K., and J. Korshover, 1973: Quasi biennial and long term fluctuations in total ozone, *Mon. Wea. Rev.*, ***101***, 426-443.

Angell, J. K., and J. Korshover, 1974: Quasi biennial and long term fluctuations in the centers of action, *Mon. Wea. Rev.*, ***96***, 778-784.

Angell, J. K., and J. Korshover, 1975: Evidence for a quasi-biennial variation in eccentricity of the north polar vortex, *J. Atmos. Sci*, ***32***, 634-635.

Baldwin, M. P., and T. J. Dunkerton, 1998. Biennial, quasi-biennial, and decadal oscillations of potential vorticity in the northern stratosphere, *J. Geophys. Res.*, **103**, 3919–3928.

Baldwin, M. P., and T. J. Dunkerton, 1999: Propagation of the Arctic oscillation from the stratosphere to the troposphere, *J. Geophy. Res.*, ***104***, 30,937-30,946.

Baldwin, M. P., 2000: The Arctic oscillation and its role in stratosphere-troposphere coupling, *SPARC News Lett.*, ***14***, 10-14.

Baldwin, M. P., et al., 2001: The Quasi Biennial Oscillation, *Rev. Geophys.*, ***39***, 179-230.

Baray, J. –L., G. Ancellet, T. Randriambelo, and S. Baldy,1999: Tropical cyclone Marlene and stratosphere troposphere exchange, *J. Geophy. Res.*, ***104***, 13953, 13970.

Baray, J. –L., V. Daniel, G. Ancellet, and B. Legras, 2000: Planetary scale tropopause fold in the southern subtropics, *Geophy. Res. Lett.*, ***27***, 353-356.

Beekkmann, M., et al., 1997: Regional and global tropopause fold occurrence and related ozone flux across the tropopause, *J. Atmos. Chem.*, ***28***, 29-44.

Bhalme, H. N., and S. K. Jadhav, 1984: The southern oscillation and its relation to the monsoon rainfall, *J. Climatol.*, ***4***, 509-520.

Bhalme, H. N., S. S. Rahalkar, and A. B. Sikdar, 1987: Tropical quasi biennial oscillation of the 10 mb wind and Indian monsoon rainfall - Implications for forecasting, *J. Climatol.*,*7*, 345-353.

Bowman, K.P., and A. J. Krueger, 1985: A global climatology of total ozone from the Nimbus-7 total ozone mapping spectrometer, *J. Geophys. Res.*, ***90***, 7967-7976.

Bowman, K. P., 1989: Global pattern of the quasi biennial oscillation in total ozone, *J. Atmos. Sci.*, ***46***, 3328-3343.

Brasseur, G., and S. Solomon, 1984: Aeronomy of the middle atmosphere, *D. Reidel Publishing Company, Dordrecht.*

Brewer, A. W., 1949: Evidence for a world circulation provided by the measurements of helium and water vapour distribution in the stratosphere, *Quart. J. Roy. Met. Soc.*, ***75***, 351-363.

Chakrabarty, D. K., et al., 1998: Long-term trend of ozone over the Indian region, *J. Geophy. Res.*, ***103***, 19245-19251.

Chang, C -P., and T. Li, 2000: A theory for the tropical tropospheric biennial oscillation, *J. Atmos. Sci.*, ***57***, 2209-2224.

Chanin, M. –L., 2001: Stratospheric ozone and its impact on climate change, *WMO Bulletin, **50**,* 41-45.

Chen, P. R., 1992: Evidence for the ionospheric response to the QBO, *Geophy. Res. Lett., **19***, 1089-1092.

Clarke, A. J., X. Liu, and S. Van Gorder, 1998: Dynamics of the biennial oscillation in the equatorial Indian and far western Pacific oceans, *J. Climate.*, ***11***, 987-1001.

Daubechies, I., 1990: The wavelet transform time-frequency localization and signal analysis, *IEEE Trans. Inform. Theory.*, ***36***, 961-1004.

De, U. S., R. R. Lele, and J. C. Natu, 1998: Breaks in southwest monsoon, *Prepublished Scientific report – 1998/3,* India Meteorological Department.

Dobson, G. M. B., et al., 1929: Measurements of the amounts of ozone in the earth's atmosphere and it's relation to other geophysical conditions: Part III, *Proc. Roy. Soc. London, A* ***122***, 456-486

Dobson, G. M. B., 1956: Origin and distribution of the polyatomic molecules in the atmosphere, *Proc. Roy. Soc. London, A* ***236***, 187-193.

.Dunkerton, T. J., 1978: On the mean meridional mass motions of the stratosphere and mesosphere, *J. Atmos. Sci.*, ***35***, 2325-2333.

Dunkerton, T. J., and D. P. Delisi, 1997: Biennial, quasi biennial and decadal oscillation of potential vorticity in the northern stratosphere, (Personnel communication)

Dutta, R. K., and M. G. Gupta, 1967: Synoptic study of the formation and movement of western depressions, *Indian J. Meteor. Geophy.*, ***18***, 45-50.

Ebdon, R. A., 1975: The quasi biennial oscillation and its association with tropospheric circulation patterns, *Meteor. Mag.*, ***104***, 282-297.

Fusco, A. C., and M. L. Salby, 1999: Interannual variations of total ozone and their relationship to variations of planetary wave activity, *J. Climate*, ***12***, 1619-1629.

Gabor, D., 1946: Theory of communications, *J. IEEE (London)* **93,** 429 –457

Garcia, R. R., and D. L. Hartmann, 1980: The role of planetary waves in the maintenance of the zonally averaged ozone distribution of the upper stratosphere, *J. Atmos. Sci.*, ***37***, 2248-2264.

Giorgetta, M. A., L. Bengtsson, and K. Arpe, 1999: An investigation of QBO signals in the east Asian and Indian monsoon in GCM experiments, *Climate Dyn.* ***15***, 435-450.

Gong, D., et al., 2001: East Asian winter monsoon and Arctic oscillation, *Geophy. Res. Lett.*, ***28***, 2073-2076.

Goswami, B. N., 1995: A multiscale interaction model for the origin of the tropospheric QBO, *J. Climate*, ***8***, 524-534.

Gouget, H., J. –P. Cammas, A. Marenco, R. Rosset, and I. Jonquieres, 1996: Ozone peaks associated with a subtropical tropopause fold and with the trade wind inversion: a case study from the campaign TROPOZ II over the Caribbean in winter, *J. Geophy. Res*, ***101***, 25,979 – 25,993.

Gray, W. M., 1984: Atlantic seasonal hurricane frequency. Part I: El Nino and 30 mb quasi biennial oscillation influences, *Mon. Wea. Rev.*, ***112***, 1649-1665.

Gray, W. M., J. D. Sheaffer, and J. A. Kinaff, 1992: Hypothesized mechanism for stratospheric QBO influence on ENSO variability, *Geophy. Res. Lett.*, ***19***, 107-110.

Hadjinicolaou, P., Pyle, J. A.. Chipperfield, M. P. and Kettleborough, J. A. 1997. Effect of interannual meteorological variability on mid-latitude O_3 , *Geophy. Res. Lett.* ***24***, 2993-2996.

Hamilton, K., 1989: Interhemispheric asymmetry and annual synchronization of the ozone quasi-biennial oscillation, *J. Atmos. Sci.*,***46***, 1019-1025.

Hamilton, K., 1995: Comments on "Global QBO in circulation and ozone. Part I: Reexamination of observational evidence", *J. Atmos. Sci.*, ***52***, 1834-1838.

Hitchmann, M. H., M. Mc Kay, and C. R. Trepte, 1994: A climatology of stratospheric aerosol, *J. Geophy. Res.*, ***99***, 20689-20700.

Hollandsworth, S. M., et al., 1995: Observational study of the quasi biennial oscillation in ozone, *J. Geophy. Res.*, ***100***, 7347-7361.

Holton, J. R., and R. S. Lindzen, 1972: An updated theory for the quasi biennial cycle of the tropical stratosphere, *J. Atmos. Sci*, ***29***, 1076-1080.

Holton, J. R., and H. C. Tan, 1980: The influence of the equatorial quasi biennial oscillation on the global circulation at 50 mb, *J. Atmos. Sci.*, ***10***, 2200-2208.

Holton, J. R., and H. C. Tan, 1982: The quasi biennial oscillation in the Northern Hemisphere lower stratosphere, *J. Met. Soc. Japan*, ***60***, 140-148.

Holton, J. R., 1989: Influence of the annual cycle in meridional transport on the quasi biennial oscillation in total ozone, *J. Atmos. Sci.*, ***46***, 1434-1439.

Holton, J. R., et al., 1995: Stratosphere-Troposphere exchange, *Rev. Geophys.*, ***33***, 4403-4449.

Hood, L. L., and D. A. Zaff, 1995: Lower stratospheric stationary waves and the longitude dependence of ozone trends in winter, *J. Geophy. Res.*, ***100***, 25,791-25,800.

Hood, L. L., and J. P. M. McCormack, 1997: An investigation of dynamical contributions to midlatitude ozone trends in winter, *J. Geophy. Res.*, ***102***, 13,079-13,093.

Jackman, C. E., et al., 1996: Past, present and future modeled ozone trends with comparisons to observed trends, *J. Geophys. Res.*, ***101***, 28,753-28,767.

James, P.M., et al., 1997: A study of ozone mini-hole formation using a tracer advection model driven by barotropic dynamics, *Meteorol. Atmos. Phys.*, ***64***, 107-121.

James, P.M., et al., 2000: Very low ozone episodes due to polar vortex displacements, *Tellus,* ***52 B***, 1123-1137.

Joseph, P. V., 1967: A case study of very low latitude occurrence of the subtropical jet stream over the Indian region, *Indian J. Meteor. Geophy.*, ***18***, 217-226.

Joseph, P. V., and J. Srinivasan, 1999: Rossby waves in May and the Indian summer monsoon rainfall, *Tellus*, ***51A***, 854-864.

Kalnay, E., et al., 1996: The NCEP/NCAR 40-year reanalysis project, *Bull. Amer. Met. Soc.*, *77*, 437 - 471.

Kanamitsu, M., and T. N. Krishnamurti, 1978: Northern summer tropical circulations during drought and normal rainfall months, *Mon. Wea. Rev*, ***106***, 331-347.

Khandekar, M. L., 1996: El Nino/Southern Oscillation, Indian monsoon and world grain yields – A synthesis, *Land based and marine hazards* M. I. El-Sabh et al., Eds., *Advances in Natural and Technological Hazards Research*, *7*, Kluwer Academic, 79-95.

Khandekar, M. L., 1998: Comments on "Space-Time structure of monsoon interannual variability", *J. Climate*, ***11***, 3057-3059.

Kiehl, J., and S. Solomon, 1986: On the radiative balance of the stratosphere, *J. Atmos. Sci.*, ***43***, 1525-1534.

Kurzeja, R. J., 1981: The transport of trace chemicals by planetary waves in the stratosphere. Part-I, Steady waves, *J. Atmos. Sci.*, ***38***, 2779-2788.

Labitzke, K., and H. Van Loon, 1988: Association between the 11-year solar cycle, the QBO and the atmosphere. Part I: the troposphere and stratosphere in the Northern Hemisphere in winter, *J. Atmos. Terr. Phy.* ***50***, 197-206.

Lau, K. –M., and H. Y. Weng, 1995: Climate signal detection using wavelet transform: How to make a time series sing, *Bull. Amer. Meteor.* Soc., ***76***, 2391-2402.

Lindzen R. S., and J. R. Holton, 1968: A theory of the quasi biennial oscillation. *J. Atmos. Sci.*, ***25***, 1095-1107.

Logan, J. A., 1994: Trends in the vertical distribution of ozone: An analysis of ozonesonde data, *J. Geophy. Res.*, ***99***, 25,553-25,585.

Magana, V., and P. J. Webster, 1996: Atmospheric circulations during active and break periods of the Asian monsoon. Preprints of the Eighth conference on the Global Ocean – Atmosphere – Land system (GOALS), *Amer. Meteorol. Soc., Atlanta, USA. Jan 28 – Feb 2*, 1996.

Mahlman, J. D., 1997: Dynamics of Transport processes in the upper troposphere. *Science,* ***276,*** 1079-1083.

Mani, A., C. R. Sreedharan, P. V. Joseph, and S. S. Sinha, 1973: Studies of the vertical distribution of atmospheric ozone in association with western disturbances over India. *PAGEOPH,* ***106-108***, 1192-1199.

McKenna, D., *et al., 1989: Diagnostic studies of the Antarctic vortex during the* 1987 Airbourne Antarctic Ozone Experiment: Ozone mini-holes, *J. Geophys. Res.*, ***94***, 11,641-11,668.

McPeters R. D., et al., 1996: Nimbus-7 Total ozone mapping spectrometer (TOMS) data products user's guide, *NASA Reference Publication (Available in the TOMS Ver-7 Data CD-ROM).*

Meehl, G. A., 1987: The annual cycle and interannual variability in the tropical Indian and Pacific Ocean regions, *Mon. Wea. Rev.* ***115***, 27-50.

Meehl, G. A., 1994: Coupled land-ocean-atmosphere processes and south Asian monsoon variability. *Science*, ***266***, 263-267.

Meehl, G. A., 1997: The south Asian monsoon and the tropospheric biennial oscillation, *J. Climate*, ***10***, 1921-1943.

Mohanakumar, K., 1996: Effects of solar activity and stratospheric QBO on tropical monsoon rainfall, *J. Geomag. Geoelectr.*, ***48***, 343-352.

Mooley, D. A., and B. Parthasarathy, 1984: Variability of the Indian summer monsoon and tropical circulation features, *Mon. Wea. Rev.*, ***111***, 967-978.

Morlet, J., 1983: Sampling theory and wave propagation, *NATO ASI Series, FL, Springer*, 233 –261

Mukherjee, B. K., K. Indira, R. S. Reddy, and Bh. V. Ramana Murthy, 1985: Quasi biennial oscillation in stratospheric zonal wind and Indian summer monsoon, *Mon. Wea. Rev.*, ***113***, 1421-1429.

Murgatroyd, R. J., and F. Singleton, 1961: Possible meridional circulations in the stratosphere and mesosphere, *Quart. J. Roy. Met. Soc.*, ***87,*** 125-135.

Naujokat, B., 1986: An update of the observed quasi biennial oscillation of the stratospheric winds over the tropics, *J. Atmos. Sci.*, ***43***, 1873-1877.

Newman, P.A., et al., 1988: The morphology and meteorology of southern hemisphere spring total ozone mini-holes, *Geophy. Res. Lett.*, ***15***, 923-926.

Nicholls, N., 1978: Air-sea interaction and the quasi-biennial oscillation, *Mon. Wea. Rev.*, ***106***, 1505-1508.

Niu, X., et al., 1992: Trends in column ozone based on TOMS data: Dependence on month, latitude and longitude, *J. Geophy. Res.*, ***97***, 14,661-14,669.

Parthasarathy, B., A. A. Munot, and D. R. Kothawale, 1994: All India monthly and seasonal rainfall series: 1871-1993, *Theor. Appl. Climatol,* ***49***, 217-224.

Pawson, S., and M. Fiorino, 1998: A comparison of reanalyses in the tropical stratosphere. Part 1: thermal structure and the annual cycle, *Climate Dyn.*, ***14***, 631-644.

Pawson, S., and M. Fiorino, 1998: A comparison of reanalyses in the tropical stratosphere. Part 2: the quasi-biennial oscillation, *Climate Dyn.*, ***14***, 645-658.

Pawson, S., and M. Fiorino, 1999: A comparison of reanalyses in the tropical stratosphere. Part 3: inclusion of the pre-satellite data era, *Climate Dyn.*, ***15***, 241-250.

Petzoldt, K., et al., 1994: Correlation between stratospheric temperature, total ozone and tropospheric weather systems, *Geophy. Res. Lett.*, ***21***, 1203-1206.

Petzoldt, K., 1999: The role of dynamics in total ozone deviations from their long-term mean over the Northern Hemisphere, *Ann. Geophysicae, 17*, 231-241.

Plumb, R. A., and Mc Ewan, A. D., 1978: The instability of a forced standing wave in a viscous stratified fluid: a laboratory analogue of the quasi biennial oscillation, *J. Atmos. Sci.*, ***35***, 1827-1839.

Raman, C. R. V., Y. P. Rao, and S. M. A. Alvi, 1980: The role of interactions with middle latitude circulation in the behaviour of southwest monsoon of 1972 and 1979, *Current Science, **49***, 123-129.

Raman, C. R. V., and Y. P. Rao, 1981: Blocking highs over Asia and monsoon droughts over India, *Nature*, ***289***, 271-273.

Ramaswamy, C., 1962: Breaks in the Indian summer monsoon as a phenomenon of interaction between the easterly and the sub-tropical westerly jet streams, *Tellus*, ***24***, 337-349.

Ramaswamy, V., et al., 2001: Stratospheric temperature trends: Observations and model simulations, *Rev. Geophys.*, ***39***, 71-122.

Randel, W. J, F. Wu, R. Swinbank, J. Nash, and A. O' Neill, 1997: Global QBO circulation derived from UKMO stratospheric analysis, (Personnel communication).

Rasmusson, E. M., X. Wang, and C. F. Ropelewski, 1990: The biennial component of ENSO variability, *J. Mar. Sys.*, ***1***, 71-96.

Reed, R.J., 1950: The role of vertical motions in ozone – weather relationships, *J. Meteorol., 7*, 263-267.

Reed, R. J., W. J. Campbell, L. A. Rasmussen, and D. G. Rogers, 1961: Evidence of a downward propagating annual wind reversal in the equatorial stratosphere, *J. Geophy. Res.*, ***66***, 813-818.

Rodgers, E. B., J. Stout, J. Steranka, and S. Chang, 1990: Tropical cyclone-upper atmospheric interactions as inferred from satellite total ozone observations, *J. Appl. Meteor.*, ***29***, 934-954.

Ropelewski, C. F., M. S. Halpert, and X. Wang, 1992: Observed tropospheric biennial variabillity and its relationship to the southern oscillation, *J. Climate*, ***5***, 594-614.

Salby, M.L., and P. F. Callaghan, 1993: Fluctuations of total ozone and their relationship to stratospheric air motions, *J. Geophys. Res.*, ***98***, 2715-2727.

Sardeshmukh, P. D., and B. J. Hoskins, 1988: The generation of global rotational flow by steady idealized tropical divergence, *J. Atmos. Sci.*, ***45***, 1228-1251.

Singh, M. S., 1963: Upper air circulation associated with the western disturbance, *Indian J. Meteor. Geophy.*, ***14***, 156-172.

Singh, M. S., 1979: Westerly upper air troughs and development of western disturbance over India, *Mausam*, ***30***, 405-414.

Solomon, S., 1999: Stratospheric ozone depletion: A review of concepts and History, *Rev. Geophys.*, ***37***, 3275-3316.

SPARC (Stratospheric Processes and Their role in Climate), 1998: Assessment of trends in the vertical distribution of ozone. *SPARC Report No. 1*, Verrieres le Buisson Cedex, France.

SPARC (Stratospheric Processes and Their role in Climate), 2000: SPARC assessment of upper tropospheric and stratospheric water vapour. *SPARC Report No. 2*, Verrieres le Buisson Cedex, France.

Staehelin, J., et al., 2001: Ozone trends: A review, *Rev. Geophys.*, ***39***, 231-253.

Stanford, J. L., and J. R. Ziemke, 1993: Rossby Gravity waves in tropical total ozone, *Geophy. Res. Lett.*, ***20***, 2239-2242.

Steinbrecht, W., et al., 2001: Interannual changes of total ozone and Northern Hemispheric circulation pattern, *Geophy. Res. Lett.*, ***28***, 1191-1194.

Stolarski, R. S., et al., 1991: Total ozone trends deduced from NIMBUS 7 TOMS data, *Geophy. Res. Lett.*, ***18***, 1015-1018.

Stout, J., and E. B. Rodgers, 1992: Nimbus-7 total ozone observations of western north Pacific tropical cyclones, *J. Appl. Meteor.*, ***31***, 758-783.

Subbaraya, B. H., and S. Lal, 1999: Space Research in India: Accomplishments and Prospects, *Stratospheric chemistry and ozone depletion, pp 44.*PRL Alumni Association, Ahmedabad.

Suhre, K., et al., 1997: Ozone-rich transients in the upper equatorial Atlantic troposphere, *Nature*, ***388***, 661-663.

Terray, P., 1995: Space-Time structure of monsoons interannual variability, *J. Climate*, ***8***, 2595-2619.

Terray, P., 1998: Answer to comments on 'Space-Time structure of monsoons interannual variability', *J. Climate*, ***11***, 3060-3061.

Tomita, T., and T. Yasunari, 1996: Role of the northeast winter monsoon on the biennial oscillation of the ENSO/monsoon system, *J. Met. Soc. Japan.*, ***74***, 399-413.

Torrence, C., and G. P. Compo, 1998: A practical guide to wavelet analysis, *Bull. Amer. Met. Soc.*, ***79,*** 61-78.

Trenberth, K. E., 1975: A quasi biennial standing wave in the Southern Hemisphere and interactions with sea surface temperature, *Quart. J. Roy. Met. Soc.*, ***101***, 55-74.

Tung, K. K., and H. Y. Yang, 1994: Global QBO in circulation and ozone: Part I: Re-examination of observational evidence, *J. Atmos. Sci.*, ***51***, 2699-2707.

Tung, K. K., and H. Y. Yang, 1994: Global QBO in circulation and ozone. Part II: A simple mechanistic model, *J. Atmos. Sci.*, ***51***, 2708-2721.

Van der Leun, J., Tang, X., and Tevini, M., 1995: Environmental effects of ozone depletion: 1994 assessment, *Ambio*, ***14***, 138.

Veryard, R. G., and R. A. Ebdon, 1961: Fluctuations in tropical stratospheric winds, *Meteorol. Mag.*, ***90***, 125-143.

Webster, P. J., 1995: The annual cycle and the predictability of the tropical coupled ocean-atmosphere system, *Meteorolo. And Atmos. Phys.*, ***56***, 33-55.

Webster, P. J., et al., 1998: Monsoons: Processes, predictability, and the prospects for prediction, *J. Geophy. Res.*, ***103***, 14,451 – 14,510.

Weng, H., and K. -M. Lau, 1994: Wavelets, period doubling, and time-frequency localization with application to organization of convection over the tropical western Pacific, *J. Atmos. Sci.*, ***51***, 2523-2541.

Wirth, V., 1993: Quasi-stationary planetary waves in total ozone and their correlation with lower stratospheric temperature, *J. Geophy. Res.*, ***98***, 8873-8882.

Wirth, V., 1995: Diabatic heating in an axisymmetric cut-off cyclone and related stratosphere-troposphere exchange, *Quart. J. Roy. Meteorol. Soc.*, ***121***, 127-147.

WMO (World Meteorological Organization), 1998: Scientific Assessment of ozone depletion: 1998, *Global Ozone Research and Monitoring Project, WMO Report No. 44,* ***Vol. I***, Geneva.

.Yasunari, T., and R. Suppiah, 1988: Some problems on the interannual variability of Indonesian monsoon rainfall. *In 'Tropical Rainfall Measurements'*, Theon, J. S and N. Fugono (edi), A. Deepak Publishing, Hampton, pp 527.

Yasunari, T., 1989: A possible link of the QBOs between the stratosphere, troposphere and sea surface temperature in the tropics, *J. Met. Soc. Japan*, ***67***, 483-493

Ziemke, J. R., and J. L. Stanford, 1994: Kelvin waves in total column ozone, *Geophy. Res. Lett.*, ***21***, 105-108.

List of Publications

1. **Sathiyamoorthy, V.,** and K. Mohankumar (2000) Characteristics of tropospheric biennial oscillation and its possible association with the stratospheric QBO, ***Geophysical Research Letters – (USA)***, Vol. 27, 5, 669-672.

2. **Sathiyamoorthy V,** K. Mohankumar and P. V. Joseph (2001) Inter-annual variability of total ozone and its relation with the Asia Pacific wave. ***Tellus B-(Sweden)*** [accepted for publication].

3. **Sathiyamoorthy, V.,** Mohankumar , K., and P. V. Joseph (2001) Synoptic and Intraseasonal Time Scale Ozone Transport over South Asia, ***National Seminar on Tropical Meteorology – TROPMET-2001.***

4. Mohankumar. K., **V. Sathiyamoorthy** and S. Sijikumar (2000) Biennial oscillation in Temperature and Monsoon activity. ***SPARC General Assembly***, November 6-10, 2000, Mar Del Plata, Argentina.

5. Mohankumar. K., and **V. Sathiyamoorthy and** P.V. Joseph (2000) Role of Asia Pacific wave on Stratosphere – Troposphere exchange. ***SPARC. General Assembly***, November 6-10, 2000, Mar Del Plata, Argentina.

6. Siji Kumar, S., **V. Sathiyamoorthy**, Anu Simon, Prince K. Xavier, V. Sajith and P. V. Joseph (2000) Does the low level jet stream split into two branches over the Arabian sea? ***Proceedings of the National Seminar – TROPMET-2000.***

7. **V. Sathiyamoorthy,** S. Sijikumar , Prince . K. X., and Mohankumar. K, (1998).Application of Wavelet Transform for the Study of Stratosphere – Troposphere Coupling Processes, *Seminar on Stratosphere Troposphere Interactions,* Cochin University of Science and Technology, Cochin, November.